COMPUTATIONAL MODELLING OF FLUID FLOW AND HEAT TRANSFER THROUGH METAL FOAM AND WIRE MESH

Thesis

Submitted in partial fulfillment of the requirements for the Degree of

DOCTOR OF PHILOSOPHY

By

BANJARA KOTRESHA
(165119ME16F02)

DEPARTMENT OF MECHANICAL ENGINEERING

NATIONAL INSTITUTE OF TECHNOLOGY KARNATAKA

SURATHKAL, MANGALORE – 575025

AUGUST, 2019

DECLARATION

By the PhD research scholar

I hereby declare that the Research Thesis entitled **"COMPUTATIONAL MODELLING OF FLUID FLOW AND HEAT TRANSFER THROUGH METAL FOAM AND WIRE MESH"** which is being submitted to the **National Institute of Technology Karnataka, Surathkal** in partial fulfilment of the requirements for the award of the Degree of **Doctor of Philosophy** in **Mechanical Engineering** is a *bonafide report of the research work carried out by me*. The material contained in this Research Thesis has not been submitted to any other Universities or Institutes for the award of any degree.

Register Number: **ME16F02**

Name of the Research Scholar: **BANJARA KOTRESHA**

Signature of the Research Scholar:

Department of Mechanical Engineering

Place: NITK-Surathkal

Date:

CERTIFICATE

This is to certify that the Research Thesis entitled **"COMPUTATIONAL MODELLING OF FLUID FLOW AND HEAT TRANSFER THROUGH METAL FOAM AND WIRE MESH"** submitted by **Mr. BANJARA KOTRESHA (Register Number: 165119ME16F02)** as the record of the research work carried out by him, *is accepted as the Research Thesis submission* in partial fulfilment of the requirements for the award of the Degree of **Doctor of Philosophy.**

R e s e a r c h G u i d e (s)

Dr. N Gnanasekaran.

Assistant Professor

Department of Mechanical Engineering

National Institute of Technology Karnataka, Surathkal

Chairman-DRPC

Department of Mechanical Engineering

National Institute of Technology Karnataka, Surathkal

Date:

ACKNOWLEDGEMENT

The two mantras - "The joy of research and joy of teaching" learnt from his guru and guiding the same to his students in a simple and effective way; there is lot to learn and inculcate from my research supervisor **Dr. N Gnanasekaran**, who became **Guru** not only to me but others too. The interest, guidance, encouragement and academic insight of my advisor has been invaluable over the last three years. He has been very generous with his time and energy, and I have learnt enormous information from him. I have been privileged to work with him and I am extremely grateful to him.

My deepest gratitude to **Prof. C. Balaji, IIT Madras** and **Mr. Arun Murthy, Director-Technical, Fluidyn Softwares and Consultancy Pvt. Ltd,** for their valuable guidance and words of advice.

I am extremely grateful to HOD, **Dr. Shrikantha S Rao** for making available all the facilities needed for the smooth progress of my research work. I would like to thank **Dr. Kumar G N** and **Dr. Arumuga Perumal** for their constant support and guidance during my research tenure. My special thanks to **Dr. Gangadharan K V** for providing DAQ facilities to conduct the experiments. I am also thankful to my RPAC committee members **Dr. Vishwanth K P** and **Dr. Arun M** for their guidance during my presentation. I would also like to thank secretary DRPC, **Dr. Jeyaraj P** for being available whenever I approached him and making my presentations happen in a smooth way.

I would like express my sincere thanks to All India Council for Technical Education (AICTE), Government of India and Department of Higher Education, Government of Karnataka for giving me an opportunity to carry out my research work at NITK under quality improvement programme (QIP).

I am extremely thankful to the department of Mechanical Engineering, Government Engineering College, Haveri, Faculty and non- teaching staff for providing the opportunity to carry out my research work at NITK. My special thanks to **Dr. K. B. Prakash**, Principal, GEC, Haveri, for supporting and helping me in getting the deputation to pursue Ph.D at NITK. I also thank all the faculties of Government Engineering College, Haveri, for their kind words and constant support to pursue Ph.D at NITK.

Words cannot explain my gratitude to my mother **Smt. B Lakshmamma** for supporting me and her blessings helped me in my research work. I would also like to thank my elder sister

ABSTRACT

The present research work expounds the numerical investigation of fluid flow and heat transfer through high porosity metallic porous mediums such as metal foam and wire mesh filled in a vertical channel. In the present study the metallic porous mediums are placed on either sides of the heater-plate assembly to enhance the heat transfer. Two different heater assemblies are considered in the present investigation which involves a uniform aluminium plate-heater assembly and a discrete aluminium plate-heater assembly. The present problem is considered as conjugate heat transfer as it involves both solid aluminium plate and fluid flow in the channel. A two dimensional computational domain is selected for the numerical investigation as the vertical channel is symmetrical about the vertical axis. The metal foam/wire mesh region is considered as a homogeneous porous medium with the Darcy Extended Forchheimer model to evaluate the characteristics of fluid flow while the local thermal non-equilibrium heat transfer model is considered for the analysis of heat transfer.

The objectives of the present research work are to quantify the effect of pore density, porosity, partially filling thickness, thickness and thermal conductivity of same pore density metal foam, finding out the isothermal condition in discrete heat source system and to determine the interfacial heat transfer coefficient for the wire mesh porous medium in mixed convection and forced convection regimes. Three different filling rates of 40%, 70% and 100% by volume in the vertical channel are also considered for the investigation for the partial filled metallic porous mediums in the vertical channel.

The results in terms of Nusselt number, Colburn j factor and overall performance factor are presented and discussed for the cases studied in this research work. This work serves as the current relevance in electronic cooling so as to open up more parametric and optimization studies to develop new class of materials for the enhancement of heat transfer.

Keywords: Vertical channel, Conjugate heat transfer, CFD, Metal foam, LTNE, Interfacial heat transfer coefficient, Brass wire mesh

Table of Contents

List of Figures

List of Tables

Nomenclature

A	Surface area of the aluminum plate (m^2)
a_{sf}	Surface area density (m^{-1})
C	Form drag coefficient (m^{-1})
C_p	Specific heat (J/kgK)
d	Diameter of the wire (m)
d_p	Pore diameter (m)
d_f	Fiber diameter (m)
f	Friction factor
Gr	Grashoff number
g	acceleration due to gravity ($9.81\ m/s^2$)
H	Metal foam total thickness, (m)
H_f	Metal foam thickness (m)
h	heat transfer coefficient (W/m^2K)
h_{sf}	Interfacial heat transfer coefficient (W/m^2K)
j	Colburn j factor
K	Permeability (m^2)
L	Length of metal foam, (m)
LTE	Local thermal equilibrium (-)
$LTNE$	Local thermal non-equilibrium (-)
Nu	Nusselt number
Nu_{sf}	Interfacial Nusselt number
Pr	Prandtl number
Q	Heat power input (W)
Re_D	Reynolds number based on hydraulic diameter

Re_H	Reynolds number based on thickness
Re_{d_f}	Reynolds number based on fiber diameter
Ri_D	Richardson number based on hydraulic diameter
Ri_H	Richardson number based on thickness
St	Stanton number $= \dfrac{h}{\rho U C_p}$
T	Temperature (K)
U, V	Velocity (m/s)
w	Width of the cell opening (m)

Greek symbols

ε	Porosity
λ	Thermal conductivity (W/mk)
λ_p	Performance factor
μ	Dynamic viscosity (N-s/m^2)
v	Kinematic viscosity (m^2/s)
ρ	Density (kg/m^3)

Subscripts

eff	Effective
f	Fluid
fe	Fluid effective
s	Solid
se	Solid effective
t	Turbulent

CHAPTER 1

INTRODUCTION

In recent times, efficient cooling is required for thermal devices such as electronics cooling, heat exchangers and geothermal applications etc. to increase thermal performance. The space available for heat dissipation is reducing as the electronic components are becoming extremely smaller which in turn increases the complexity of the problem. Natural convection is most useful for cooling the electronic device by considering air as the working fluid which is more economical due to less maintenance and easy cooling, but in some cases due to more heat flux, the natural convection is not sufficient to cool such devices. Hence, in these cases forced convection is useful to improve heat transfer but it requires additional pumping power. Interestingly, mixed convection also takes place at very low fluid velocities wherein the buoyancy driven flow dominates the forced convection flow. There are different efficient cooling methods available to cool the electronic equipment such as heat pipes, heat sinks, perforated plates, porous medium etc.. Recent times, porous mediums are also considered as a promising candidate for increasing the heat transfer rate in various engineering applications.

The flow of fluid and heat transfer through the porous medium is a new emerging branch of fluid mechanics and heat transfer. The use of porous medium in industrial applications for the enhancement of heat transfer has received a considerable attention among researchers. Porous mediums such as wire meshes, perforated plates and metal foams are also extensively considered for the enhancement of heat transfer in many thermal engineering applications.

1.1 POROUS MEDIUM

A porous medium is defined as a material consisting of solid matrix with interconnected voids (Kaviany, 1991, Nield and Bejan, 2006). The fluid flows through the voids (pores) of the porous medium, in simple single phase flow the voids are saturated with single fluid. The solid phase of the porous medium may be rigid or

it may undergo small deformation. The examples of naturally available porous medium are beach sand, limestone, human lungs and wood etc.

Among metallic porous mediums the metal foams are receiving considerable attention by the researchers as it is having various advantages compared to other porous mediums available in the market (Zhao, 2012).

1.2 APPLICATIONS OF POROUS MEDIUM

The fluid flow and heat transfer through the porous medium is of interest in various engineering disciplines like mechanical, chemical, geological, environmental, petroleum etc. (Kaviany, 1991). Figure 1 depicts some applications of porous medium in pictorial form.
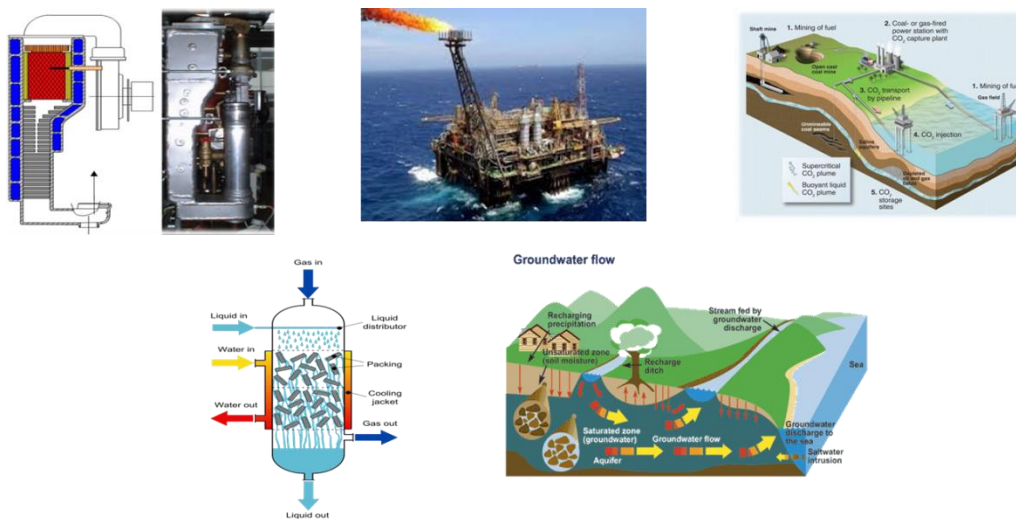
Figure 1.1 Applications of porous medium

1.3 SOME DEFINITIONS RELATED TO POROUS MEDIUM

1.3.1 Porosity (ε)

It is very important property of the porous medium which is calculated based on the solid and pore volumes as the porous medium is composed of two material constituents. It is defined as the ratio of total void volume to the total volume of the porous medium. Similarly the surface porosity is defined as the ratio of void area to the total area.

$$\varepsilon = \frac{V_{void}}{V_{total}} = 1 - \frac{V_{solid}}{V_{total}} \qquad (1.1)$$

where V_{void} is the void volume, V_{total} is total volume of the porous medium and V_{solid} is the solid volume present in the porous medium. The value of the porosity for any porous medium varies from 0 to 1, if the porosity value is near to 1 then it is called highly porous and if it is near to 0 then it is less porous. The porosity plays significant role in the prediction of pressure drop across any porous medium.

There are different methods available for the measurement of porosity of any given porous medium. They are listed below (Bear 1968):

1. Direct method

2. Optical method

3. Computed tomography method

4. Imbibition methods

5. Water saturation method

6. Water evaporation method

7. Mercury intrusion porosimeter

8. Gas expansion method.

1.3.2 Permeability (K)

It is defined as the ability of the porous material to allow the fluid to pass through it. It depends on the porosity as well as shape of the porous structures. It is derived from the Darcy law. It is expressed in m^2. The fluid passes rapidly through the porous medium if permeability is high and vice versa. The permeability of the porous medium can be calculated from experimental pressure drop or analytical expressions given by many researchers for different type of porous medium (Arunn N., 2015). The permeability is given by the following expression based on Darcy law.

$$K = u_p \frac{\mu \Delta x}{\Delta P} \qquad (1.2)$$

Where u_p is the superficial velocity, μ is the dynamic viscosity of the fluid and $\frac{\Delta P}{\Delta x}$ is the pressure gradient across the porous medium thickness.

The permeability is calculated analytically from the following expression mentioned in Eq. (1.3) for simple geometries.

$$K = \frac{D_p{}^2 \varepsilon^3}{180 \, (1 - \varepsilon)^2} \qquad\qquad (1.3)$$

where D_p is diameter of the fibre or ligament of the porous structure and ε is volumetric porosity of the porous medium. The constant 180 is taken from the best fit from the experimental data. Permeability of any porous medium can also be calculated from the experimental results of pressure drop obtained with curve fitting and comparing with each term of simple Darcy law or with Darcy Extended Forchheimer equation each (Arunn N., 2015, Nield and Bejan, 2006).

1.3.3 Form coefficient

The form coefficient is one of the important parameter among two hydraulic parameters of the porous medium. It depends on the form or shape of the fibre or solid part of the porous obstruction (Lage et al. 2005). Form coefficient can be determined either by analytically or experimentally. The form drag coefficient can be expressed as

$$C = \frac{\Delta P_f / L}{\rho u_p{}^2} \qquad\qquad (1.4)$$

where ΔP_f is pressure drop because of the form drag alone.

1.3.4 Superficial velocity

The superficial or seepage velocity is the product of porosity and average velocity of the fluid over the porous volume.

$$u_p = \varepsilon \, \overline{U} \qquad\qquad (1.5)$$

Where $\overline{U}$ is the average velocity of the fluid over the volume V_f.

4

1.4 FLOW THROUGH POROUS MEDIUM

1.4.1. Equation of continuity

The conservation principle is applied on the porous continuum based on the intrinsic average velocity which is the product of volume averaged velocity and porosity of the porous medium. The conservation of mass is professed by the equation of continuity as given in Eq. (1.6) (Kaviany, 1991, Nield and Bejan, 2006).

$$\varepsilon \frac{\partial \rho_f}{\partial t} + \nabla \cdot \left(\rho_f \, u_p \right) = 0 \qquad (1.6)$$

where ρ_f is the fluid density, ε is porosity and u_p is seepage velocity.

1.4.2 Darcy Law

The basic governing law of fluid flowing through the porous medium is the Darcy's law represented in Eq. (1.7). It states that the fluid flow rate through the porous medium is proportional to pressure gradient and viscosity of the fluid over a given distance (Kaviany, 1991, Arunn N., 2015).

$$\nabla P = - \frac{\mu \, u_p}{K} \qquad (1.7)$$

The term u_p is called the Darcy velocity or superficial velocity or seepage velocity or filtration velocity etc., which is lower than the actual velocity. The Darcy law is valid only for very low velocity incompressible and isothermal flows.

1.4.3 Darcy Extended Forchheimer Law

When pore or particle diameter based Reynolds number increases in the order of 1 to 10, the linearity in the Darcy law collapses because of form drag due to solid phase of the porous medium (Nield and Bejan, 2006). Hence, Darcy extended Forchheimer is the extension of Darcy law and defines the inertial effects of the fluid flow, which accounts the form drag coefficient or inertial resistance coefficient as represented in

Eq. (1.8). The form drag coefficient depends on the internal structure of porous medium, porosity and pore size.

$$-\nabla P = \frac{\mu \, u_p}{K} + \frac{\rho c_F}{\sqrt{K}} \, |u_p| u_p \qquad (1.8)$$

The modified Darcy law represented in Eq. (1.7) is initially represented by Dupuit (1863) and Forchheimer (1901). The second term in the RHS of Eq. (1.8) is termed as Forchheimer term where c_F is called Forchheimer constant. The transition of flow from laminar to turbulent occurs when the permeability based Reynolds number is greater than 150 (Neild and Bejan, 2006).

1.4.4 Darcy Brinkman Equation

The effect of fluid –fluid viscous shear always present in a viscous flow is identified by Brinkman (1949) other than the viscous drag due to fluid-solid in a porous medium. The Brinkman combined stokes flow and Darcy flow to obtain Darcy Brinkman equation as represented in Eq. (1.9) (Neild and Bejan, 2006, Arunn. N., 2015).

$$\nabla P = -\frac{\mu \, u_p}{K} + \mu_{eff} \, \nabla^2 u_p \qquad (1.9)$$

where μ_{eff} is effective viscosity

1.5 HEAT TRANSFER THROUGH POROUS MEDIUM

The heat transfer through the porous medium takes place through both the phases i.e. solid (ligaments or fibres) and fluid (flowing inside the porous medium). In some situations the temperature of the solid is in equilibrium with fluid flowing inside the porous medium, this scenario is identified as local thermal equilibrium (LTE). But this is always not true; hence there exist a temperature gradient at the interface between the solid obstacle and the adjacent fluid, this scenario is recognized as local thermal non-equilibrium (LTNE).

1.5.1 Local Thermal Equilibrium Model (LTE)

Local thermal equilibrium model assumes that the solid and fluid phases of the porous medium are in thermal equilibrium i.e. $T_s = T_f = T$. The net heat transfer between the phases of the porous medium is zero since the heat conduction in both the phases takes place simultaneously (Nield and Bejan, 2006). The conservation of energy is applied to both the phases of the porous medium and is given in Eq. (1.10 – 1.11).

For solid
$$(1 - \varepsilon)(\rho c)_s \frac{\partial T_s}{\partial t} = (1 - \varepsilon)\nabla.(k_s \nabla T_s) + (1 - \varepsilon)\, q_s''' \qquad (1.10)$$

For fluid
$$\varepsilon(\rho c_p)_f \frac{\partial T_f}{\partial t} + (\rho c_p)_f\, u_p.\nabla T_f = \varepsilon\, \nabla.(k_f \nabla T_f) + \varepsilon\, q_f''' \qquad (1.11)$$

For local thermal equilibrium condition, add Eq. (1.10) and (1.11)

$$(\rho c)_{eff} \frac{\partial T}{\partial t} + (\rho c)_f\, U.\nabla T = \nabla.(k_{eff} \nabla T) + q_{eff}''' \qquad (1.12)$$

where
$$(\rho c)_{eff} = (1 - \varepsilon)(\rho c)_s + \varepsilon\, (\rho c_P)_f \qquad (1.13)$$

$$k_{eff} = (1 - \varepsilon)\, k_s + \varepsilon\, k_f \qquad (1.14)$$

$$q_{eff}''' = (1 - \varepsilon)q_s''' + \varepsilon\, q_f''' \qquad (1.15)$$

Equation (1.13-1.15) represents the effective heat capacity, effective thermal conductivity and effective heat generation.

1.5.2 Local Thermal Non-Equilibrium Model (LTNE)

The local thermal non-equilibrium model considers the temperature gradient at the interface between the solid and fluid phases of the porous medium. The heat transfer between the solid and fluid regions is taken into account by the convection term and is represented in Eq. (1.16) and (1.17) (Nield and Bejan, 2006). The energy equations for both solid and fluid phases of the porous medium are given by Eq. (1.16 – 1.17).

For solid
$$(1 - \varepsilon)(\rho c)_s \frac{\partial T_s}{\partial t} = (1 - \varepsilon)\nabla.(k_s \nabla T_s) + (1 - \varepsilon)\, q_s''' + h_{sf} a_{sf}(T_f - T_s) \qquad (1.16)$$

For fluid

$$\varepsilon(\rho c_p)_f \frac{\partial T_f}{\partial t} + (\rho c_p)_f u_p . \nabla T_f = \varepsilon \nabla . (k_f \nabla T_f) + \varepsilon q_f''' + h_{sf} a_{sf} (T_s - T_f)$$ (1.17)

where   surface area density for simple case is

(1.18)

$$a_{sf} = 6 (1 - \varepsilon)/d_p$$

Interfacial heat transfer coefficient correlation given by Wakao et al. (1979)

$$Nu_{sf} = 2.0 + 1.1 \, Pr^{1/3} Re_p^{0.6} \left(\frac{\varepsilon d_p}{d_h} \right)^{0.6}$$ (1.19)

d_h is the pore scale hydraulic diameter

Different correlations are available for calculating surface area density and also for interfacial heat transfer coefficient based on the type of the porous medium (Wakao et al. 1979, Zukauskas, 1987, Calmidi and Mahajan, 2000, Tian et al. 2004).

1.6 METAL FOAMS

Metal foams are new class of porous medium which consists of solid matrix made of metal with empty or fluid filled voids. There are two types of metal foams available: (i) open cellular and (ii) closed cellular. In open foams the voids are connected through the open pores while in case of closed cellular foams the voids are connected with open channels but separated by a solid wall. The metal foams can have a high value of porosity up to 0.99. The number of pores per inch (PPI) may vary from 5 to 100. The open cell and closed metal foams are shown in Fig. 1.2.

(a)   (b)
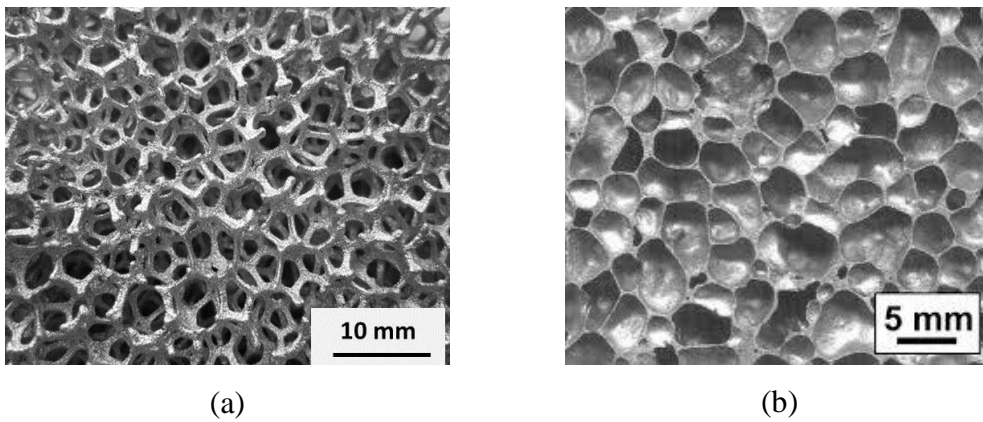
Figure 1.2 Metal foams (a) Open cell (b) Closed cell

1.6.1 Advantages of Metal Foams

The following are the advantages of the metal foams (Zhao (2012))

- Excellent stiffness to weight ratio.
- Low density with good shear and fracture strength.
- Damping factor is larger than the solid metals (order of 10).
- Able to absorb energy at almost constant pressure.
- High thermal conductivity.
- Ability to increase turbulence
- High surface contact area.
- Light weight

1.6.2 Applications of Metal foams

The distinctive properties of the metal foams made them to use in variety of thermal applications. The high porosity metal foams are more popular and are used as a good candidate for heat dissipation in electronics industry. The following are some of the applications of metal foams.

- Compact heat exchangers
- Geothermal applications
- Electronics cooling
- Building and construction industry
- Heat shields and etc.

1.7 CLOSURE

A brief introduction of heat transfer enhancement techniques as well as the some important parameters of porous medium was given in this chapter. The basics of fluid flow through the porous medium and heat transfer models are also explained. A brief introduction of metal foam was also presented at the end of the chapter. The next chapter gives the literature survey carried out in the present research work.

CHAPTER 2

LITERATURE REVIEW

A heat exchanger system is required for utilization, recovery and conversion of energy in any commercial, domestic and industrial application. The thermal efficiency of any thermal system can be increased by improving the heat exchange process which in turn reduces the cost of the overall system. It is very important to design the thermal systems encountered in the engineering applications to increase the efficiency and for smooth working. There are different techniques available for the enhancement of the heat transfer in wide variety of engineering applications. Some of the examples are micro-channel, heat sinks, extended surfaces, phase change materials, nano-fluid, porous media etc. The fluid flow and heat transfer through porous medium is one of the interesting subjects since it involves fluid flow through the pores, heat conduction through the solid fibres and convection between solid fibres and adjacent fluid flowing through the pores. Many researchers considered the metal foam porous medium as the desirable candidate for the enhancement of heat transfer as well as in terms of hydrodynamic performance compared to other porous medium.

In recent times, metals foams have started receiving considerable attention among the researchers in thermal sciences because of their high thermal conductivity and good mechanical properties. One of the promising and interesting features of metal foams is the existence of many voids in the structure as compared to regular metals; as a result, they have very large specific surface area that is available for heat transfer. In view of this, metal foams are being used as thermal management solutions in electronic cooling, compact heat exchanger etc.

2.1 COMPLETELY FILLED METAL FOAM CHANNEL

Several researchers have reported the study of flow behaviour and heat transfer enhancement through natural and forced convection in a vertical channel or between parallel plates. The vertical channel with heating can be considered as a good example

for applications like chimney, solar panels or Trombe walls (Gan, 1997). A computational fluid dynamics code is developed for the prediction of gravity flow through the Trombe wall for different parameters which affects the flow such as height and width of the channel, wall insulation and heat gains.

Thermal transport in high porous metal foams has extensively been reviewed by Zhao (2012). The review mainly focuses on forced convection of single phase, flow boiling and pool boiling heat transfer and thermal radiation in high porosity cellular metal foams. It has been reported that extensive work has been carried out on forced convection through metal foams which results in development of the compact heat exchangers. The review also reports that very limited studies have been carried out on phase change and radiation within the metal foam.

Boyd and Hooman (2012) performed 3D numerical study on metal foam heat exchanger for different cooling methods such as air and water cooling. In the simulation a graphite block of thickness 1 mm is placed between the cooling channel and the cell of the fuel cell system. One end of the graphite foam is heated because of the reactions taking place in the fuel cell and other end is cooled by air. The porous aluminium metal foam is considered in the cooling channel. The study concludes that the performance of an air cooled metal foam heat exchanger was found to be same as that of a water cooled heat exchanger for a fuel cell application with same pressure drop.

Lu et al. (2006) analytically studied the thermal performance of the metal foams filled in pipes. The flow and heat transfer through the metal foams is predicted using Brinkman Extended Darcy flow model and local thermal non-equilibrium model respectively. The effect of microstructure properties of the metal foam such as porosity, pore size, thermal conductivity ratio and finally the effect of Reynolds number on the heat transfer performance is analysed. It is concluded that the small pore size and low porosity play an important role in achieving higher overall thermal performance.

Mancin et al. (2013) experimentally studied forced convection through twenty one aluminium and copper metal foams. They considered metal foam samples of different Pores per Inch (PPI) from 5 to 40 and with porosity varying from 0.89 to 0.95 and for two different thickness of the metal foam such as 20 and 40 mm. They studied the effect of geometrical properties, mass flow rate and heat flux on the fluid flow including heat transfer. They proposed correlations for the heat transfer coefficient and the pressure drop. The results showed that the 20 mm thick foam shows higher efficiency even after having half of heat transfer area compared to 40 mm thick foam.

Numerical investigation of metal foams confined in a parallel plate for different aspect ratios has been carried out by Jeng and Tzeng (2007). In the study the air is blown from the slot provided at the top of the channel on to the metal foam confined in a channel. Highly porous and high permeability uncompressed metal foam is considered in the numerical computations. It is reported that the Nusselt number was 20 times more in metal foam compared to non-metal case.

Wang et al. (2011) used a cubical structured model for analysing fluid flow and heat transfer through open and closed cellular porous medium and the model results showed good agreement with the experimental results.

Calmidi and Mahajan (2000) studied forced convection in high porous metal foams both experimentally and numerically. They analysed different pore density aluminium metal foams with varying porosity of 0.89 – 0.97, considering air as the working fluid. They reported that thermal dispersion is negligible in the foam – air combination due to the high conductivity of the solid matrix of the metal foams. The heat transfer coefficient remained constant at a particular velocity for varying heat flux. They also developed correlation to calculate interfacial heat transfer coefficient for metal foams.

Kamath et al. (2013) conducted convective heat transfer experiments on aluminium and copper metal foams completely filled in a vertical channel. The study is carried out for three different thicknesses of the metal foams for same metal foam PPI but having different porosities. It is concluded that pressure drop was not significant with increase in the thickness of the metal foam but the heat transfer increases with

increase in the thickness and finally it has been showed that the heat transfer performance of copper metal foams was better than aluminium foams only by 4 %.

Lin et al. (2016) performed numerical simulations to study the thermal performance of aluminium metal foams filled in a horizontal channel by considering local thermal equilibrium (LTE) and local thermal non-equilibrium thermal (LTNE) models and concluded that the LTNE model gives the same performance as the LTE model at higher air velocities.

Khashan and Al-Nimr (2005) numerically solved the forced convection of non-Newtonian fluid flow through the homogeneous porous medium filled in a channel to assess the local thermal equilibrium model. The power law model is assumed for defining the non-Newtonian behaviour of the fluid with Darcy-Brinkman-Forchheimer flow model for the prediction of hydrodynamic characteristics through the porous medium. The study reports the favourable circumstances for the assumption of local thermal equilibrium model.

Jiang et al. (1999) considered a parallel plate channel filled with homogeneous porous medium for the numerical prediction of fluid flow and convection heat transfer. The study investigates the effect of LTE, LTNE and thermal dispersion. It was concluded that the LTNE thermal model is best suited for the prediction of heat transfer through metallic porous medium.

Badruddin et al. (2007) numerically solved conduction, convection and radiation through a porous medium filled in a square cavity with LTNE thermal model using finite element discretization method. The numerical study reports the effect of various parameters on heat transfer such as interfacial heat transfer coefficient, conductivity ratio, Rayleigh number and radiation. The study concluded that the Nusselt number increases with Rayleigh number and at higher conductivity ratio the effect of radiation on overall Nusselt number is negligible.

Jiang and Ren (2001) carried out a numerical study of forced convection through porous medium filled in a channel using LTNE thermal model. The problem domain

solved consists of a horizontal channel in which the top and bottom walls are given heat flux condition. It is suggested that LTNE thermal model is best suited for numerical prediction of convective heat transfer through porous medium. It is also reported that the viscous dissipation has negligible effect on the heat transfer.

Khashan et al. (2006) predicted the natural convection through the porous medium filled in a cavity using LTNE condition numerically. The effect of different parameters on the flow and heat transfer was investigated by taking into account the Boussinesq approximation. They observed that at higher Rayleigh number the effect of Forchheimer term becomes more prominent.

Hayes et al. (2008) performed a thermal modelling of metallic heat exchanger by using concept of porous medium and LTNE thermal model both numerically and experimentally. They developed a Nusselt number correlation for metal matrix heat exchanger.

Phanikumar and Mahajan (2002) carried out experimental and numerical investigations on buoyancy induced flow and heat transfer in high porosity metal foams. The results showed that the LTNE model predicts the thermal performance well with the experimental results compared to the LTE model. The effects of thermal non-equilibrium were seemed to be significant for high Rayleigh and Darcy numbers.

Liu et al. (2017) reported simulations for forced convection in open cell metal foams by employing the Kelvin structure model to predict the pressure drop and thermal performance. The numerical results were compared with the experimental data and also with the semi-empirical models. A good agreement between all the three was achieved.

Kamath et al. (2011) performed experiments on high porosity aluminium metal foams having different pore densities filled in a vertical channel. A heater plate assembly is placed at the centre of the channel and aluminium metal foams are placed on either side of the assembly to enhance heat transfer. They reported that the heat transfer

increases as metal foam PPI increases with the expense of pressure drop. Finally, the Nusselt number correlation in terms of Reynolds number, porosity and Prandtl number was developed in the range of parameters studied.

Kim et al. (2000) performed experiments to calculate the pressure drop and the thermal performance through porous fins in a heat exchanger. The aluminium metal foams of different PPIs with porosities ranging from 0.89 to 0.96 are considered for the analysis and it has been concluded that the friction is lower for higher PPI due to large surface area; hence, the porous fins with low porosity and low permeability are preferred for compact heat exchangers of plate fin types.

Kim et al. (2001) performed experimental study on forced convection through aluminium metal foams filled in a channel heated asymmetrically. The test setup is prepared from Plexiglas in which metal foams with 10, 20 and 40 PPIs and constant porosity of 0.92 were considered in the analysis. They reported that higher PPI metal foam enhances heat transfer at the expense of friction factor. It is also mentioned that with the help of non-dimensional Darcy number, the friction factor and Nusselt number can be predicted from simple permeability measurement.

Bhattacharya et al. (2002) calculated the thermal properties of high porosity metal foams both analytically and experimentally by considering air and water as working fluids. The aluminium metal foams of different PPI and porosities are placed in the in the wind tunnel to determine the effective thermal conductivity, inertial coefficient and permeability. They reported that the ratio defined as the cross section of the porous structure to the intersection of fibres and the porosity of fibre play an important role in the calculation of effective thermal conductivity of the metal foam.

Boomsma et al. (2003) manufactured aluminium metal foam with 2.3 mm average cell diameter and developed a compact heat exchanger in which forced convection experiments were performed with water as working fluid. The performance of heat transfer was calculated for working fluid as 50% water-ethylene glycol solution. The problem geometry considered consists of a channel in which aluminium metal foam is

filled completely in the channel. They concluded that the efficiency of compressed metal foams was higher compared to several available heat exchangers and the thermal resistance decreases with the presence of metal foams compared to the other heat exchangers.

Venugopal et al. (2010) performed forced convection experiments through metallic porous structures in a vertical channel. The porous medium used for the experiments was made of metallic perforated plates. The commercially available 1.5 mm thick brass perforated sheets with 3 mm stamped holes are considered to prepare the porous medium. The study is conducted for different Reynolds number and recorded pressure drop as well as temperature distribution on the aluminium plate. According to their parametric study, they concluded that the decrease in porosity increases the Nusselt number and the porosity value of 0.85 provides 4.52 times higher heat transfer than that of the clear channel flow.

Mancin et al. (2012) experimentally studied the effect of different heights of the foam on the performance of heat transfer. The aluminium metal foam of 20PPI, porosity of 0.93 with two different aspect ratios was considered in the analysis. The pressure gradient for 20 mm and 40 mm foam heights was found to be equal but the heat transfer coefficient obtained for 20 mm foam height was found to be higher than that of 40 mm foam height. They also experimentally studied the performance of heat transfer for copper metal foam by forced convection (Mancin et al. (2012)). They reported that the heat transfer coefficient increases with increasing mass flow rate but the effect of heat flux on the heat transfer coefficient was found to be insignificant.

Guerroudj and Kahalerras (2012) numerically studied the effects of mixed convection in an inclined channel filled with heated porous blocks. A parallel plate channel with three discrete porous blocks attached to the bottom wall is considered and investigation is performed for different inclination angle. They reported that the inclination angle of the channel plays an important role in the calculation of flow and heat transfer and obtained a maximum Nusselt number at a channel angle of $+90^0$. They also found that the optimum channel inclination of -30^0 gives maximum heat transfer at lower Darcy number.

Dukhan et al. (2014) conducted hydrodynamic experiments on 20PPI aluminium metal foam with a porosity of 0.876 for different Reynolds number varying from Darcy to turbulent regime with water as working medium. Aluminium metal foams are brazed on to the inner surface of the wall of the aluminium pipe. They identified flow and transition regimes such as Pre-Darcy, transition to Darcy and Darcy regime based on the Reynolds number. They observed that the Darcy regime is narrow but the Forchheimer regime is wide for the range of parameters studied.

Ly et al. (2016) showed the use of numerical Fast Fourier Transform (FFT) model to compute the permeability from the digital images of the porous media. They considered different microstructures of the porous media and validated with the benchmark problems. They also studied the complex microstructure of the porous medium with varying porosities. Their results have shown good agreement with the values reported in literature.

The dependence of metal foams ligament shape (micro structure) on the radiative heat transfer has been evaluated using Monte Carlo technique by Cunsolo et al. (2016). The idealized geometries for the study are generated using Kelvin structure methodology. Two different types of metal foam ligaments structure were analysed: concave shape and porosity varying structure. The results show that the ligament shapes have a significant impact on the radiative heat transfer. They also highlighted the significance of the effect of surface area on heat transfer.

Celik et al. (2017) numerically investigated the interfacial heat transfer coefficient for a porous media in mixed convection by using pore scale model. The volume averaging technique has been used for solving the representative volume. It was also reported that in buoyancy driven flows the height of the porous media has a significant effect on the interfacial heat transfer coefficient and the correlations available for forced convection can also be used for mixed convection for low porosity porous media.

Solmus (2015) numerically studied the forced convection heat transfer through graphite foam filled in a rectangular channel and compared the performance of graphite foam with aluminium metal foam. The hydrodynamics and thermal performance metal foam porous medium is predicted using Brinkman-Forchheimer extended Darcy model and LTNE thermal model. The bottom wall of the channel was assigned heat input while the top wall was kept insulated. The results reveal that the graphite foam give better heat transfer performance compared to aluminium metal foam. They also noticed the large temperature difference between fluid and solid phases of the graphite metal foam in the parameters studied.

Gangapatnam et al. (2017) studied heat transfer through metal foams completely filled in a vertical duct both numerically and experimentally. The problem domain consists of vertical channel filled with 20PPI metal foam of aluminium material. The experimentally obtained results are compared with the analytical equations and obtained important properties of metal foam. These properties in turn used in numerical simulation and compared the numerical results with experimental results. The study also finds out the optimum thickness of the channel for obtaining maximum heat transfer. The LTE and LTNE thermal models are used to predict the thermal performance and the study concluded that the LTNE model is better than LTE model.

Nazari et al. (2015) experimentally studied the behaviour of porous insert into the circular tube in which the nanofluid is flowing. The circular pipe is made of aluminium and aluminium metal foam of porosity 0.5 is filled completely in the pipe for the enhancement of heat transfer. Al_2O_3/water nanofluid is flowing through the pipe while the pipe wall is maintained isothermal. The results obtained using nanofluid is then compared with water fluid case to see the thermal performance. The study concludes that the use of porous medium inside the circular tube improves heat transfer compared to the plain tube.

Ghosh (2008) analytically studied forced convection heat transfer through high porosity metal foams confined between the parallel plates by assuming a simple cubic structure of the metal foam. The analytical model considers the conduction and convection at the microscopic level and the expression developed resembles the

equations of conventional extended surfaces like fin. It is found that the metal foam struts cross connection enhances the heat transfer and the excess temperature between the fluid and solid phase of the foam decreases with increase in pore density and porosity.

Tamayol and Hooman (2011) theoretically studied the forced convection heat transfer through metal foams using the concept of thermal resistance. The intricate structure of the metal foam ligaments is modelled as cylinders arranged in a cubic array method. The metal foams are filled in the channel which was made of rectangular and tubular shapes. The interfacial heat transfer between the solid ligaments and adjacent fluid, conduction in the ligaments and convection from the solid walls is considered in the investigation. The basic simple convection principles are used in this approach to develop the model which solves the forced convection through the metal foams and it is suggested that the methodology can be used for investigating the effect of different parameters on the thermal performance.

2.2 PARTIALLY FILLED POROUS MEDIUM IN A CHANNEL

Xu et al. [1] conducted an analytical study of forced convection study on metal foams partially filled in a parallel-plate channel. A layer of two metal foams are attached to the bottom and top wall of the parallel plate channel and channel core is empty hence it forms a partial filling. Both top and bottom walls are subjected to the constant heat flux condition. The results showed that the friction factor can be reduced by increasing the porosity and decreasing the pore density and the overall performance of the metal foam become maximum when the hallow ratio is less than 0.3.

Hajipour and Dehkordi (2012) carried out analytical and numerical studies on porous medium partially filled in a parallel plate channel through mixed convection by using nano-fluids. The wall of the vertical channel is maintained at different isothermal temperatures and the metal foam layer is attached to the left wall of the vertical channel. They conclude that the presence of nanoparticles increases the velocity and also the temperature especially at higher heat flux.

Bernardo et al. (2014) conducted experimental and numerical studies on metal foam partially filled in a horizontal channel. The study is concentrated on the mixed convection effects through the metal foam in the channel and heat losses to the external ambient which is attached to the top wall of the channel. The heat is added to the channel from the bottom wall and it is being carried from the metal foam by air. They present the results in terms of temperature profiles for both with and without metal foam and calculated the amount of heat given to the surrounding.

Hajipour and Dehkordi (2014) performed experimental and numerical studies on mixed convection through metal foam partially inserted into the vertical channel. The channel is made of copper and 50% of the channel is partially filled with metal foam. In the numerical study, a two dimensional computational domain was considered as the channel was symmetrical. A transient analysis is carried out to see the effect of nanofluid flow rates on the flow and heat transfer. They reported that the volume concentration of 0.3% of nanofluid gives 20% and 5% increase in heat transfer and pressure drop respectively, compared to the distilled water.

Sener et al. (2016) carried out experimental study on aluminium metal foam filled in a rectangular channel for calculating pressure drop and heat transfer. The channel is filled with 10 and 20 pore density metal foam in four different ways such as completely filled, concave, convex and in triangular. Air is considered as working fluid and the Reynolds number varies from 968 to 29624, hence the results are presented for both laminar and turbulent zones. In case of fully filled case the metal foam of 20 PPI shows highest heat transfer whereas in case of partially filled channel the metal foam of 10 PPI gives the highest thermal performance. They concluded that heat transfer in the channel increases with increasing filling rate of the foam.

Lu et al. (2016) carried out analytical studies on forced convection through horizontal plate channel partly filled with metal foams. A two dimensional horizontal channel is considered in which the bottom wall is heated. The Brinkman-extended Darcy flow model is considered along with LTNE thermal model and coupling between the foam free region and foam region is considered in the investigation. They predicted that the

velocity distribution and temperature profile for the entire domain for different pore densities and also for different porosities of the metal foam. It is reported that the porosity, pore density and height of the metal foam plays an important role in the prediction of fluid flow through the channel. The thermal resistance in the metal foam filled channel is because of metal foam and fluid flowing in it and it is suggested that the optimized heat transfer can be obtained by reducing the thermal resistance part.

Lu et al. (2017) performed analytical study on forced convection heat transfer through parallel plate heat exchangers partly filled with metal foams in the channel. The two different types of channel configurations are studied such as symmetrical and asymmetrical. In symmetrical channel the metal foams are filled inside the channel while in case of asymmetrical channel the metal foam is filled outside the channel. The velocity and temperature distribution in the channel is predicted for both the scenarios of the channel configurations. The study concludes that the flow ratio plays an important role in the prediction of flow and heat transfer through partially filled channels.

2.3 DISCRETE HEAT SOURCES WITH/WITHOUT POROUS MEDIUM IN THE CHANNEL

In this electronic era, the electronic components are becoming increasingly smaller; as a result, the area available for heat dissipation becomes very less which in turn increases the heat flux at the chip level. The convection heat transfer study through discrete heat sources in channels is very important to analyse the cooling rate in order to increase the performance and efficiency of the electronic components. Rao et al. (2002) performed numerical study on mixed convection in a vertical channel with surface radiation including the discrete heat source in each wall. They reported that the wall surface temperature reduces by 50% when surface of wall changes to good emitter from good reflector. The surface emissivity plays an important role in the decrease of wall peak temperatures.

Baskaya et al. (2005) experimentally studied the forced convection in a rectangular channel with an array of discrete heat sources. The discrete heat sources are flush mounted and air is considered as working fluid. The result reveals that the heat

transfer enhancement depends on the limit of Grashof and Reynolds number. As Grashof number increases the heat transfer enhances due to buoyancy flow.

Dogan et al. [4] investigated mixed convection with discrete heat sources in a rectangular channel. The discrete heat sources are placed at top and bottom of the channel. They reported that for a given Grashof number as Reynolds number decreases the enhancement of heat transfer takes place at the last rows of the channel due to secondary flow induced by buoyancy and also suggested few guidelines for the design of electronic equipment.

Bautista and Mendez (2005) studied laminar forced convection through the discrete heat sources in a rectangular channel analytically and numerically. The study involves the conjugate heat transfer for the heated strip which is placed in a substrate that generates heat continuously. The contact between the heated strip and substrate is modelled by using non-dimensional parameter.

Linhui et al. (2006) experimentally performed natural convection study on vertical plate with discrete heat sources and developed correlation for heat transfer in terms of heating space and Rayleigh number. They reported that heat transfer from the discrete heat sources to the steel plate is not considered as uniform.

Sudhakar et al. (2009) used CFD and ANN to predict the optimal discrete heat sources configuration with conjugate heat transfer in a vertical duct. FLUENT software is used for solving the vertical duct to get temperature data as compared to configuration of the heat sources. They reported that ANN is predicting the heat source temperatures accurately and faster than the CFD code.

Radhakrishnan et al. (2010) carried out experimental and numerical studies to optimize the multiple heaters in an enclosure. The multiple heat sources are placed in a staggered manner and they used response surface method to maximize and minimize the heat input and the temperature deviation from the target temperature respectively.

Hotta et al (2013) conducted experiments to determine the optimal heat source configuration by natural convection for protruding heat sources and the study also includes the effects of surface radiation. They reported that the highest heat generating heat source should be placed at the bottom of the substrate board and heat transfer can be increased by painting the heat sources by black paint.

Ajmera and Mathur (2015) experimentally studied mixed convection in an enclosure having multiple ventilations with discrete heat source. They concluded that the heater which is placed near to enclosure inlet experiences lowest temperature and other heat sources gives the same temperature until Grashof number reaches a critical value.

Durgam et al. (2017) carried out experimental and numerical studies to get optimal heat source configuration both by natural and forced convection in a horizontal channel. The optimal distribution of the heat sources is defined based on the geometric parameter λ. They also studied the effect of thermal conductivity of the substrate and reported that the thermal conductivity of the substrate plays a very important role in the enhancement of heat transfer.

Silva et al. (2004) studied the optimal space distribution of heat sources on a wall by forced convection analytically and numerically. Their results showed that optimal spacing of the heat sources depends on the Reynolds number and they must be distributed non-uniformly on the wall.

Many researchers considered porous mediums of different types for the enhancement of heat transfer through the discrete heat source system in their studies and some authors considered metal foams in the investigation because of the noteworthy properties of metal foams. Some of the literature on the same is discussed below.

Kamath et al. (2014) carried out experimental investigation of heat transfer enhancement in a vertical channel filled with high porous metal foam with discrete heat sources. A discrete heat assembly which is combination of Bakelite and aluminium strips is placed inside the vertical channel at the centre and metal foam of 20 mm thickness is placed on either side of the assembly for increasing the heat

transfer. Initially, all the heat sources are assigned with equal heat inputs to see the temperature distribution on all the aluminium strips. Later the heat inputs on the heat sources are distributed such that the bottom heater carries more heat, middle heater is assigned with half of the bottom and top heater is defined with half of the heat input of middle. They used ANN and GA, a hybrid technique, to optimize the heat inputs to the heat sources so as to achieve isothermal condition on all the sources. They reported that the heat transfer increases by 5 times with the use of metal foam compared to the clear channel case.

Chen et al. (2013) performed a numerical study for the forced convective cooling of discrete heat sources by using metal foam layers. A horizontal channel in which four discrete heat sources are placed on the bottom plate and metal foam layers are attached to each heat sources is considered for the investigation. The flow and heat transfer through the metal foam layer is predicted using Darcy-Brinkman-Forchheimer flow and LTNE thermal models. The study reported that the temperature of solid and fluid phases decreases with increasing heat exchange between the solid – fluid interface and there exist local thermal equilibrium between the porous layer and the fluid. The concept of LTE is applicable for lower porosity, Darcy number and fibre diameter or at higher PPI and conductivity ratio.

Hadim and Chen (1994) carried out a mixed convection analysis in a vertical channel filled with porous medium with discrete heat sources at the left wall. The mixed convection problem is solved by considering Boussinesq approximation in the solution. They reported that as Darcy number decreases the flow separation point remains the same but the reattachment point moved still downstream and the average Nusselt number increases with increasing Darcy number. It is also identified that increase in the Darcy number decreases the average Nusselt number and bottom heat source experiences more heat transfer.

Hadim and Bethancourt (1995) performed a numerical study on forced convection in a channel partially filled with porous medium with discrete heat sources on the bottom wall. The flow in the channel is assumed to be laminar and flow through metal

foam layer is modelled using Darcy-Brinkman-Forchheimer model. The porous medium is assumed as homogeneous isotropic medium and fluid flowing through it is in thermal equilibrium with solid matrix of the porous medium. The effect of heater width and spacing between the heaters is analysed in the study. The result showed that by increasing the spacing of heat source there is negligible change in the heat transfer but the decrease of pressure drop is found to be significant.

Angirasa and Peterson (1999) numerically studied the turbulent forced convection in a channel filled with thin porous material of high porosity having a flush mount heat source on the channel wall. A two dimensional computational domain is consider in which a finite heat source is placed on the bottom wall of the channel. The study reports that the high porosity porous medium is suitable for enhancement of heat transfer because of good mixing and distribution of the flow.

Huang et al. (2005) performed the enhancement of heat transfer from the multiple heated blocks with porous covers in a channel. Finite volume discrete heat sources are placed on the bottom wall of channel and these heat blocks are covered by porous layers. A Darcy-Brinkman-Forchheimer flow model is considered for the prediction of flow through the porous layers. They concluded that the second and subsequent blocks cause flow recirculation which in turn increases the heat transfer because of the porous covers.

Yucel and Guven (2009) numerically studied the low Reynolds number forced convection in a channel with discrete heat sources which are covered by porous medium at the bottom wall. The simulation is carried out assuming a steady laminar flow in the channel and the channel walls are kept adiabatic. The effects of different flow parameter were also analysed. The study reveals that the high thermal conductivity porous medium covered on the solid blocks enhances the heat transfer significantly and decreases the maximum temperature on the heated blocks.

Sivasankaran et al. (2011) studied the effect of two discrete heat sources in a rectangular porous enclosure with heat generating system under natural convection. In

this study the size of the top heater is varied by keeping the length of the bottom heater constant and the natural convection effects are modelled using Boussinesq approximation. It has been reported that for smaller heater length ratio, heat transfer at both the heaters are found to be high.

Huang and Chen (2012) performed a numerical study on mixed convection through discrete porous covering heated blocks in a vertical channel. The flow characteristic in the channel is predicted using Darcy-Brinkman-Forchheimer flow model along with Boussinesq approximation to incorporate the buoyancy effects. They reported that the heat transfer rate increases from both sides of the heated blocks by the use of porous cover.

Sankar et al. (2013) performed a numerical study on natural convection through vertical annular enclosure filled with porous medium with internal heat generation along with discrete heating. A two dimensional axisymmetric computational domain is considered in which one wall consists of discrete heat source. The Darcy-Brinkman-Forchheimer flow and LTE thermal models are considered for homogeneous porous medium for prediction of flow and heat transfer. Natural convection in the cylindrical enclosure is modelled using Boussinesq approximation. The study concludes that by placing the heater at the middle of the inner annulus highest heat transfer rate is achieved and the hot spots are minimized rather than placing at top or bottom portion of inner wall. They also noticed the importance of location and size of the heater in enhancement of heat transfer.

Ghorab (2015) carried out a numerical investigation of forced convection heat transfer through four discrete sources in a heat exchanger with nonporous and partially filled porous channel by varying the exit height. The convergent nozzle is considered in which discrete heat sources and metal foams at each discrete heater are placed on the bottom wall of the channel. A thermal equilibrium is assumed between the solid and fluid phase of the porous medium. The results show that the Nusselt number increases by 20-40% in the partly filled porous convergent channel compared to nonporous.

2.4 CHANNEL FILLED WITH WIRE MESH POROUS MEDIUM

Many researchers used metallic porous medium to enhance heat transfer in cooling of electronics component. Higher porosity, low weight ratio, ability to increase turbulence etc. are the advantages of metallic porous medium. Ozdemir and Ozguc (1997) performed forced convection experiments on wire mesh screen porous medium filled in the channel for a Reynolds number (based on wire diameter) range of 1.5 to 12. They obtained Ergun's constants based on the relationship between pressure drop and flow rate. The study reports that the Ergun's equation can be obtained if the specific area of the wire mesh is calculated from the geometrical properties.

Muralidhar and Suzuki (2001) performed a numerical study on flow and heat transfer through the regenerator which was made using wire mesh for pulsating flow of gas. The physical geometry consists of a tube filled with wire mesh porous medium. They employed a non-Darcy flow and LTNE thermal model for the regenerator mesh for the prediction of flow and heat transfer. The results revealed that the higher order harmonics contribute significantly to the value of friction factor.

Tian et al. (2004) experimentally studied the forced convection heat transfer through copper mesh screens. Two types of copper mesh screens are analysed in the study and are prepared from transient liquid phase bonding method and brazing the plane weave wire mesh screens. These wire meshes are then filled in a parallel flow channel to find the flow and heat transfer characteristics. It is found that the friction factor is not only a function of porosity of the wire screens but is also a function of orientation of the mesh. A correlation for calculating the surface area density of the wire mesh is proposed. They reported that the overall thermal performance strongly depends on the surface area density as well as porosity of the porous medium but not based on the orientation of the wire mesh.

Li and Peterson (2006) determined the thermal conductivity of the wire mesh screen layers both theoretically and experimentally. They reported that the effective thermal conductivity of the wire screens can be obtained as high as 4-35% compared to the thermal conductivity of the wire metal when there exist good contact between the

wires. It is also suggested that the contact condition between the layers of wires plays a crucial role in the calculation of effective thermal conductivity.

Xu et al. (2007) performed both experimental and numerical studies on forced convection through the metallic wire mesh structures. The experimental results are compared to the numerical results to validate the methodology. The brazed metallic wire structures are filled inside the channel and uniform water flow is maintained to predict the heat transfer. Under steady state conditions, uniform heat flux was applied for different mesh configurations in the study. The result reveals that the friction factor is independent of inlet velocity for Reynolds number greater than 2000. It also reported that the surface area density and porosity of the wire mesh plays important role in the heat transfer for a given velocity of the fluid.

Dyga and Placzek (2010) studied the forced convection heat transfer through a channel with and without the wire mesh by considering air and water as working fluid. The results show that the efficiency of the heat exchanger was found to increase by the use of wire mesh. It is also noted in the study that in water-wire mesh combination gives higher pressure drop compared to air-wire mesh combination. Hence, it is suggested that the combination of air and wire mesh increases the intensity of the heat exchange compared to water-wire mesh combination.

Zhao et al. (2013) developed new analytical methodology to calculate the porosity, surface area density and thermal conductivity of square and diamond shaped wire screen meshes. The study includes various parameters such as wire diameter, number of meshes, pattern of stacking and compactness factor and the results were found agreeing with the existing methods available in the literature.

Ma et al. (2016) performed experiments on sintered woven wire mesh with inhomogeneous porosity to study the performance of flow and heat transfer. The test specimen consists of two parts of same thickness and wire diameter but having different porosities and is sandwiched between two copper electrodes. An infrared camera is used for the measurement of temperature on the solid part of the wire mesh. The results show that the friction factor decreases and Nusselt number increases with

increase in the Reynolds number for the same test piece and concluded that the average porosity has great influence on the heat transfer.

Kurian et al. (2016) experimentally studied the mixed convection through the brass wire mesh filled in a vertical channel by considering air as working fluid. Three different wire mesh porosities are considered in the analysis and are made of brass material. The brass wire meshes of same size are placed on either side of a heater plate assembly for enhancing heat transfer. The test section is placed in the wind tunnel. The pressure drop and temperature excess is recorded for different flow rates of the fluid. It is showed that the wire mesh structure performs almost the same as metal foam of same porosity. It is suggested that the wire mesh porous medium can be used for the enhancement of heat transfer with moderate pressure drop.

Tu et al. (2016) performed hydrodynamic and heat transfer studies by performing experiments on a circular tube by inserting mesh in to the cylinder. The test section consists of concentric cylinders in which hot fluid flows through the core and cold fluid flows in the annulus in the flow direction. The cylinder mesh having PPI 30, 60 and 120 are considered in the investigation with tap water as working fluid. It is observed that the wire mesh of 60 PPI is found as optimum based on the obtained results. The study reveals that the heat transfer increases by 2.3-2.6 times compared to without mesh case.

Fu et al. (2017) experimentally investigated the enhancement of heat transfer using wire mesh attached to the tubes with the help of twin wire arc thermal spraying method. The aluminium wire mesh of different wire diameters is taken and three different porosities of the wire mesh were prepared. These wire meshes are then connected to the aluminium tubes by using thermal spraying method. The results obtained are compared with plain tube and tube-wire. They concluded that the sprayed wire mesh heat exchangers enhance the heat transfer compared to the plain tube.

Huang et al. (2017) numerically studied the effect of metal cylinder inserts filled in a circular tube in a laminar flow. The effect of different parameters like pore type, porosity, length of the spacer and clearance is studied in detail. The parametric study

shows that the Nusselt number increases by 2.15 to 7.17 times than the plain tube and concluded that the porous metal wire mesh inserts enhances heat transfer compared to other porous inserts for the same pumping power. The clearance between the tube wall and metal insert plays a significant role in the heat transfer augmentation.

2.5 SUMMARY OF LITERATURE AND RESEARCH GAPS

From the above literature, it is clear that there are numerous analytical, experimental and numerical research works on porous mediums like metal foams, wire meshes, perforated plates etc. completely or partially filled in the channels. The investigation mainly focuses on the prediction of hydrodynamic and thermal characteristics of the porous medium. Some of the highlights of the literature are as follows.

- The use of porous medium showed significant improvement in heat transfer as it increases the surface area available for the heat transfer and fluid flow.
- The open cellular metal foams received considerable attention compared to closed cellular metal foams.
- The wire mesh porous mediums also shown a significant role in the enhancement of heat transfer as similar to metal foams and the advantage of using the wire mesh reduces the total operating cost.

Based on the above literature review the authors found some of the research gaps as follows.

- The numerical study of mixed convection heat transfer through different pore density, high porosity metal foams filled in the vertical channel is essential in order to design efficient cooling heat exchanger system.
- The study on effect of thickness and thermal conductivity of the metal foam is also limited.
- There is no correlation available for the calculation of interfacial heat transfer coefficient for the wire mesh porous medium.
- The study of hydrodynamic and heat transfer characteristics through wire mesh porous mediums in completely and partially filled channel is also limited in the literature.

31

- The solution of heat transfer through the discrete heat sources embedded in the channel is also important in the design of electronic equipment.

2.6 MOTIVE AND SCOPE FOR THE PRESENT WORK

Aforementioned review of literature, it can be seen that the numerical analysis on metal foams is formidable but is essential in order to understand their flow and heat transfer characteristics as exploration of detailed parametric studies by way of experiments can be very time consuming and expensive. Numerical investigations on mixed convection are even more complex and are expectedly inadequate in the literature. Also, the numerical investigations of parametric and optimization studies of forced convection through highly porous metal foams and wire meshes are necessary but complex due to the structure of the porous media. In harmony with this, this thesis focuses on numerical simulation of fluid flow and heat transfer in a vertical channel with and without open cell porous metal foams as well as wire mesh porous medium.

2.7 OBJECTIVES OF THE WORK

1. To develop a numerical model for the analysis of fluid flow and heat transfer through mixed convection in a vertical channel with and without open cell porous metal foams.
2. To investigate the effect of thickness and thermal conductivity of the high porosity metal foams filled in a vertical channel.
3. To investigate the effect of partial filling of the metal foam on fluid flow and heat transfer in a vertical channel.
4. To propose a suitable interfacial heat transfer coefficient for the analysis of wire mesh porous media.
5. Development of a suitable thermal model for finding out optimal distribution of heat sources for the application of electronic cooling using metal foams.

2.8 CLOSURE

The detailed description of the literature survey on metal foams, wire mesh and other porous mediums are given in this chapter.

CHAPTER 3

MATHEMATICAL MODELING OF FLUID FLOW AND HEAT TRANSFER THROUGH METAL FOAMS

3.1 INTRODUCTION

This chapter elucidates the methodology used for the prediction of fluid flow and heat transfer through high porosity metal foam filled in a vertical channel. It also explains the governing equations considered for solving the open space and metal foam regions of the channel along with the details of numerical model. Finally, the grid independency study and validation of the methodology are presented.

3.2 PROBLEM GEOMETRY

The problem geometry consists of an aluminium plate cum heater plate assembly which is placed inside a vertical channel. Aluminium metal foams are placed on both sides of the aluminium plate as shown in Figure 3.1. The dimensions of the aluminium plates considered are 250 x 150 x 3 (all in mm). The channel size considered in this study is similar to the experimental setup studied by Kamath et al. (2011).

The aluminium metal foam of different pore density (PPI) is considered for the investigations. The size of metal foam is 250 x 150 x 10 (all in mm) and porosity of the aluminium metal foams varies from 0.90 to 0.95. The properties of the metal foam considered for the present study are taken from Kamath et al. (2011) and are listed in Table 3.1. Table 3.1 also gives the uncertainties in the measured values of the permeability and the form drag coefficient as reported in Kamath et al. (2011).

Table 3.1 Properties of aluminium metal foam considered in the present study

PPI	Porosity	Permeability 10^7, m^2	Uncertainty %	Form drag coefficient	Uncertainty %
10	0.95	2.480	±7.95	94.98	±2.45
20	0.90	2.177	±9.67	208.82	±2.21
30	0.92	1.644	±9.83	148.97	±3.68
45	0.90	0.420	±5.87	397.01	±5.80
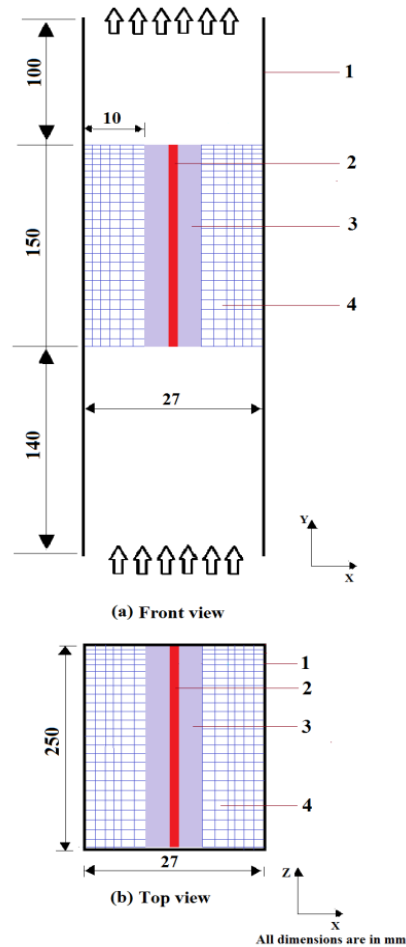
Figure 3.1 Schematic of the vertical channel filled with metal foam (1) Side wall of the channel (2) Heater (3) Aluminium plate (4) Metal foam

3.3 COMPUTATIONAL DOMAIN AND BOUNDARY CONDITIONS

Since the vertical channel is symmetry about the vertical axis, only one half of the vertical channel is considered for the numerical computations. A two dimensional computational domain that consists of the heater, the aluminium plate and the metal foam filled on one side of the plate, upstream and downstream of the channel as shown in Figure 3.2 is chosen for carrying out the numerical investigations. While the heater is assigned with a known heat flux as the boundary condition, a uniform velocity and zero pressure (p = 0) are assumed at the inlet and the outlet of the channel, respectively. Since the channel is symmetric about the vertical axis, the axis is defined with symmetry boundary condition and the side walls of the channel are set to adiabatic conditions.

The figure shows the computational domain with the following boundary conditions labeled:

Pressure outlet (top):
$$P = 0, \quad \frac{\partial U}{\partial y} = 0, \quad \frac{\partial V}{\partial y} = 0$$

Symmetry (upper right):
$$\frac{\partial T}{\partial x} = 0, \quad U = 0, \quad \frac{\partial V}{\partial x} = 0$$

Adiabatic wall (left):
$$U = V = 0, \quad \frac{\partial T}{\partial x} = 0$$

Heat flux (right):
$$\frac{Q}{A} = -K_s \frac{\partial T}{\partial x}$$

Symmetry (lower right):
$$\frac{\partial T}{\partial x} = 0, \quad U = 0, \quad \frac{\partial V}{\partial x} = 0$$

Velocity inlet (bottom):
$$U = 0, \quad V = V_\infty, \quad T = T_\infty$$
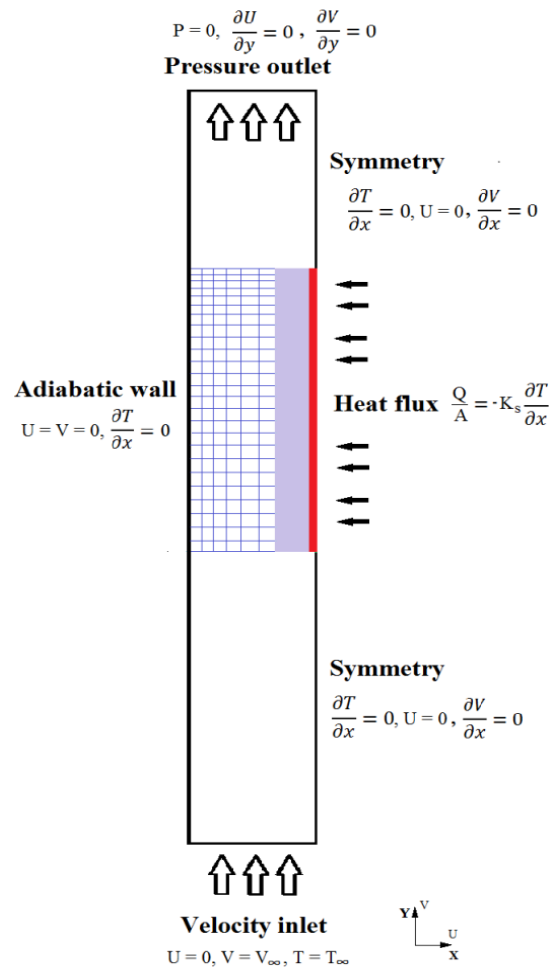
Figure 3.2 Computational domain and boundary conditions

3.4 NUMERICAL DETAILS

The computations are carried out using the commercially available ANSYS FLUENT 15.0 (2017). Air is considered as the working fluid and is flowing through both the open region and metal foam region of the channel. The velocity of the air is varied from 0.05 to 3.0 m/s and the Reynolds number based on the hydraulic diameter of the channel varies from 150 to 9000. In this range, the flow is assumed to be laminar, transition and turbulent flows. Whenever Reynolds number lies between 0 and 2300, the flow is assumed to be laminar, when it is between 2300 and 6000 the flow is considered to be in the transition regime and when it is greater than 6000 the flow is assumed to be turbulent. Therefore, to capture the transition and turbulent characteristics of the flow, a three equation transition turbulence model i.e., k-kl-ω transition model (ANSYS (2017), Walters and Coklja (2008)) and two equation

35

turbulence model i.e., k-ω model is considered in the foam free region of the vertical channel (ANSYS (2017)). The Reynolds number inside the aluminium metal foam is calculated based on the pore diameter of the metal foams and is found to be less than 150. In view of this, a laminar flow is considered in the metal foam region, as turbulent flow occurs only when the pore diameter based Reynolds number is greater than 150 (Nield and Bejan, 2005).

The governing equations solved for the open region are similar to that of open pipe flow and in the governing equations the effect of porosity, permeability etc. are considered for the metal foam region. The Reynolds averaged Navier-Stokes (RANS) equations are given as

Continuity equation:
$$\frac{\partial(\rho_f u_i)}{\partial x_i} = 0 \tag{3.1}$$

Momentum equations:
$$\frac{\partial(\rho_f u_i u_j)}{\partial x_j} = -\frac{\partial p}{\partial x_i} + \frac{\partial}{\partial x_j}\left((\mu_f + \mu_t)\left(\frac{\partial u_i}{\partial x_j} + \frac{\partial u_j}{\partial x_i}\right)\right) + \rho_f g\beta(T - T_\infty) \tag{3.2}$$

Energy Equation:
$$\frac{\partial(\rho_f u_j T)}{\partial x_j} = \frac{\partial}{\partial x_j}\left(\left(\frac{\mu_f}{Pr_f} + \frac{\mu_t}{Pr_t}\right)\frac{\partial T}{\partial x_j}\right) \tag{3.3}$$

More details on k-kl-ω transition and k-ω models are available in FLUENT help manual. The metal foam in the present numerical study has been considered as an isotropic homogeneous porous medium using the Darcy Extended Forchheimer model which involves the inertia and viscous effects because of the form drag coefficient and permeability of the porous metal foam. The governing equations considered for solving the high porous metal foam region are as follows.

Continuity equation:
$$\frac{\partial(\rho_f \varepsilon u_i)}{\partial x_i} = 0 \tag{3.4}$$

Momentum equations:
$$\frac{\partial(\rho_f u_i u_j)}{\partial x_j} = -\varepsilon\frac{\partial p}{\partial x_i} + \frac{\partial}{\partial x_j}\left(\mu_f\left(\frac{\partial u_i}{\partial x_j} + \frac{\partial u_j}{\partial x_i}\right)\right) - \varepsilon\left(\frac{\mu_{eff}}{K}u_i + \rho_f C\,|u|u_i\right) \tag{3.5}$$

Energy Equation:
LTNE

i. For Fluid $\varepsilon \dfrac{\partial(\rho_f\, C_{p.f}\, u_j T)}{\partial x_j} = k_f\, \varepsilon \dfrac{\partial}{\partial x_j}\left(\dfrac{\partial T_f}{\partial x_j}\right) +$ (3.6)

$$h_{sf} a_{sf}\left(T_s - T_f\right)$$

ii. For solid $k_s\,(1-\varepsilon)\dfrac{\partial}{\partial x_j}\left(\dfrac{\partial T_s}{\partial x_j}\right) = h_{sf} a_{sf}\left(T_f - T_s\right)$ (3.7)

where μ_{eff} is the effective viscosity taken equal to the fluid viscosity, K is the permeability, ρ is density of air, h_{sf} is the interfacial heat transfer coefficient, a_{sf} is the surface area density, C is the form drag coefficient and ε is porosity of the metal foam.

It is pertinent to mention that the thermal dispersion in the metal foam is assumed to be negligible and is neglected in the present numerical investigation due to the interaction between high thermal conductivity of solid matrix of metal foams and low thermal conductivity air as working fluid according to Calmidi and Mahajan (2000). Also, the flow mixing due to tortuous path of the metal foam is not considered in the present numerical simulation. The metal foam region is modelled as a single fluid region in which FLUENT uses a superficial velocity formulation calculated based on the volumetric flow rate through the porous region. At the interface between metal foam and the free foam regions, continuity conditions on the energy and shear stress are applied. The Coupled scheme is used for pressure velocity coupling with pseudo transient under relaxation scheme. A second order discretization is used for pressure, momentum, turbulent kinetic energy, laminar kinetic energy, specific dissipation rate and energy equations. The convergence criteria for the continuity and momentum equation are set as 10^{-5}, for k-kl-ω is set below 10^{-3} and for the energy equation is set below 10^{-10}.

At lower flow rates the flow variables takes more time for convergence. In order to overcome this problem, initially only the flow variables are solved for the complete problem geometry considered for the solution which includes both porous region as well as non-porous region of the channel. After getting the converged flow variable results the solution of energy equation for both porous and non-porous medium is

activated. This approach improved the convergence of the both flow and temperature variables.

The flow within the metal foam/wire mesh porous medium is considered as laminar as Reynolds number calculated based on permeability is in terms of orders of 10 and the open region of the channel is considered to be laminar, transition and turbulent based on the Reynolds number of the flow calculated with the hydraulic diameter of the channel as characteristic length. A boundary layer mesh is created near the wall of the channel in order to capture the flow physics near the wall and the dimensionless wall distance (Y plus) is limited to 5.0. A very popularly known k-ε turbulence model is initially considered for capturing the turbulent features of the flow in the open region of the channel and it is observed that the convergence of the variables were taken more CPU time. When the same solution is carried out using k-ω turbulence model the convergence was faster than the k-ε turbulence model and it is found that the both hydrodynamic and thermal results obtained with the use of both the turbulence models were same.

The surface area density (a_{sf}) and interfacial heat transfer coefficient (h_{sf}) for the metal foams used for the simulations (see Eq. (3.6) and Eq. (3.7)) are calculated based on the expressions given by Calmidi and Mahajan (2000) and are as follows.

Surface area density
$$a_{sf} = \frac{3\pi \, d_f\left(1 - exp^{-((1-\varepsilon)/0.04)}\right)}{\left(0.59 \, d_p\right)^2} \tag{3.8}$$

Interfacial heat transfer coefficient
$$\frac{h_{sf} \, d_f\left(1 - exp^{-((1-\varepsilon)/0.04)}\right)}{\lambda_f} = 0.52 \; Re_{d_f}^{0.5} Pr^{0.37} \tag{3.9}$$

where λ_f is thermal conductivity of the fluid, Pr is the Prandtl number, Re_{d_f} is the Reynolds number based on the fiber diameter and is calculated as $Re_{d_f} = \left(\frac{u \, d_f\left(1 - exp^{-((1-\varepsilon)/0.04)}\right)}{\varepsilon v}\right)$, d_f is the fiber diameter. The fiber diameter, pore diameter and the surface area density calculated for the metal foams used for the simulations are listed in Table 3.2. The surfaces area density calculated for all the metal foams are in good agreement with literature (refer Kopanidis et al., 2010).

Table 3.2 Surface area density of the metal foams used in the present study

Pore density (PPI)	Fiber diameter d_f (mm)	Pore diameter d_p (mm)	Porosity	Surface area density a_{sf} (m^{-1})
10	0.445	4.952	0.95	360.60
20	0.451	3.416	0.90	960.65
30	0.216	2.324	0.92	936.38
45	0.184	1.654	0.90	1671.76

3.5 GRID INDEPENDENCE STUDY

Grid independency study is carried out in order to fix the optimal grids for the numerical computations. To accomplish this, simulations are performed for 10PPI aluminium metal foam with a heat input of 20W. Detailed grid sensitivity calculations were done for three different grids of 26130, 56700 and 88400 to determine the optimal size of the mesh. Table 3.3 lists the pressure drop and excess temperature for three grid sizes for 10 PPI metal foam. From Table 3.3, the grid size of 56700 nodes is seen to be optimum in terms of pressure drop and excess temperature. Hence, further calculations are done with 56700 nodes.

Table 3.3 Results of the grid independence study for 10PPI aluminium metal foam (Re =3000)

Cells	Pressure drop (ΔP)	Excess temperature (ΔT)	Deviation (%)	
			$|\Delta P|$	$|\Delta T|$
26130	27.60	7.74	0.22	0.94
56700	27.56	7.70	0.07	0.42
88400	27.54	7.66	Base Line	

3.6 VALIDATION STUDIES

3.6.1 Pressure Drop

The variation of pressure drop with fluid inlet velocity for a range of 0.05 to 3 m/s for all the metal foam pore densities is shown in Figure 3.3. For the purpose of comparison, the experimental results of Kamath et al. (2011) are also shown in the figure. The figure confirms that the agreement between the results of the present study with the values of Kamath et al. (2011) is good. The pressure drop per unit length increases as the inlet velocity increases for all the metal foams, as expected the variation becomes non-linear at higher velocities. The pressure drop increases as the PPI increases which is seen in Figure 3.3. However, the 30 PPI metal foam shows a lower pressure drop compared to 20PPI metal foam, since the porosity of the 30 PPI foam is (0.92) more compared that of the 20PPI foam (0.90). In view of this, the obstruction to the flow reduces for the case of 30 PPI.
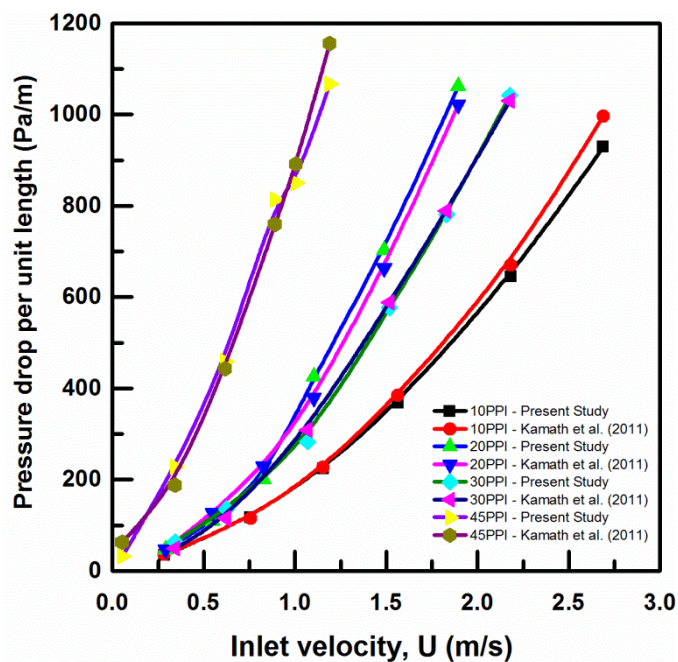
Figure 3.3 Variation of pressure drop per unit length with velocity for different metal foams and comparison with experimental benchmarks

3.6.2 Excess Temperature

The excess temperature is defined as the temperature difference between average temperature obtained on the aluminium plate and inlet temperature of the fluid. Figure

3.4 shows a comparison of the temperature differences obtained in the present study with those obtained experimentally by Kamath et al. (2011). The temperature excess obtained for clear channel simulation matches well with the experimental result for heat input of 20 W. For metal foams at very low velocities, a large difference between the experiments and simulations is seen. However, this deviation reduces as inlet velocity increases. The results obtained in the present simulations are similar to the results obtained by Lin et al. (2016). The temperature difference is in good agreement with experimental results for higher velocities.
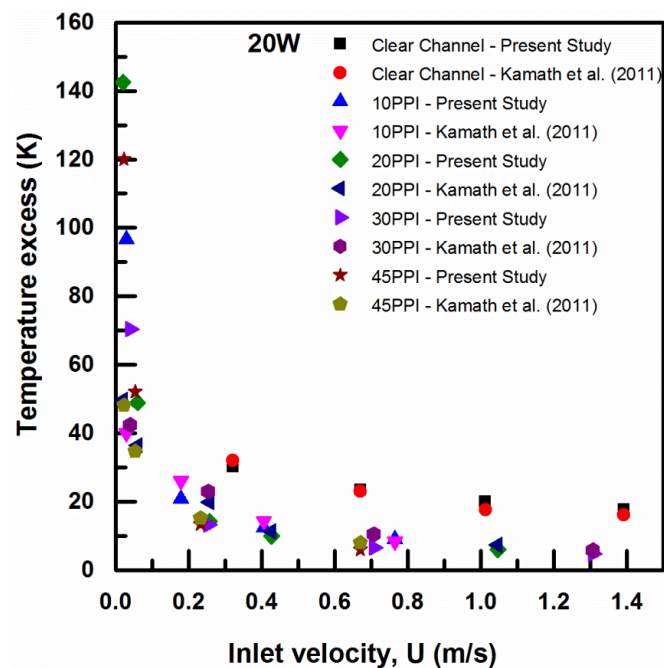
Figure 3.4 Comparison of temperature difference for various metal foams obtained in this study with experimental benchmarks

Based on the above comparison, it is clear that the numerical results are in good agreement with the experimental results and this serves as the validation of the methodology adopted in this study.

3.7 CLOSURE

The numerical methodology adopted for the solution of fluid flow and heat transfer through the metal foam porous medium is explained in detail in this chapter. The numerical results are validated by comparing with the available experimental results. The next chapter gives the numerical results of different PPI of the metal foams.

CHAPTER 4

MIXED CONVECTION THROUGH HIGH POROSITY METAL FOAMS FILLED IN A VERTICAL CHANNEL

4.1 INTRODUCTION

The effect of pore densities and porosities of high porosity metal foams in mixed convection is numerically investigated and explained in this chapter. The problem geometry, computational domain, boundary conditions, details of numerical setup considered for the present numerical investigation is already discussed in chapter 3. The grid independence study along with validation of the methodology was discussed in chapter 3.

The aluminium metal foam of different pore densities 10, 20, 30 and 45 PPI with porosity varying from 0.90 to 0.95 is considered in the present investigation. The results in terms of pressure drop, friction factor, heat transfer coefficient, Nusselt number, Colburn j factor and overall thermal performance factor for all the metal foams considered in the study are plotted and discussed.

4.2 RESULTS AND DISCUSSION

4.2.1 Flow Measurements

The variation of pressure drop with fluid inlet velocity for a range of 0.05 to 3 m/s for all the metal foam pore densities is shown in Figure 4.1. The pressure drop per unit length increases as the inlet velocity increases for all the metal foams. The variation of pressure drop is linear at lower velocities but becomes non-linear at higher velocities as expected. However, the 20 PPI metal foam shows a higher pressure drop compared to 30 PPI metal foam, as the porosity of the 20 PPI foam is (0.90) less compared that of the 30 PPI foam (0.92).
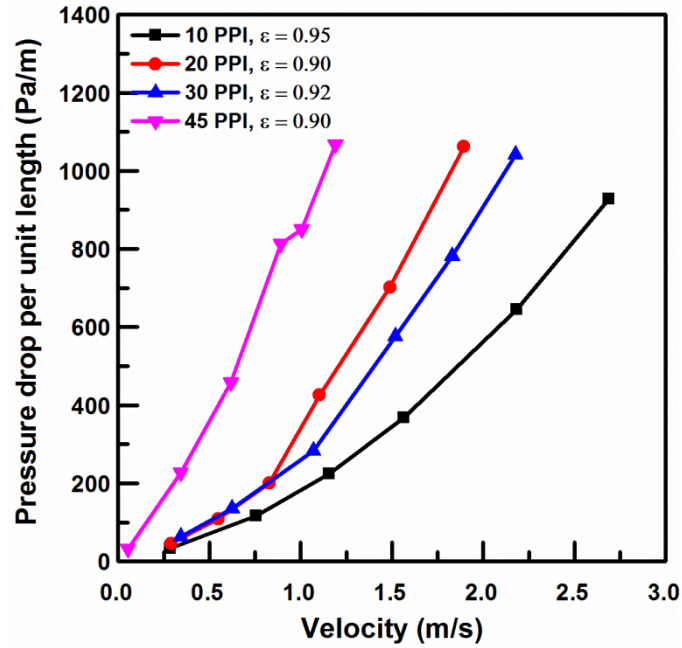
Figure 4.1 Variation of pressure drop with velocity for different metal foams PPI

The friction factor f is calculated based on the metal foam thickness is given by Eq. (4.1)

$$f = \frac{\Delta p}{\left(\frac{L}{H}\right)\left(\frac{\rho V^2}{2}\right)}$$ (4.1)

Figure 4.2 shows the variation of friction factor with Reynolds number for all the metal foams considered. The friction factor is higher for 45 PPI metal foam since the pressure drop is more as seen in Figure 4.1. This is because the number of fiber ligaments are more in case of 45 PPI metal foam compared to other metal foams.
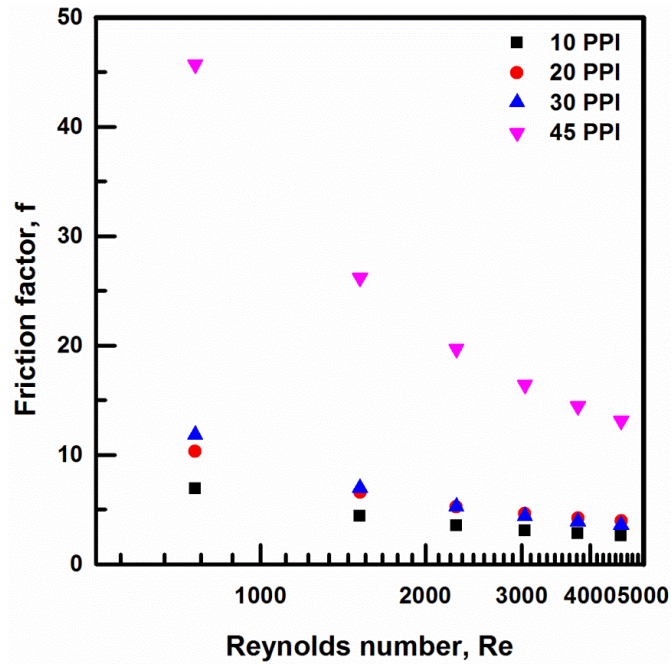
Figure 4.2 Variation of friction factor with Reynolds number for different metal foam PPI

4.2.2 Results of Heat Transfer

The metals foams considered in the present study are made of aluminium material with thermal conductivity of 165 W/mK (Kamath et al. (2011)). Since the metal foams are placed on both sides of aluminium plate with the heater sandwiched in between, the power input given to the heater is equally divided to both sides of the aluminium plates. Computations are done for only one half of the channel in view of the symmetry as already mentioned. The expression for the wall heat transfer coefficient and Nusselt number are given by

Wall heat transfer coefficient

$$h = \frac{Q}{A\Delta T} \tag{4.2}$$

Nusselt number

$$Nu = \frac{hD_h}{\lambda_{eff}} \tag{4.3}$$

where Q is the power input to the heater (W), A is the surface area of the aluminium plate exposed to the metal foam (m^2), ΔT is the temperature difference between average temperature of the aluminium plate (T_{avg}) and ambient temperature (T_∞) i.e., ($T_{avg} - T_\infty$), D_h is the hydraulic diameter of the channel (m), λ_{eff} is the effective

thermal conductivity of the metal foam. The effective thermal conductivity is calculated as $\lambda_{\text{eff}} = \lambda_s^{(1-\varepsilon)} \times \lambda_f^{\varepsilon}$ where λ_s is the thermal conductivity of the metal foam and λ_f is the thermal conductivity of air (Kamath et al. (2011)).

The non-dimensional numbers like Reynolds number, Grashof number and Richardson number are defined based on the hydraulic diameter of the vertical channel along with the properties of air taken at an inlet temperature of 30°C and are given by.

Reynolds number
$$Re = \frac{VD_h}{\nu} \qquad (4.4)$$

Grashof number
$$Gr = \frac{g\beta\Delta TD_h{}^3}{\nu^2} \qquad (4.5)$$

Richardson number
$$Ri = \frac{Gr}{Re^2} \qquad (4.6)$$

Wall Heat Transfer Coefficient

As expected, the wall heat transfer coefficient increases as the velocity increases. Figure 4.3 shows the heat transfer coefficient for different PPI metal foams for a heat input of 40W. The heat transfer coefficient increases as the pore density of the metal foam increases. The enhancement in heat transfer with the use of foams is clearly seen in Figure 4.3. At a velocity of 1 m/s, the channel filled with 45 PPI metal foam case gives a heat transfer enhancement of 336% compared to the clear channel. The 45 PPI metal foam is having better heat transfer compared to the other metal foams studied because of more surface area for the heat transfer. The figure also shows the wall heat transfer coefficient for different heat inputs obtained for clear channel simulations.
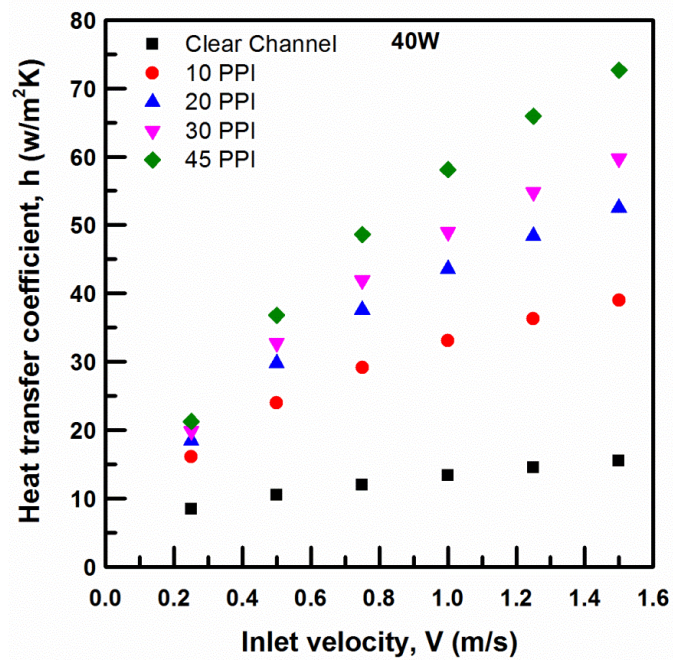
Figure 4.3 Heat transfer coefficient for all metal foams

The variation of average Nusselt number for different metal foams with respect to the flow Reynolds number is shown in Figure 4.4. The Nusselt number increases with Reynolds number as expected but the increase is not linear and is mainly due to the metal foam which can also be seen from this plot. The results of Nusselt number obtained match well with the experimental results obtained by Kamath et al. (2011) with a maximum deviation of ±15%. At lower Reynolds number the buoyancy driven flow dominates while at higher Reynolds number forced convection dominates as expected. At a particular Reynolds number the Nusselt number increases with pore density of the metal foam.
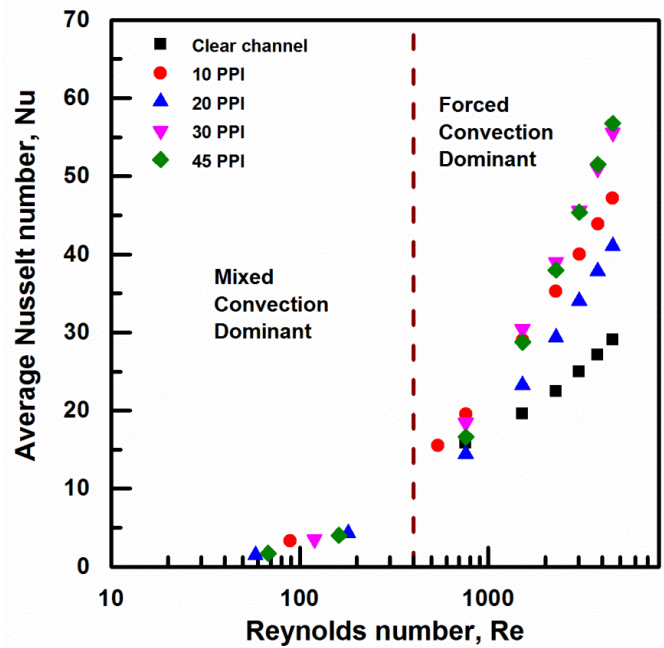
Figure 4.4 Variation of Nusselt number with Reynolds number

Figure 4.5 shows the classification of flow regimes based on the Reynolds number. The drastic change in Nusselt number with respect to Reynolds number for all the metal foams is observed at a Reynolds number of 400. When Re > 400, the Nusselt number strongly depends on the Reynolds number that can be identified as forced convection regime. Below this value, the variation of Nusselt number with Reynolds number is weak, hence it is identified as mixed convection regime.

Figure 4.6 shows the variation of Nusselt number with respect to Richardson number. Based on the slope of the curves the regimes can be classified as forced convection and mixed convection. It is clear that the changes in curves are noticed when Richardson number (Ri) is 1. The Nusselt number is found to be dependent on the Richardson number when Ri is less than one and the regime can be identified as forced convection. For Ri > 1, variation of Nusselt number with Richardson number is weak and the regime is identified as mixed convection region.
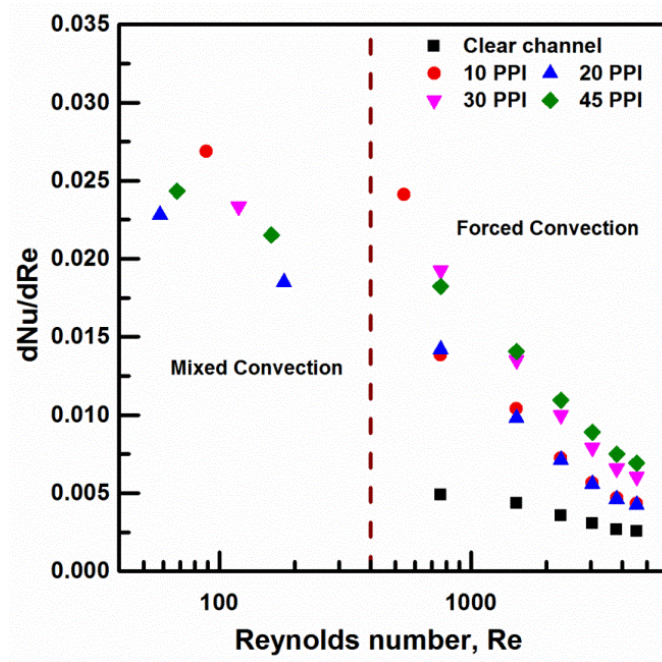
Figure 4.5 Flow regimes based on Reynolds number
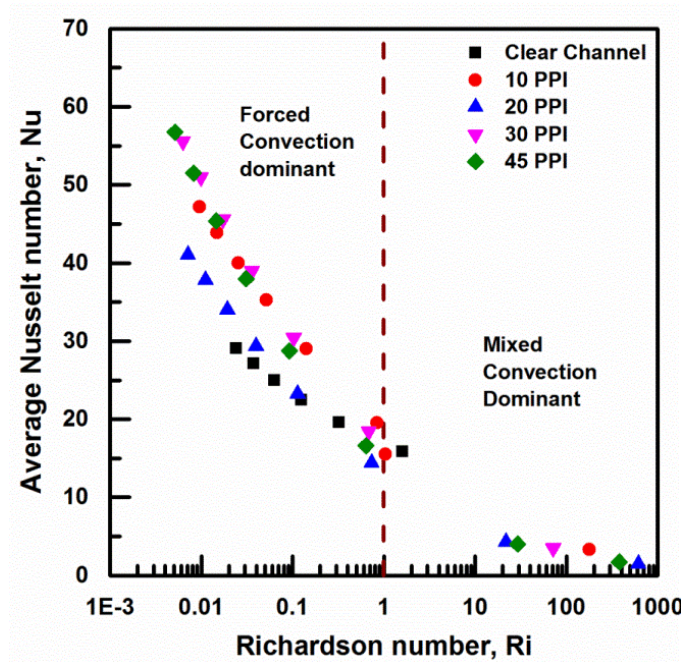
Figure 4.6 Variation of Nusselt number with Richardson number

The Nusselt number obtained in the present study is compared with the correlation available in the literature. Kamath et al. (2011) developed a correlation for Nusselt number based on the Reynolds number, Richardson number and porosity of the metal

foam by using the experimental data with an RMS error of ±10.87% which is given by Eq. (4.7) and valid for a range of parameters specified in Eq. (4.8). A parity plot, shown in Figure 4.7, between the Nusselt numbers obtained based on correlation proposed in (Kamath et al. (2011)) and the Nusselt number based on the present simulation, shows very good agreement with a deviation of ±15%.

$$Nu_{porous} = 0.223 Re^{0.723} \varepsilon^{6.81} (1 + Ri^{0.46} Re^{-0.73}) \qquad (4.7)$$

$$0.005 \leq Ri \leq 1032$$
$$24 \leq Re \leq 3730 \qquad (4.8)$$
$$0.9 \leq \varepsilon \leq 0.95$$
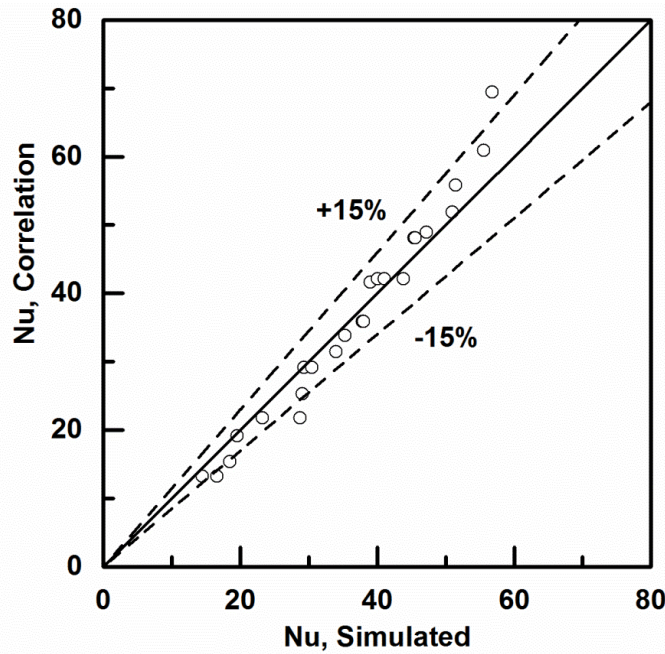
Figure 4.7 Parity plot showing agreement between Nusselt number based on correlation and Nusselt number based on present simulations

The Colburn j factor which describes heat transfer performance of heat exchanging device is given by Eq. (4.9)

$$j = St. Pr^{\frac{2}{3}} \qquad (4.9)$$

Figure 4.8 shows the variation of Colburn j factor with Reynolds number. The figure shows a decrease of Colburn j factor with the increase in flow rate for all the metal

foams. A similar trend is observed in Boomsma et al. (2003), Venugopal et al. (2010). The Colburn j factor is found to be higher for all the metal foams considered in the study compared to the clear channel case. It is clear from the plot that the metal foams are good candidates for the enhancement of heat transfer at lower flow rates. At a particular Reynolds number the Colburn j factor increases with increase of metal foam PPI, the 45 PPI metal foam gives better performance compared to other metal foams studied.
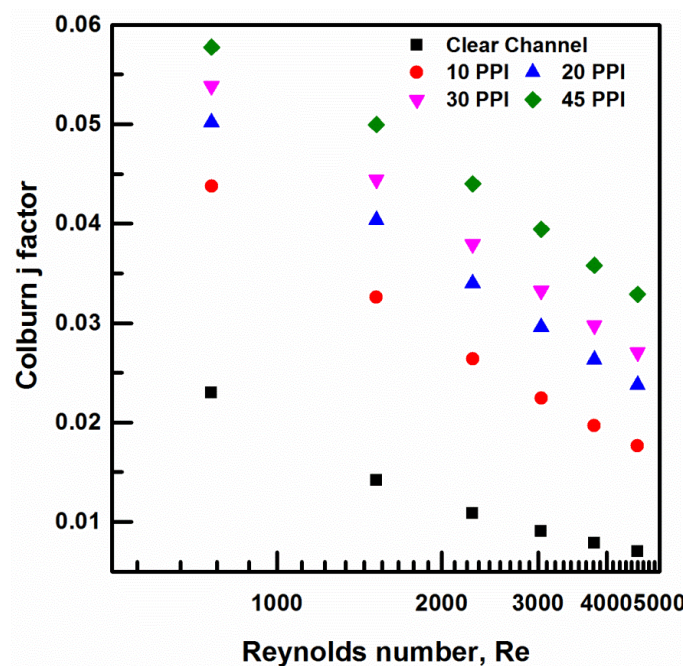
Figure 4.8 Variations of Colburn j factor with Reynolds number.

The overall performance of the metal foams can be analysed by using a performance factor similar to that defined in Manglik (2003) and is given by Eq. (4.10).

$$\lambda_p = \frac{j}{f^{\frac{1}{3}}}$$

(4.10)

Figure 4.9 shows the variation of performance factor (λ_p) with Reynolds number. The figure shows a general decrease of performance factor with the increasing flow rates. Among all the metal foams studied 30 PPI metal foam gives higher performance compared to other pore densities. The variation of performance factors for 20, 30 and 45 PPI metal foams does not show much variation in the Reynolds number range

between 750 and 1600, but 10 PPI metal foam shows a variation in the performance factor for the same range of Reynolds number. The performance factor for 30 PPI metal foam is higher compared to 45 PPI metal foam because the friction factor is less for 30 PPI compared to 45 PPI as seen in Figure 4.2.
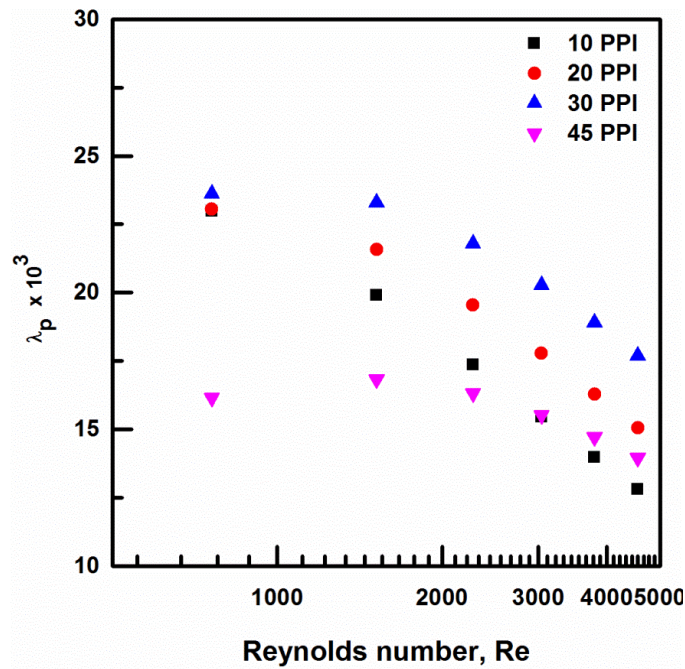
Figure 4.9 Variations of performance factor with Reynolds number.

4.3 CONCLUSIONS

In this chapter, numerical simulations of flow assisted mixed convection in a vertical channel filled with high porosity metal foams were carried out by using commercially available ANSYS Fluent 15.0 software. The aluminium metal foams were placed on either side of the aluminium plate to enhance the heat transfer. Four different types of metal foam PPI 10, 20, 30 and 45 were considered in the numerical simulation whose porosity varies from 0.90 to 0.95. The numerical results were validated with experimental results. The key conclusions obtained in this study are.

- The Darcy Extended Forchheimer porous model predicts the pressure drop with a maximum deviation of 8% compared to the experimental results.

- The heat transfer coefficient and Nusselt number increases as metal foam PPI increases. At inlet velocity of 1 m/s, the channel filled with 45 PPI metal foam gives 1.77 times higher heat transfer compared to 10 PPI metal foam. Therefore, metal foams can be used for the heat transfer enhancement in the thermal engineering applications.
- Distinct flow regimes can be identified based on the variation of Nusselt number with Reynolds and Richardson numbers.
- Based on the comparison of metal foam in terms of friction factor and overall performance factor, 30 PPI metal foam is seen to give better thermal performance compared to other metal foams.

4.4 CLOSURE

The detailed description of the mixed convection heat transfer through high porosity aluminium metal foam was elucidated in this chapter. Four different types of pore density metal foams with varying porosities were considered for the analysis. The effect of partial filling of the metal foams on pressure drop and heat transfer is explained in the next chapter.

CHAPTER 5

MIXED CONVECTION HEAT TRANSFER THROUGH PARTIALLY FILLED HIGH POROSITY METAL FOAMS

5.1 INTRODUCTION

This chapter discusses about the numerical simulation of mixed convection heat transfer through metal foams partially filled in a vertical channel. The methodology adopted to solve the complex structure of the metal foam is explained and the results in terms of pressure drop, Nusselt number and overall performance factor are presented and discussed.

5.2 PROBLEM STATEMENT

In this study, a vertical channel in which a heater is sandwiched between two plates is considered for the numerical model. The aluminium metal foams are placed on both sides of the aluminium plates to enhance heat transfer as shown in Figure 5.1. The aluminium plates are having dimensions of 250 x 150 x 3 (all in mm). The aluminium metal foams of four different pores per inch (PPI) 10, 20, 30 and 45 are considered for predicting the characteristics of flow and heat transfer.

Aluminium metal foams of four different PPIs with porosity varying from 0.90 to 0.95 are considered for the present numerical investigations. The metal foams are partially filled in the vertical channel with 40%, 70% and 100% volume proportions to determine the characteristics of flow and performance of heat transfer. Three different thicknesses of the metal foam are filled in the channel for each PPI and are represented as $H_f = 0.4H$, $H_f = 0.7H$ and $H_f = H$. Table 5.1 gives the properties of metal foams considered for the present study along with the uncertainties in the measured values of the permeability and the form drag coefficient.
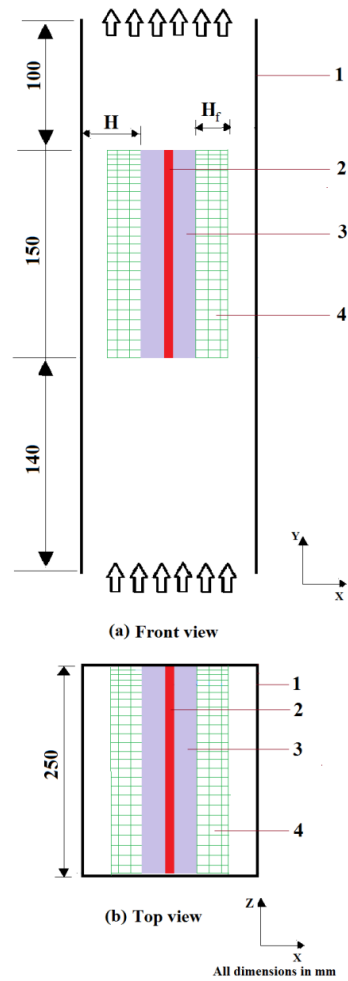
Figure 5.1 Schematic of the vertical channel filled with metal foam (1) Side wall of the channel (2) Heater (3) Aluminium plate (4) Metal foam

Table 5.1 Characteristics of metal foams

Material	PPI	Porosity	Permeability 10^7, m^2	Uncertainty %	Form drag coefficient	Uncertainty %
	10	0.95	2.480	± 7.95	94.98	± 2.45
Aluminium (Kamath et al. (2011))	20	0.90	2.177	± 9.67	208.82	± 2.21
	30	0.92	1.644	± 9.83	148.97	± 3.68
	45	0.90	0.420	± 5.87	397.01	± 5.80
Copper (Kamath et al. (2013))	10	0.88	1.742	± 19.20	176.75	± 4.60

5.2 COMPUTATIONAL DOMAIN AND BOUNDARY CONDITIONS

It is clear from Figure 5.1 that the vertical channel is symmetrical about the Y axis, hence the computational domain considered for the simulation consists of only one half of the vertical channel as shown in Figure 5.2. A two dimensional computational domain consisting of the heater, the aluminium plate, partially filled metal foam on one side of the plate, upstream and downstream of the channel is considered for the numerical study. The inlet to the channel is defined with uniform velocity inlet boundary condition; the outlet is defined with zero pressure (p =0) and the heater is assigned with a known heat flux boundary condition. The vertical axis is defined with symmetry boundary condition and the side walls of the channel are set to adiabatic boundary conditions. At the interface between the metal foam free region and foam region of the vertical channel, continuity in the shear stress and energy is applied as mentioned by many researchers.
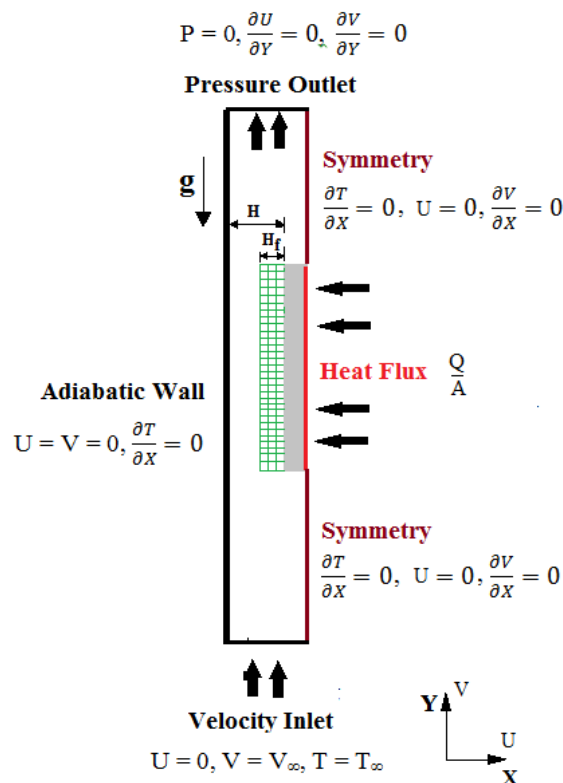
Figure 5.2 Computational domain with boundary conditions

5.3 NUMERICAL DETAILS

The details of numerical parameters and the governing equations used for the prediction of flow and heat transfer through the open space and metal foam region of the channel is as same as mentioned in the section 3.3 of chapter 3. At the interface between the porous medium and free region (open channel) the continuities of velocity, fluid temperature, shear stress and heat flux at the fluid-porous interface are considered as shown below.

Velocity
$$V \mid_{y^+} = V \mid_{y^-} \tag{5.1}$$

Fluid temperature
$$T_f \mid_{y^+} = T_f \mid_{y^-} \tag{5.2}$$

$$\left(k_{fe} \frac{\partial T_f}{\partial y} + k_{se} \frac{\partial T_s}{\partial y} \right)_f \mid_{y^+} = k_f \frac{\partial T_f}{\partial y} \mid_{y^-} \tag{5.3}$$

Shear stress
$$\frac{\mu_f}{\varepsilon} \frac{\partial v}{\partial y} \mid_{y^+} = \mu_f \frac{\partial v}{\partial y} \mid_{y^-} \tag{5.4}$$

Heat flux
$$k_s \frac{\partial T_s}{\partial y} \mid_{y^+} = h_{sf} (T_s - T_f) \mid_{y^-} \tag{5.5}$$

The surface area density (a_{sf}) for the aluminium and copper metal foam considered in the present study are calculated based on the Eq. (3.8) proposed by Calmidi and Mahajan (2000) and interfacial heat transfer coefficient (h_{sf}) is calculated from Eq. (5.6) given by Zukauskas (1987).

Interfacial heat transfer coefficient

$$\frac{h_{sf} d_f \left(1 - \exp^{-\left(\frac{(1-\varepsilon)}{0.04} \right)} \right)}{\lambda_f} = \begin{cases} 0.76 \ \mathrm{Re}_{d_f}^{0.4} \mathrm{Pr}^{0.37}, \left(1 \le \ \mathrm{Re}_{d_f} \le 40 \right), \\ 0.52 \ \mathrm{Re}_{d_f}^{0.5} \mathrm{Pr}^{0.37}, \left(40 \le \ \mathrm{Re}_{d_f} \le 10^3 \right), \\ 0.26 \ \mathrm{Re}_{d_f}^{0.6} \mathrm{Pr}^{0.37}, \left(10^3 \le \ \mathrm{Re}_{d_f} \le 2 \times 10^5 \right) \end{cases} \tag{5.6}$$

where λ_f is thermal conductivity of the air, Pr is the Prandtl number, Re_{d_f} is the Reynolds number based on the fiber diameter and is calculated as $Re_{d_f} = \left(\frac{u \, d_f \left(1 - exp^{-((1-\varepsilon)/0.04)} \right)}{\varepsilon v} \right)$, d_f is the fiber diameter. The fibre diameter, pore diameter (Kamath et al. (2011, 2013)) and the surface area density calculated for the metal foams used for the simulations are listed in Table 5.2. The surfaces area density calculated for all the metal foams is in good agreement with literature (Kopanidis et al. (2010)).

Table 5.2 Metal foams surface area density

Material	Pore density (PPI)	Fiber diameter d_f (mm)	Pore diameter d_p (mm)	Porosity ε	Surface area density a_{sf} (m^{-1})
Aluminium	10	0.445	4.952	0.95	360.60
	20	0.451	3.416	0.90	960.65
	30	0.216	2.324	0.92	936.38
	45	0.184	1.654	0.90	1671.76
Copper	10	0.687	4.644	0.88	822.83

5.4 RESULTS

5.4.1 Grid Independence Study

A grid size of 56700 nodes is selected for the further computational investigation as it is seen to be optimum in terms of pressure drop and excess temperature compared to other grid sizes. The detail of grid sensitivity study is already discussed in section 3.5 of chapter 3.

5.4.2 Validation of the Numerical Model

The comparison of pressure drop and excess temperature obtained for 10 PPI metal foam filled channel with experimental benchmarks is presented and discussed in section 3.6.

5.4.3 Flow Measurements

The velocity distribution in the channel based on the effect of different key parameters is shown in Figure 5.3. Figure 5.3(a) shows the effect of metal foam porosity and PPI on the velocity distribution of the channel for $H_f = 0.7H$. The velocity of the air in the open region increases as PPI increases and decreases as porosity increases, whereas in the metal foam region the velocity decreases as PPI increases and increases as porosity increases. The velocity in the open region is higher and smaller in the metal foam region for 30PPI metal foam compared to 20PPI metal

foam. This is because the porosity of the 30PPI metal foam is more compared to 20PPI metal foam. Similar results are observed for metal foam thickness of 0.4H and 1H.

The velocity distribution obtained in the present study for 10PPI metal foam is compared with analytical results obtained by Lu et al. (2016) as shown in Figure 5.3 (b). It is evident from the figure that the results of the numerical simulations obtained in this study are in good agreement with the analytical results available in literature.
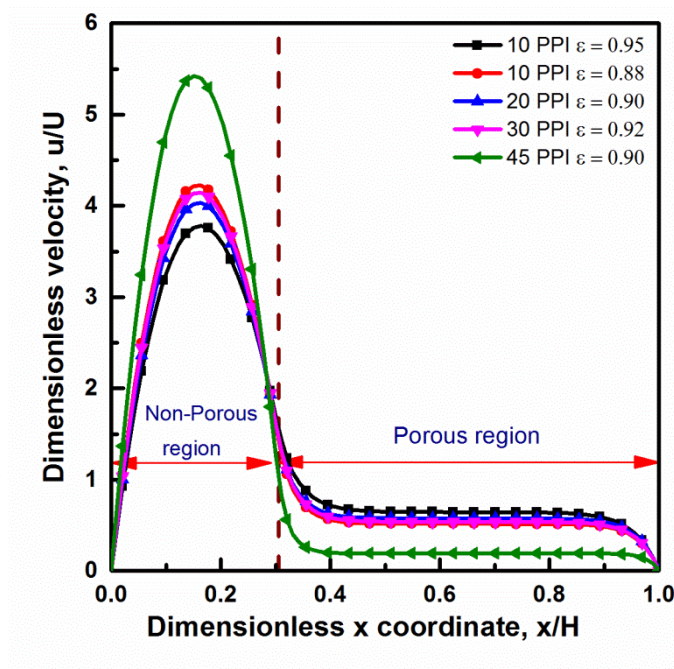
Figure 5.3 (a) Velocity distribution: effect of PPI and porosity on the velocity distribution
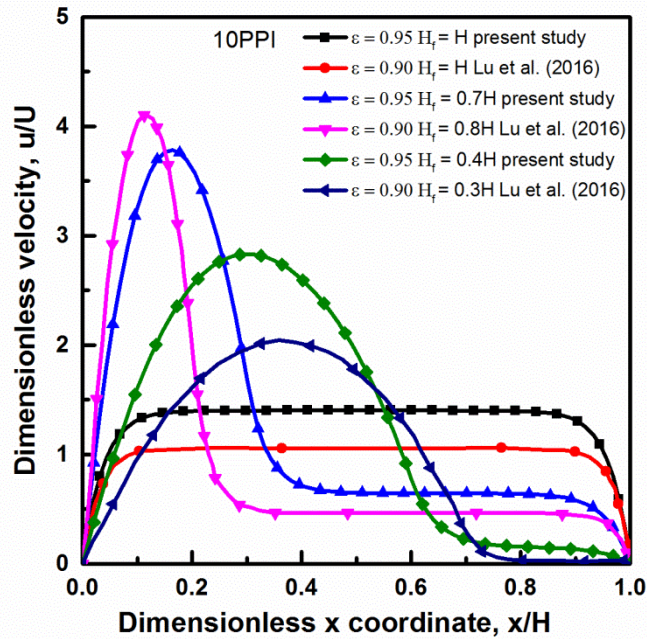
Figure 5.3 (b) Velocity distribution; comparison of effect of dimensionless thickness for 10 PPI metal foam obtained in the present study with analytical benchmarks.

Figure 5.4 shows the variations of pressure drop with respect to the inlet velocity, thickness and PPI of the metal foam in the partly filled channel. The effect of dimensionless thickness of the metal foam on the pressure drop for 10PPI metal foam is shown in Figure 5.4 (a). The pressure drop increases with respect to the increase of fluid inlet velocity for all the thickness of the metal foam. It is clear from the figure that at a particular velocity the pressure drop increases with increase in the metal foam thickness. At a fluid inlet velocity of 1 m/s, the pressure drop for the channel filled with 70% (H_f = 0.7H) 10 PPI metal foam is almost 49% of the completely filled (H_f = H) channel. Similarly, the pressure drop for the channel filled with 40% (H_f = 0.4H) results in 34% and 18% of the 70% (H_f = 0.7H) and completely filled (H_f = H) 10 PPI metal foam channel, respectively. The effect of pore density of the metal foam on the pressure drop for all the metal foams is shown in Figure 5.4 (b). The pressure drop increases as the metal foam PPI increases at a particular velocity for all the thickness of the metal foam. The pressure drop for 30PPI metal foam is smaller compared to 20PPI metal foam because of the porosity of the metal foams as discussed earlier.

61
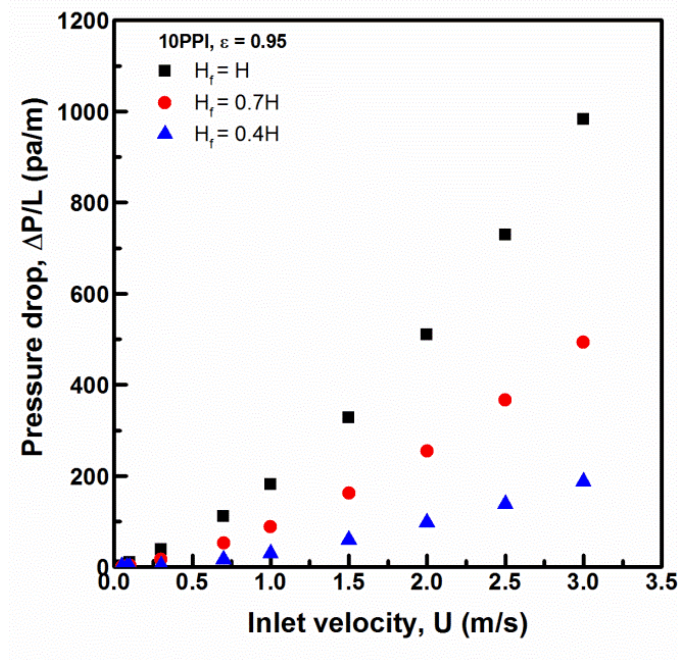
Figure 5.4 (a) Pressure drop: effect of thickness on pressure drop for 10PPI metal foam
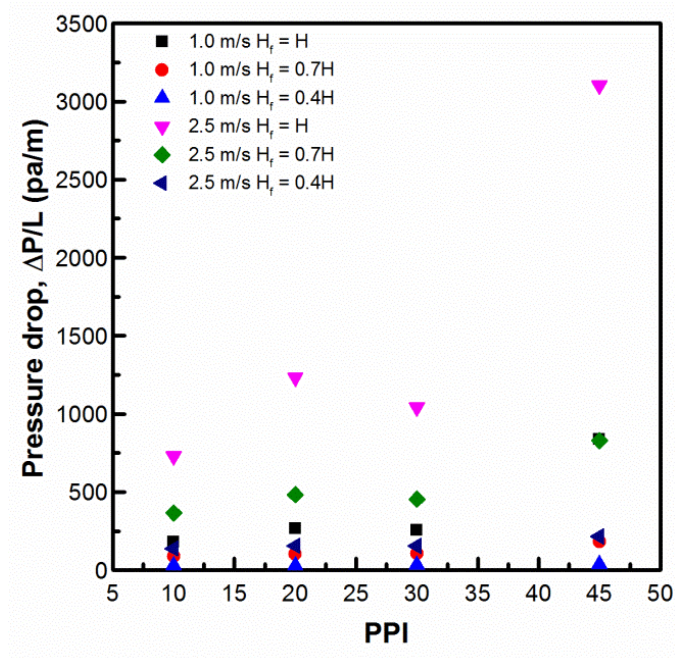
Figure 5.4 (b) Pressure drop: pressure drop variation with respect to metal foam PPI

The friction factor based on hydraulic diameter is calculated for the metal foams and is given by Eq. (5.7)

$$f = \frac{\Delta P}{\left(\frac{L}{D_h}\right)\left(\frac{\rho U^2}{2}\right)} \tag{5.7}$$

Figure 5.5 shows the friction factor variations with respect to the Reynolds number. The friction factor shows a general decrease with respect to Reynolds number for all the metal foam thicknesses. The variations of the friction factor with respect to Reynolds number for 10PPI ($\varepsilon = 0.95$) metal foam for different thicknesses are shown in Figure 5.5 (a). The channel filled with 40% (H_f =0.4H) metal foam shows very less value of friction factor since the pressure drop is low compared to other two thicknesses. Figure 5.5 (b) shows the friction factor variations with respect to Reynolds number for different pore densities. The friction factor increases with the increasing pore density of the metal foam. The metal foam of 45 PPI shows higher friction factor compared to other pore densities since it shows higher pressure drop compared to other PPIs.
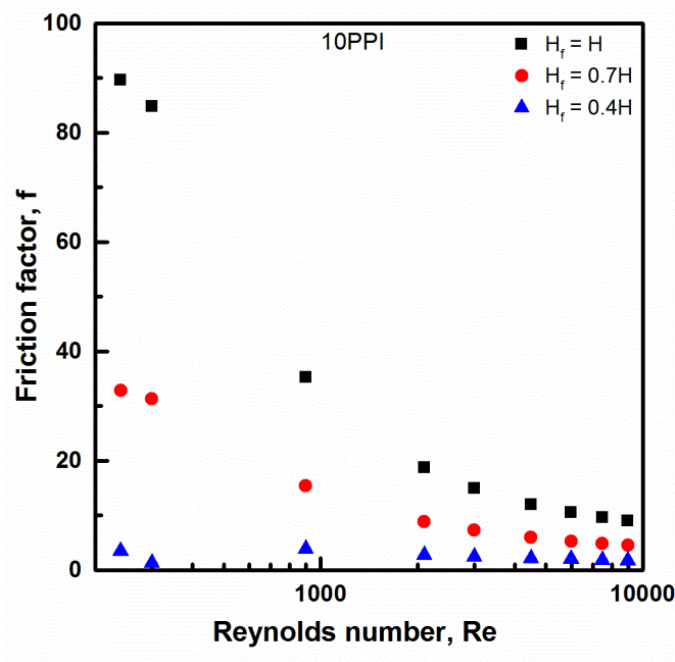
Figure 5.5 (a) Friction factor: effect of metal foam thickness on friction factor for 10PPI metal foam
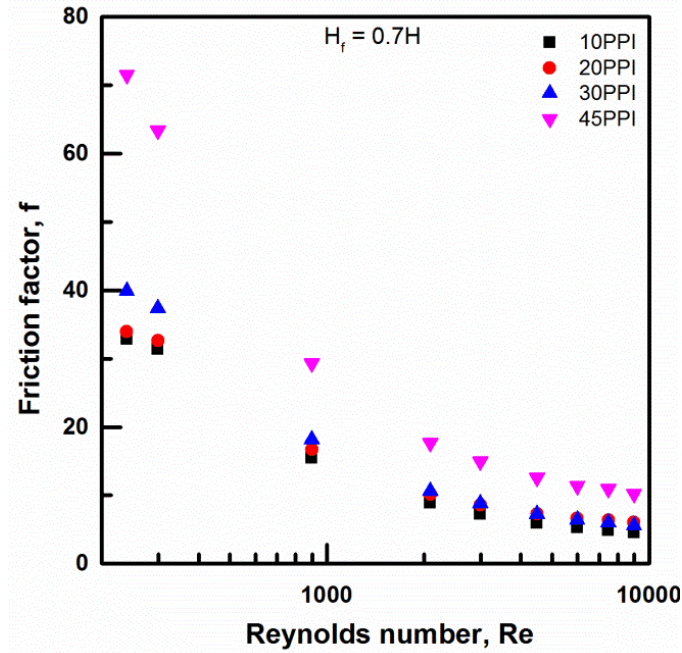
Figure 5.5 (b) Friction factor: effect of metal foam pore density on friction factor

5.4.4 Results of Heat Transfer

In the present study, the metal foam made of aluminium material is considered with a thermal conductivity of 165 W/mK (Kamath et al. (2011)). The wall heat transfer coefficient and Nusselt number are computed from following equations.

Wall Heat transfer coefficient

$$h = \frac{Q}{A\Delta T} \qquad (5.8)$$

Nusselt Number

$$Nu = \frac{hD_h}{\lambda_f} \qquad (5.9)$$

where Q is the total power input to the heater (W), A is the surface area of the aluminum plate attached to the metal foam (m^2), ΔT is the temperature difference between aluminum plate average temperature (T_{avg}) and ambient temperature (T_∞) i.e., ($T_{avg} - T_\infty$), D_h is the hydraulic diameter of the channel (m), λ_f is the thermal conductivity of the air.

The non-dimensional numbers are defined based on the hydraulic diameter of the channel. The Reynolds number, Grashof number and Richardson number are specified as.

64

| Reynolds number | $$Re = \dfrac{VD_h}{\nu}$$ | (5.10) |

| Grashof number | $$Gr = \dfrac{g\beta\Delta TD_h{}^3}{\nu^2}$$ | (5.11) |

| Richardson number | $$Ri = \dfrac{Gr}{Re^2}$$ | (5.12) |

The effect of inlet velocity and pore density of the metal foam on the excess temperature is shown in Fig. 5.6. The temperature excess decreases with increasing inlet velocity of the fluid for all the thicknesses of the metal foam, shown in Fig. 5.6 (a). However, the temperature excess decreases with increasing metal foam thickness in the channel at a particular velocity. Similar type of result is also observed for other PPI metal foams. The temperature difference in general decreases as pore density increases at a particular velocity for all the thicknesses as shown in Fig. 5.6 (b). But the temperature excess increases slightly for 45 PPI metal foam of partially filled channel. This may be due to the fact that the porosity of the 45 PPI (0.90) metal foam is smaller compared to 30PPI metal foam (0.92).
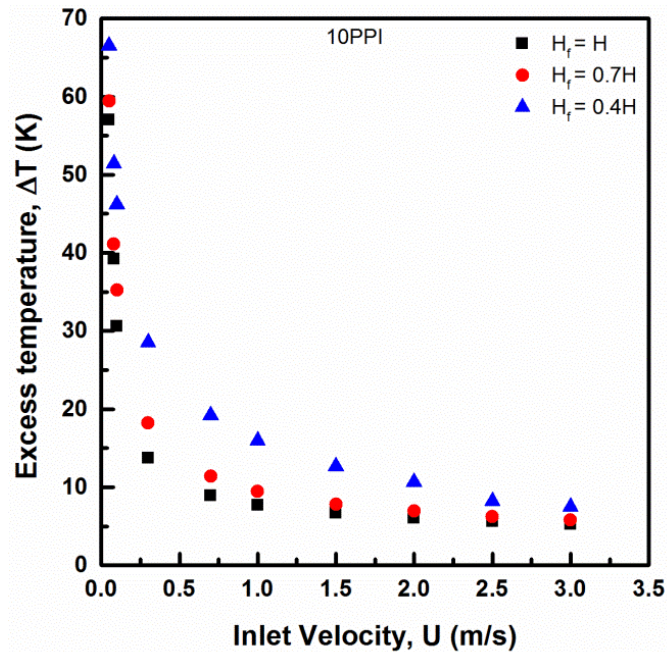
Fig. 5.6 (a). Excess temperature; the effect of metal foam thickness on excess temperature for 10PPI metal foam
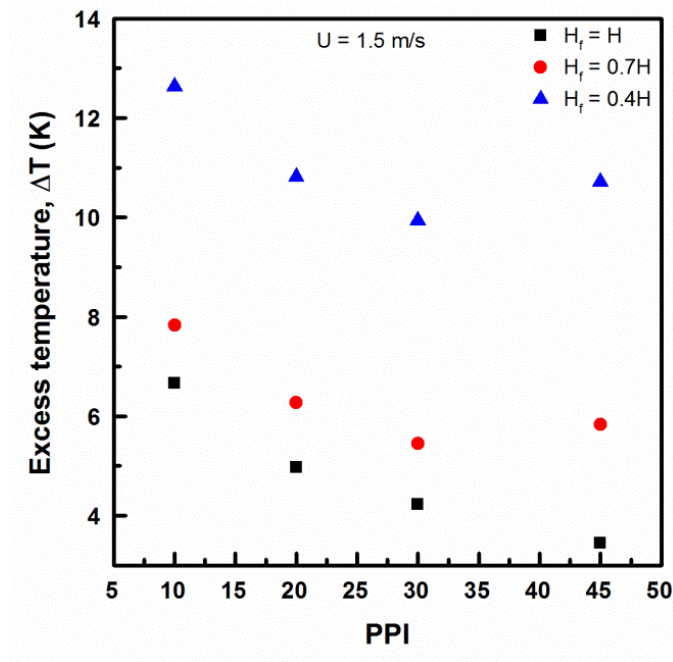
Fig. 5.6 (b). Excess temperature; the effect of PPI on the excess temperature at velocity of 1.5 m/s

The variation of Nusselt number with respect to Reynolds number for 10PPI metal foam and pore density is shown in Figure 5.7. The increase of Nusselt number with the increase of Reynolds number for all thicknesses for 10PPI metal foam is shown in Figure 5.7 (a). The channel completely filled with metal foam case shows a higher Nusselt number compared to partly filled channel. The channel filled with a volume average of 40% and 70% of metal foam predicts average Nusselt number of 62% and 86% compared to completely filled channel case. The slope of the Nusselt number curves changes at Reynolds number of 400, the regime below Re = 400 the variation of Nusselt number is not much significant; so, the regime can be identified as mixed convection regime. When Re is greater than 400, the Nusselt number strongly depends on the Reynolds number so this regime is identified as forced convection regime. Figure 5.7 (b) shows the variations of Nusselt number for the channel filled with 70% metal foam for all the pore densities. Similar results are obtained for 40% filling rate of the channel. The variations of Nusselt number with respect to pore density of the metal foam at a Reynolds number of 3000 is shown in Figure 5.7 (c). The Nusselt number increases as metal foam pore density increases because the

number of fibers increases as PPI increase which in turn increases the interfacial surface area for heat transfer. From the figure it is clear that the 70% filled channel with higher PPI metal foam gives higher heat transfer rate compared to completely filled lower PPI metal foam. For example, at Re=3000, the 20 PPI metal foam with 70% filling rate and 10 PPI completely filled channel provide almost the same heat transfer rate; whereas, 70% filled 30 PPI metal foam gives 1.12 times higher heat transfer compared to completely filled 10 PPI and 70% filled 20 PPI metal foam. The pressure drop obtained for 70% filled 30 PPI metal foam is 41% lesser compared to completely filled 10 PPI metal foam case. This proves that partly filled channel with higher PPI metal foam can be used for the enhancement of heat transfer with minimum pressure drop.
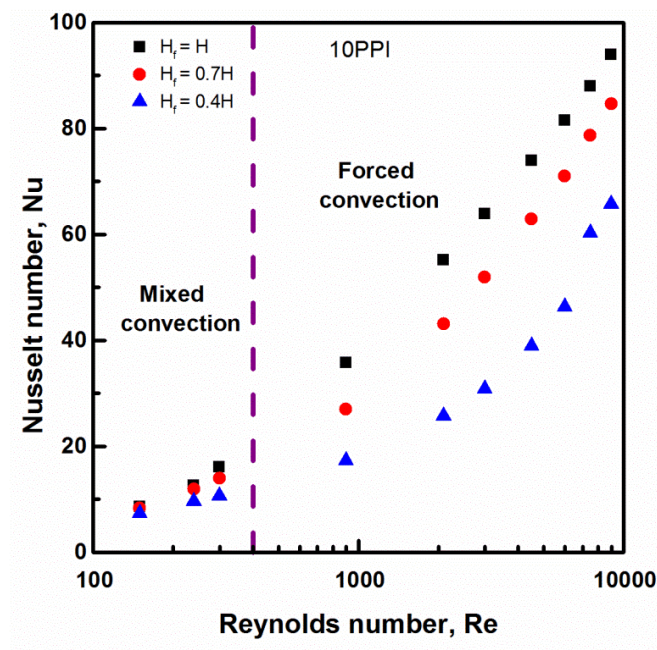
Figure 5.7 (a) Average Nusselt number: Nusselt number variations with Reynolds number for different thicknesses of 10PPI metal foam
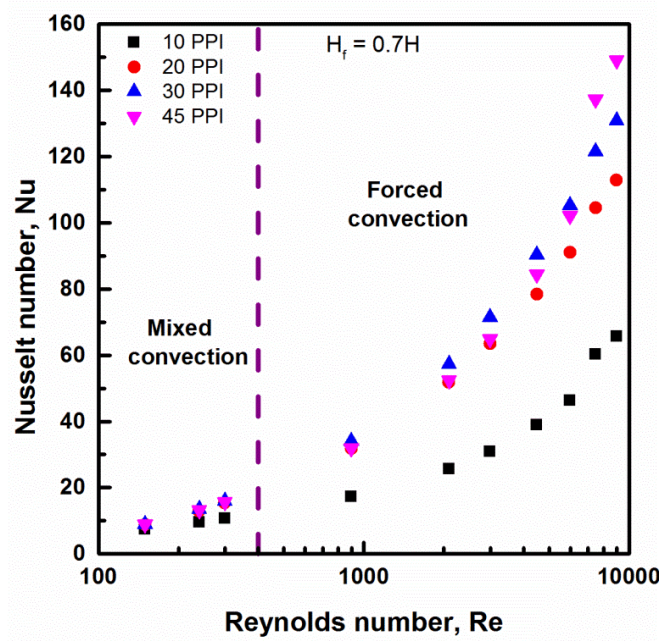
Figure 5.7 (b) Average Nusselt number: Nusselt number variations for all PPI metal foams completely filled case
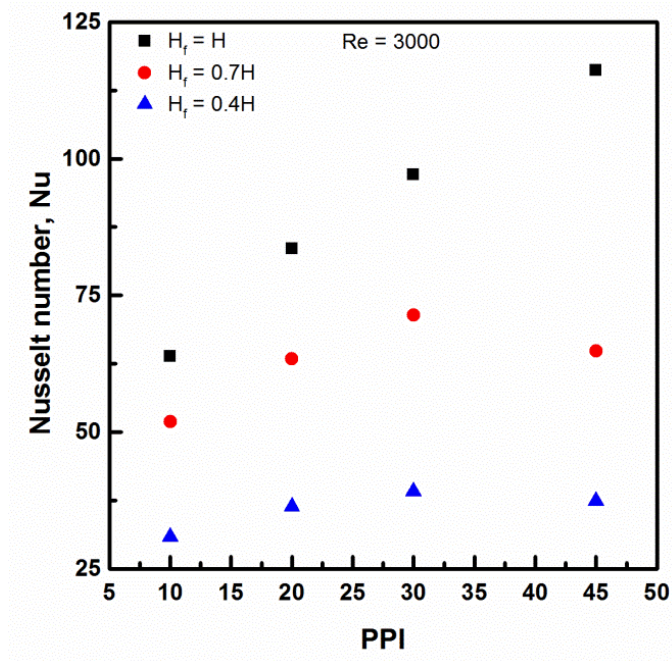
Figure 5.7 (c) Average Nusselt number: the effect of PPI on Nusselt number for all the thicknesses at Re = 3000.

Figure 5.8 shows the effect of Richardson number on the Nusselt number for 10PPI metal thickness and for different pore densities of the metal foam. The Nusselt number decreases with increasing Richardson number for all the thicknesses of the metal foams studied and such a result is shown in Figure 5.8 (a) for a representative case of 10 PPI metal foam. The region in which the Nusselt number is strong dependent on the Richardson number is identified as forced convection region and it occur when the Richardson number is less than 1. When the value of Richardson number is greater than 1, the Nusselt number is not dependent on the Richardson number, this regime is recognized as mixed convection regime. The Nusselt number variations with respect to Richardson number for different pore densities are shown in Figure 5.8 (b). Forced and mixed convections for different pore densities are also clearly seen from this plot. At a particular Richardson number, the Nusselt number increases with increasing pore density of the metal foam.
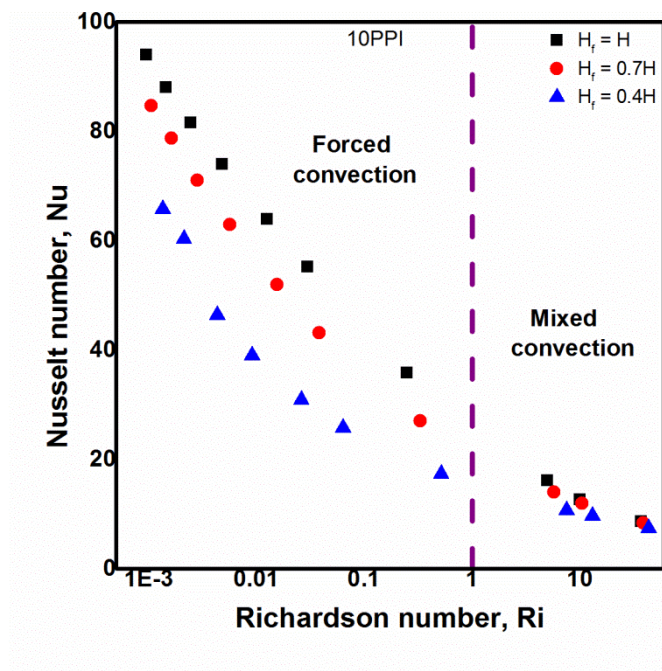
Figure 5.8 (a) Average Nusselt number: Nusselt number variations with Richardson number for different thicknesses of 10PPI metal foam
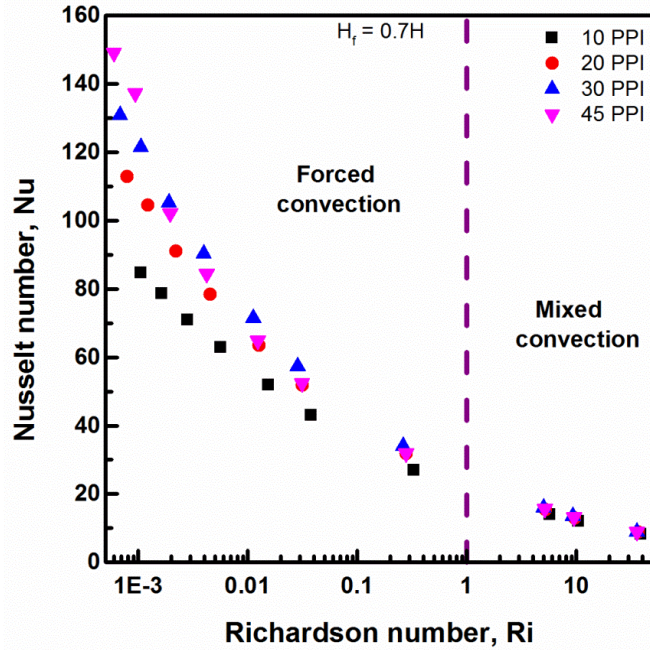
Figure 5.8 (b) Average Nusselt number: the effect of PPI on Nusselt number for $H_f =$ 0.7H.

The thermal performance of a heat exchanging device can be calculated by using Colburn j factor which is given in Eq. (5.13)

$$j = St.Pr^{\frac{2}{3}} \qquad (5.13)$$

Figure 5.9 shows the variation of Colburn j factor with respect to the Reynolds number. The Colburn j factor shows a general decrease with increasing flow rate for all the thicknesses of 10PPI metal foams considered for the present study and the result is shown in Figure 5.9 (a). The channel completely filled with the metal foam shows higher value of Colburn j factor compared to the partially filled cases but all the thicknesses give higher thermal performance in the lower flow rates as noticed from the study. A similar type of tendency is observed in the metal foams as well as other porous mediums reported in literature (Boomsma et al. (2003)). As the thermal performance increases with increasing thickness of the metal foams, 70% partly filled (Hf = 0.7H) case gives same performance as completely filled (Hf = H) channel at higher Reynolds number. Figure 5.9 (b) shows the variations of Colburn j factor with respect to Reynolds number for different pore densities. It is clear from the plot that

30PPI metal foam gives higher thermal performance compared to other PPI metal foams.
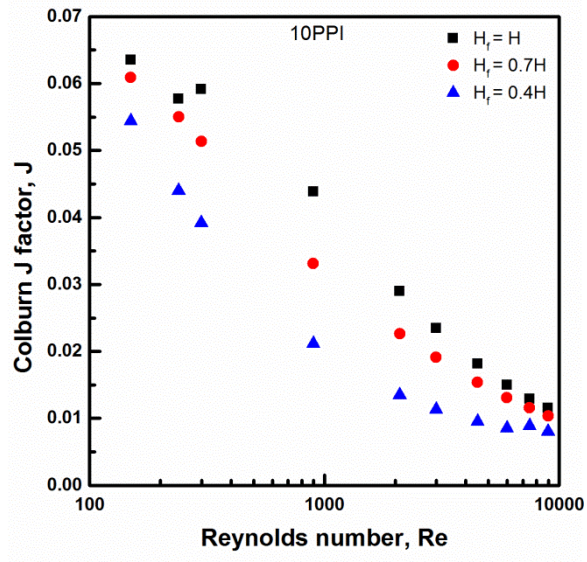
Figure 5.9 (a) Colburn j factor variations with Reynolds number; for 10PPI metal foam thicknesses
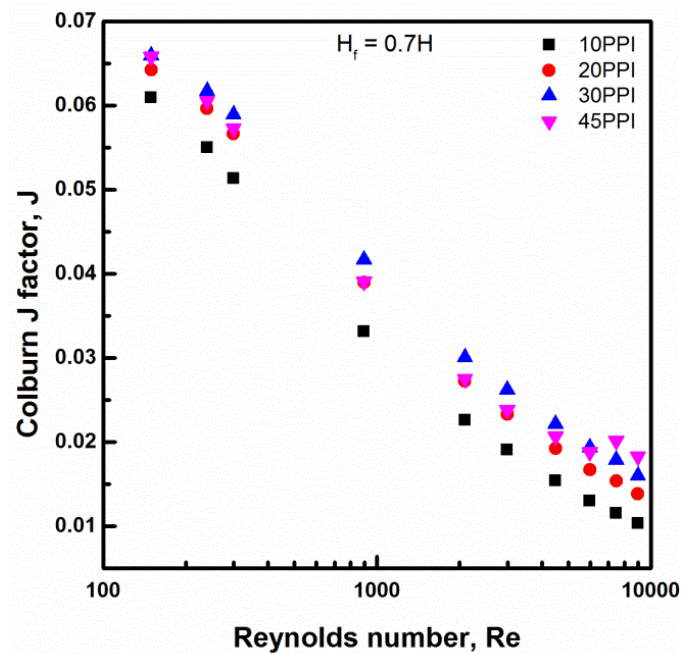
Figure 5.9 (b) Colburn j factor variations with Reynolds number; for different pore densities of 0.7H thickness.

The overall performance of the metal foams can be analysed by using a performance factor, which compares the heat transfer coefficient to the pumping power of the fluid, as mentioned by Manglik (2003) and is given by Eq. (5.14)

$$\lambda_p = \frac{j}{f^{\frac{1}{3}}} \qquad (5.14)$$

Figure 5.10 shows the performance factor (λ_p) variations with respect to Reynolds number for various thicknesses of 10PPI metal foam and for different pore densities of 0.7H thickness. The performance factor shows overall decrease with the increasing flow rates for all the pore densities and for all the thickness studied. Figure 5.10 (a) shows the performance factor for 10PPI metal foam. At lower Reynolds number, the partly filled channel gives higher performance compared to completely filled metal foam channel, whereas at higher Reynolds number the completely filled channel gives higher performance compared to partly filled one. The performance of the partly filled channel with thickness $H_f = 0.7H$ is the same as that of $H_f = H$ for all the Reynolds number considered. From this, it is clear that the partly filled channel with thickness $H_f = 0.7H$ is better since the pressure drop reduces almost 50% compared to the completely filled channel. The variation of performance factor for different pore densities of the metal foams for the thickness of $H_f = 0.7H$ is shown in Figure 5.10 (b). The performance factor decreases with the increasing flow rates for all the pore densities studied. The 30PPI metal foam gives higher performance among all the PPIs studied for all the thicknesses.
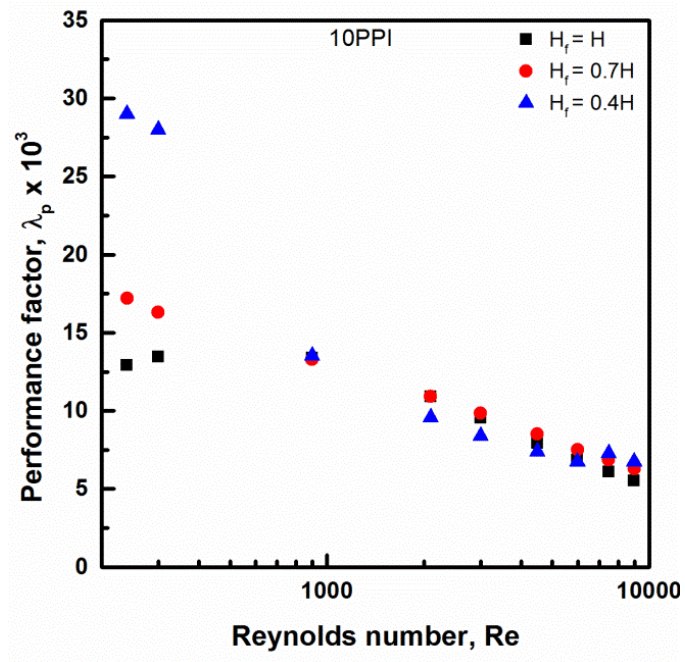
Figure 5.10 (a). Variations of performance factor with Reynolds number; for 10PPI metal foam thicknesses
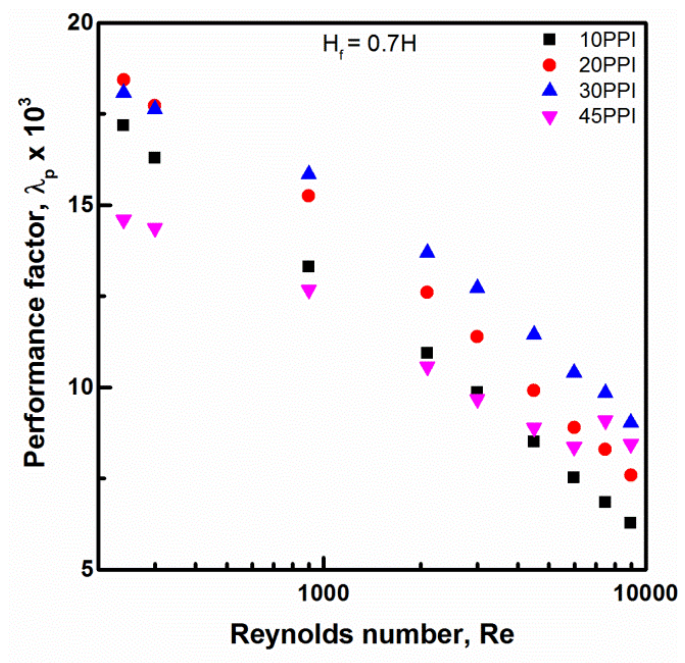
Figure 5.10 (b) Variations of performance factor with Reynolds number; for different pore densities of 0.7H thickness.

5.4.5 Effect of porosity and thermal conductivity

To compare the flow and thermal performance of different materials of the metallic foams, the numerical simulation is carried out for 10PPI copper metal foam which is having a porosity of 0.88. The characteristics of copper metal foam were also given in Table 5.1 and 5.2. The copper metal foam of 10 PPI is compared with same pore density (10 PPI) aluminium metal foam having a porosity of 0.95.

The variation of Nusselt number with respect to Reynolds number for both the aluminium and copper metal foams is shown in Figure 5.11. The Nusselt number increases with the increasing flow rate for both the thicknesses as well as both the metal foams. The copper metal foam shows higher Nusselt number for each thickness compared to aluminium metal foam. The variation of Nusselt number among the metal foams is not much significant at low Reynolds number but there is a significant change at high flow rates.
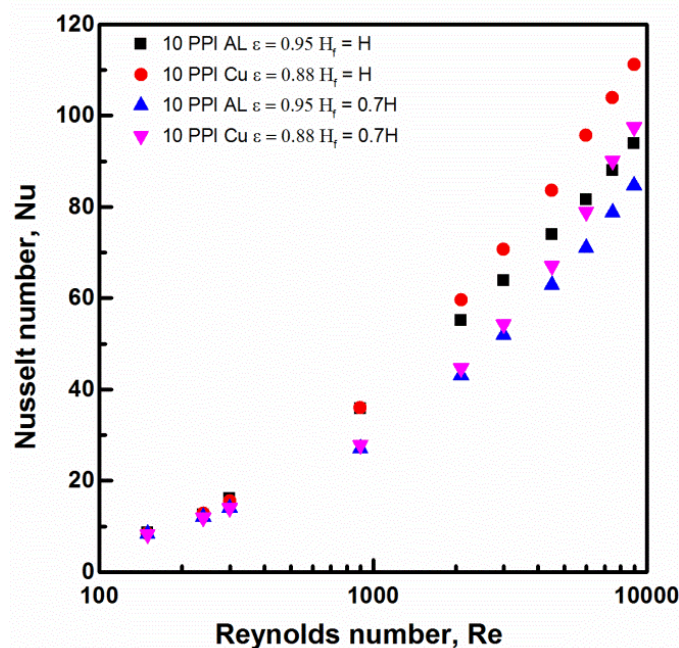
Figure 5.11 Comparison of Nusselt number variations with Reynolds number for 10PPI aluminium and copper metal foams

The variations of Colburn j factor and Performance factor with respect to Reynolds number for both aluminium and copper metal foams are shown in Figure 5.12. The

Colburn j factor decreases with increasing fluid flow rate. The copper metal foam gives better performance compared to aluminium metal foam. The performance factor also decreases with increasing flow rates for both the metal foams. At lower flow rates the aluminium metal foam gives higher thermal performance compared to the copper metal foam. Whereas, at higher flow rates the aluminium and copper metal foams give the same thermal performance for the range of Reynolds studied.
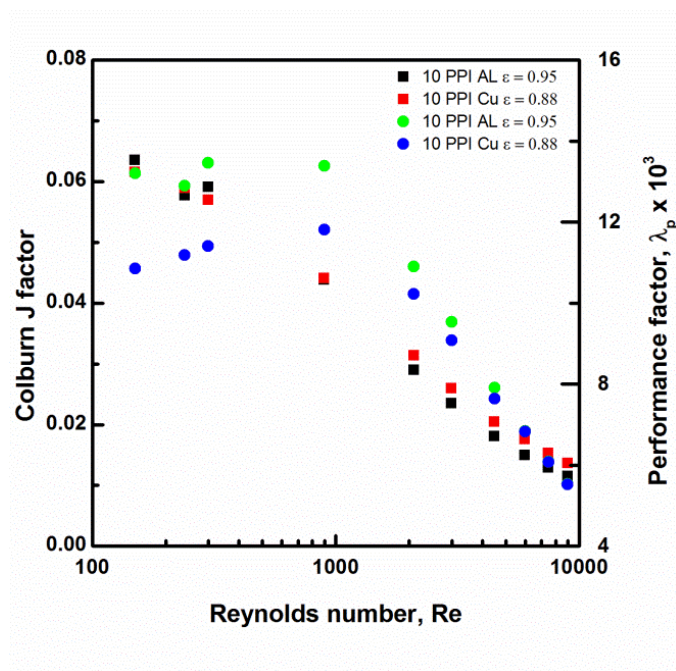
Figure 5.12 Comparison of Colburn j factor and Performance factor with Reynolds number for 10PPI aluminium and copper metal foams

5.5 CONCLUSIONS

In this chapter, the numerical simulations of mixed convection heat transfer through metal foams partially filled in a vertical channel were carried out by using commercially available ANSYS Fluent 15.0 software. In this study different types of metal foam material and three different partial filling of the metal foams have been considered. The velocity distributions predicted in the foam free region and foam region are in good agreement with the analytical results. Some of the concluding remarks are as follows.

- The velocity in the foam free region and the pressure drop in the channel increase as the metal foam filling rate increases and also they both increase with increase in metal foam PPI for each thickness. The pressure drop obtained for the filling rate of 70% ($H_f = 0.7H$) is almost an average of 50% of the completely filled case for 10 PPI metal foam. So, the pumping power required for the fluid flowing through the channel thereby reduces to 50%. Similarly, the 40% ($H_f = 0.4H$) filling rate gives an average of 34% of the 70% ($H_f = 0.7H$) filling rate and an average of 18% of the completely filled ($H_f = 1H$) 10 PPI metal foam channel. It is evident from the results that the pumping power required for the fluid increases as filling rate increases.

- The heat transfer rate increases with increasing filling rate as well as increases with increase in metal foam PPI for each thickness studied. The channel filled with 70% ($H_f = 0.7H$) and 40% ($H_f = 0.4H$) 10 PPI metal foam predicts an average heat transfer rate of 86% and 62% of the completely filled channel, respectively. At Re=3000, the 70% filled 30 PPI metal foam gives 1.12 times higher heat transfer rate compared to completely filled 10 PPI and 70% filled 20 PPI metal foam with lesser pressure drop. The pressure drop obtained for 70% filled 30 PPI metal foam is 41% lesser compared to completely filled 10 PPI metal foam case. This proves that partly filled channel with higher PPI metal foam can be used for the enhancement of heat transfer with minimum pressure drop.

- Based on the comparison of Colburn j factor and overall performance factor, 30 PPI metal foam with 70% filling rate can be used for enhancement of heat transfer with lower pressure drop.

5.6 CLOSURE

This chapter explained the detailed description of the prediction of mixed convection heat transfer through the partially filled metal foam in the vertical channel. Three different filling rates of the metal foams were considered in the numerical study. The metal foam thickness and thermal conductivity effect on flow and heat transfer characteristics are explained in the next chapter.

CHAPTER 6

EFFECT OF THICKNESS AND THERMAL CONDUCTIVITY OF METAL FOAMS FILLED IN A VERTICAL CHANNEL

6.1 INTRODUCTION

In this chapter the effect of thickness and thermal conductivity of highly porous metal foams filled in a vertical channel is studied numerically. Three different thicknesses and two different materials of the metal foam are considered for the present analysis to see the effect on hydrodynamic and thermal performance.

6.2 PROBLEM STATEMENT

The numerical model consists of a heater sandwiched between two aluminium plates that are placed inside a vertical channel. Metal foams are placed on both sides of the aluminium plate as shown in Figure 6.1. The dimensions of the aluminium plates are 250 x 150 x 3 (all in mm). High thermal conductivity metal foams such as aluminium and copper with thicknesses of 10, 20 and 30 (all in mm) are considered for the flow and thermal analysis. The dimensions of the channel considered in this study are referred from Kamath et al. (2011).

The porosity of the metal foams considered for the present simulations varies from 0.85 to 0.95. Table 6.1 shows the properties of the metal foams considered for the present study. The uncertainties in the measured values of the permeability and the drag coefficient are also reported in Table 6.1.

6.3 BOUNDARY CONDITIONS

From Figure 6.1 it is clear that the vertical channel is symmetry about the Y axis, hence only one half of the vertical channel is considered for computations. A two dimensional computational domain which consists of the heater, the aluminium plate and the metal foam filled on one side of the plate is shown in Figure 6.2. The inlet and outlet of the channel are defined with velocity and pressure, respectively. The heater side of the plate is assigned with the heat flux boundary condition and all side walls of

the channel are set to adiabatic boundary conditions. The channel is symmetric about the vertical axis; therefore, symmetry boundary is assigned to the axis.
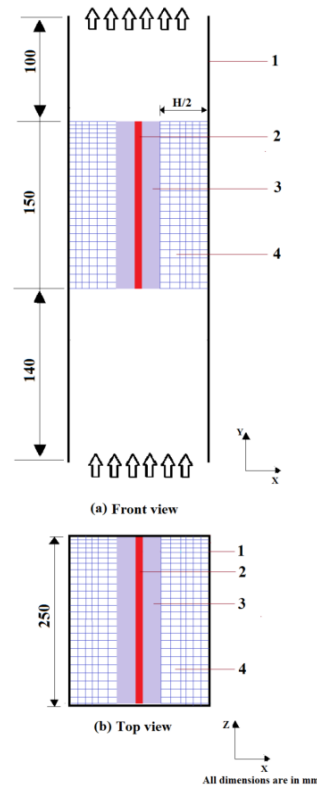
Figure 6.1 Computational domain of the vertical channel filled with metal foam (1) side wall of the channel (2) heater (3) aluminium plate (4) metal foam

Table 6.1 Properties of metal foams considered in the present study (Kamath et al. (2013))

Sample	L x W x H/2 mm^3	Porosity	Permeability 10^7, m^2	Uncertainty %	Form drag coefficient, m^{-1}	Uncertainty %
Aluminum 10 PPI	250x150x10	0.9481	2.480	±7.95	94.98	±2.45
	250x150x20	0.9417	6.706	±29.90	167.56	±3.34
	250x150x30	0.9449	3.304	±10.0	197.09	±1.85
Copper 10 PPI	250x150x10	0.8769	1.742	±19.20	176.75	±4.60
	250x150x20	0.8596	4.779	±23.24	225.48	±2.20
	250x150x30	0.8683	1.819	±11.61	248.60	±2.25

Figure with labels:

$P = 0, \frac{\partial U}{\partial y} = 0, \frac{\partial V}{\partial y} = 0$
Pressure outlet

Symmetry
$\frac{\partial T}{\partial x} = 0, U = 0, \frac{\partial V}{\partial x} = 0$

Adiabatic wall
$U = V = 0, \frac{\partial T}{\partial x} = 0$

Heat flux $\frac{Q}{A} = -K_s \frac{\partial T}{\partial x}$

Symmetry
$\frac{\partial T}{\partial x} = 0, U = 0, \frac{\partial V}{\partial x} = 0$

Velocity inlet
$U = 0, V = V_\infty, T = T_\infty$
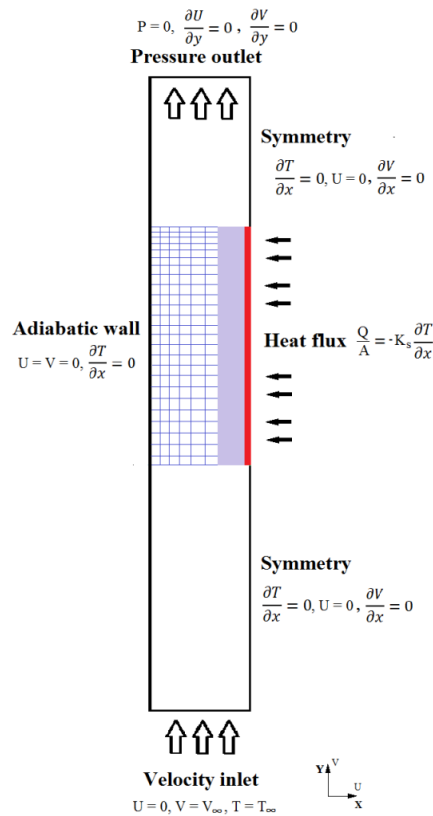
Figure 6.2 Computational domain and boundary conditions

6.4 NUMERICAL SIMULATIONS

The details of governing equations and numerical parameters are same as discussed in section 3.4 of chapter 3.

The surface area density (a_{sf}) and the interfacial heat transfer coefficient (h_{sf}) for the metal foams used for the present simulations are calculated based on the equations proposed by Calmidi and Mahajan (2000) and Zukauskas (1987), respectively. Table 6.2 represents the surface area density based on the fibre diameter, pore diameter and porosity (Kamath et al. (2013)). The surface area density calculated for the metal foams is in agreement with literature (Kopanidis et al. (2010)).

Table 6.2 Metal foams surface area density

Sample	Thickness mm	Fiber diameter d_f (mm)	Pore diameter d_p (mm)	Porosity	Surface area density a_{sf} (m^{-1})
Aluminium 10 PPI	10	0.445	4.952	0.9481	360.60
	20	0.526	4.982	0.9417	440.25
	30	0.488	4.967	0.9449	400.53
Copper 10 PPI	10	0.687	4.644	0.8769	822.83
	20	0.703	4.732	0.8596	824.72
	30	0.695	4.688	0.8683	824.49

6.5 RESULTS AND DISCUSSION

6.5.1 Grid Independence Study

In the present study, three different thicknesses and two different metal foams are considered for the simulations. Grid independency study is carried out for each thickness in order to determine the optimal size of the mesh. The number of nodes considered for the grid independency study for each thickness of the metal foam is listed in Table 6.3. The deviation in pressure and temperature is reported for an inlet velocity of 1 m/s and the heat input of 20W.

Based on the grid independence study, the optimum grids are highlighted in Table 6.3 for three different thicknesses of the metal foams. Grid sizes of 56700, 66740 and 95410 are found to be optimum for 10 mm, 20 mm and 30 mm respectively.

Table 6.3 Results of the grid independence study for aluminium metal foam

Thickness	Cells	Pressure drop (ΔP)	Temperature difference (ΔT)	Deviation (%)	
				|ΔP|	|ΔT|
	26130	27.60	7.74	0.22	0.94
10 mm	**56700**	27.56	7.70	0.07	0.42
	88400	27.54	7.66	Base Line	
	46020	19.98	6.99	0.06	0.60
20 mm	**66740**	19.96	6.96	0.07	0.17
	105000	19.97	6.95	Base Line	
	57330	25.07	6.88	0.18	0.39
30 mm	**95410**	25.09	6.88	0.10	0.27
	147600	25.12	6.86	Base Line	

6.5.2 Validation of Numerical Results

6.5.2.1 Pressure drop

The variation of pressure drop with respect to the inlet velocity of the fluid for 10 mm thick aluminium metal foam is shown in Figure 6.3. The results of pressure drop obtained in the present study are compared with the experimental data of Kamath et al. (2011). Comparison is done for the velocity range of 0.05 – 3 m/s and the results of the present simulations are in reasonable agreement with the results reported in Kamath et al. (2011). The pressure drop increases as the inlet velocity increases for the metal foam.
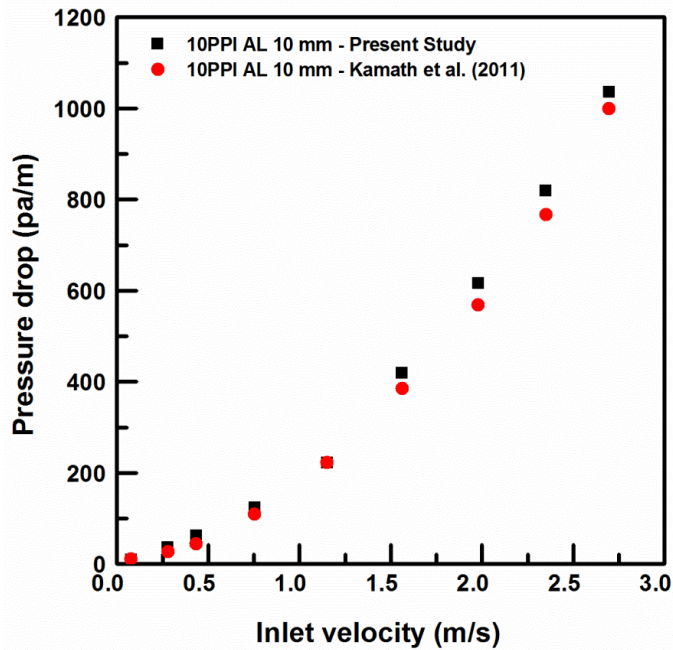
Figure 6.3 Pressure drop comparison with experimental benchmarks for 10 mm metal foam

6.5.2.2 Excess temperature

The excess temperature obtained for the clear channel case and 10 mm thick 10 PPI aluminium metal foam is compared with the experimental results of Kamath et al. (2011) and is shown in Figure 6.4. An excellent matching between simulations and experiments is noticed for the heat input of 20W. In case of very low velocities, a large deviation is seen between the experiments and simulations; however, this deviation reduces as the inlet velocity increases. The figure also shows the comparison of LTE and LTNE thermal models with the experimental benchmarks. The LTE thermal model is under predicting the excess temperature compared to experimental results; whereas, the excess temperature predicted by LTNE thermal model is agreeing well with the experimental results. It is clear that the LTNE thermal model is found suitable for predicting heat transfer through the metal foams compared to LTE model.
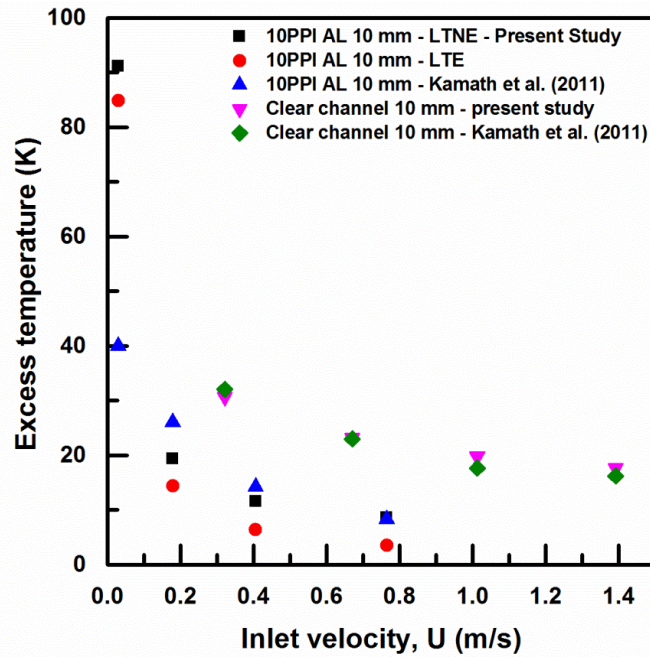
Figure 6.4 Comparison of temperature difference for 10 mm thick metal foam

For the purpose of validation of the present methodology, numerical results of pressure drop and excess temperature are compared with the experimental results reported in literature. Therefore, this analysis serves as the validation of the present study.

6.5.3 Flow Measurements

The variation of the pressure drop with respect to the inlet velocity of the fluid for the aluminium and the copper metal foams are shown in Figure 6.5 and Figure 6.6 respectively. The pressure drop in the channel increases with increasing thickness of the metal foam as expected for both the aluminium and the copper metal foams. All aluminium metal foams are having almost same porosity, so the pressure drop variation with the foam thickness is not much significant. At lower velocities the pressure drop for all the thicknesses is almost same but it varies as velocity increases. The metal foams having thickness of 30 mm show higher pressure drop compared to the other two thicknesses for both the metal foams. The copper metal foam shows higher pressure drop compared to the aluminium metal foam because of the lower porosity value.
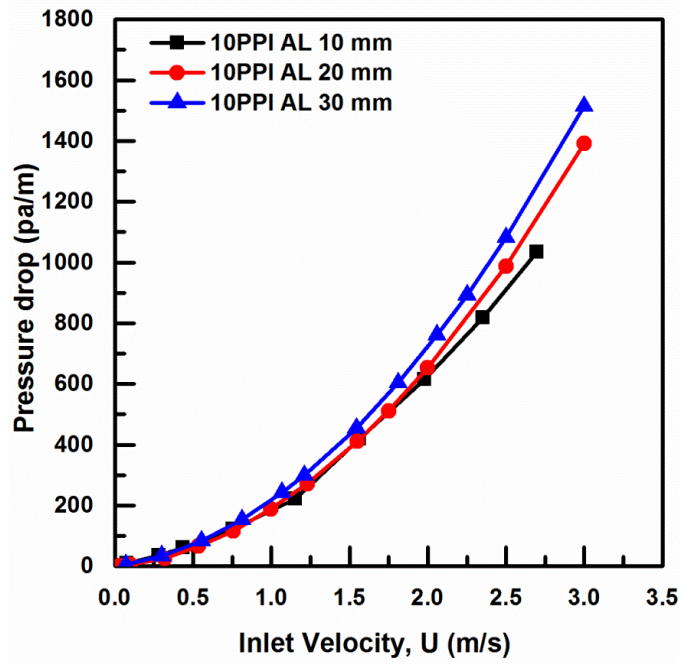
Figure 6.5 variation of pressure drop for aluminum metal foams
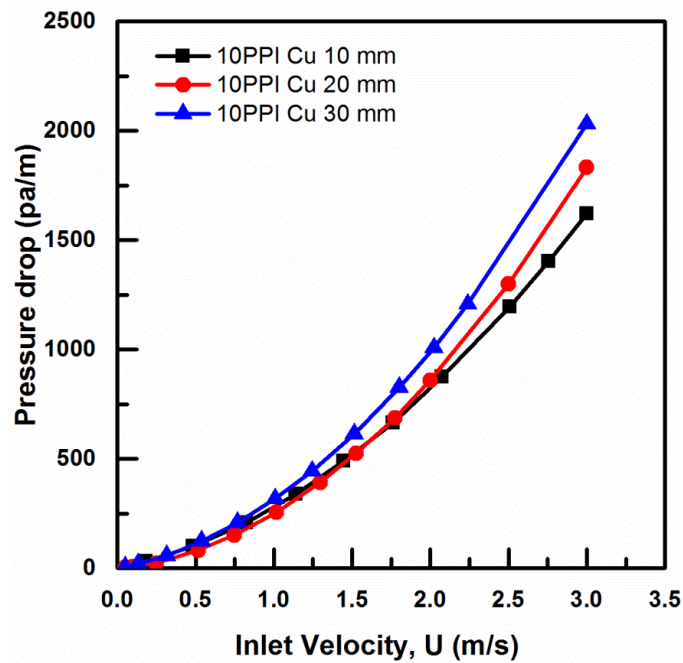
Figure 6.6 variations of pressure drop for copper metal foams

Equation (6.1) represents thickness based friction factor for the metal foam

$$f = \frac{\Delta P}{\left(\frac{L}{H}\right)\left(\frac{\rho U^2}{2}\right)} \qquad (6.1)$$

Friction factor calculated for different Reynolds number is shown in Figure 6.7. As seen from figure the friction factor for both the metal foams decreases with increasing Reynolds number and is higher for 30 mm copper metal foam because the pressure drop is more as seen in Figure 6.6. As metal foam thickness increases the number of fibre ligaments increases that obstructs the flow which in turn increases the friction factor.
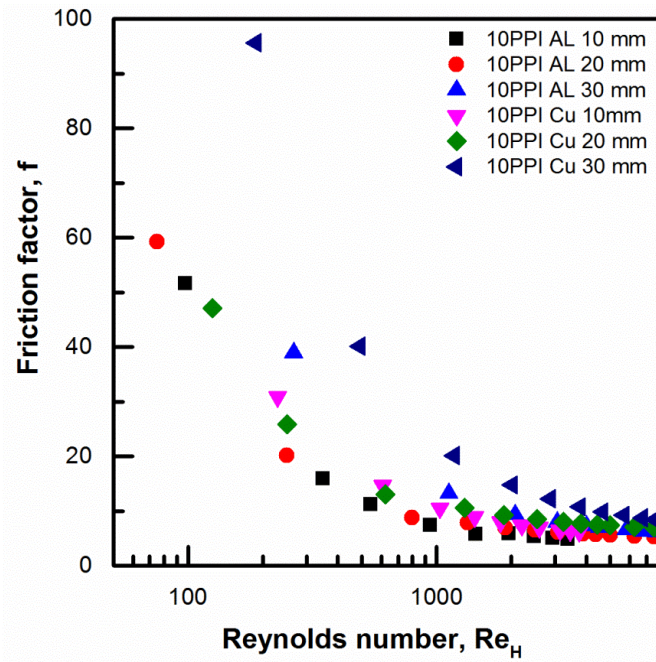
Figure 6.7 Friction factor variation with Reynolds number

The friction factor for aluminium and copper metal foams of 10 mm thickness is compared with the other porous medium available in literature to check the robustness of the present simulations and is shown in Figure 6.8. Table 6.4 shows the type of porous medium and its properties used for the present simulations. The friction factor is calculated based on the thickness of the metal foam. The numerical results match very well with the experimental results available in literature.

Table 6.4 Details of porous medium used for comparison

	Type of porous media	Thickness (mm)	Porosity
Kamath et al. (2011)	45 PPI Aluminum foam	10	0.90
Kamath et al. (2013)	10 PPI Copper foam	10	0.86
Tian et al. (2004)	Copper wire screens	10	0.80
Kim et al. (2004)	Aluminum lattice frame material (LFM)	10	0.94
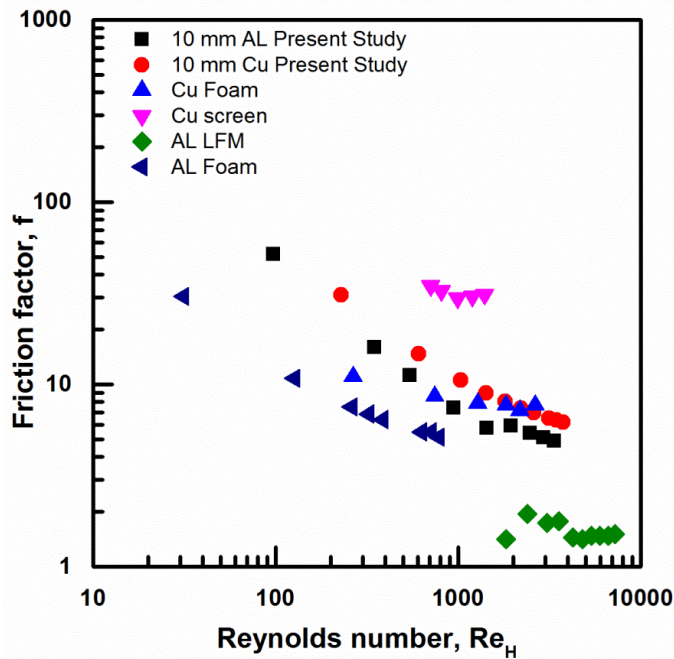
Figure 6.8 Friction factor of the present study compared with other porous medium

6.5.4 Results of Heat Transfer

The thermal conductivity of the aluminium and the copper metal foams is considered to be 165 and 380 W/mK, respectively (Kamath et al. (2013)). The power input to the heater is equally divided to both sides of the aluminium plates because of the fact that the heater is sandwiched between them. Therefore, the computations are performed

for only one half of the channel. Equations (6.2) and (6.3) are used to calculate wall heat transfer coefficient and Nusselt number.

Wall heat transfer coefficient

$$h = \frac{Q}{A\Delta T} \qquad (6.2)$$

Nusselt number

$$Nu = \frac{hH}{\lambda_f} \qquad (6.3)$$

where Q is the input power to the heater, A is the aluminium plate surface area exposed to the metal foam (m^2), ΔT is the temperature difference between average temperature of the aluminium plate (T$_{avg}$) and ambient temperature (T$_\infty$) i.e., (T$_{avg}$ − T$_\infty$), H is the total thickness of the metal foam (m), λ_f is the thermal conductivity of the fluid.

The non-dimensional Reynolds number given in Eq. (6.4) is defined based on the total thickness of the metal foam and the properties of air are taken at an inlet temperature of 30°C.

Reynolds number

$$Re = \frac{UH}{\nu} \qquad (6.4)$$

Figure 6.9 shows the variation of the temperature difference with respect to the inlet air velocity for three different heat inputs for aluminium metal foam of 10 mm thickness. The temperature difference decreases with increasing flow rate for all three heat inputs considered for the numerical simulations. The variation of the heat transfer coefficient with respect to the velocity of the fluid for 10 mm aluminium metal foam is shown in Figure 6.10. The heat transfer coefficient increases with increasing inlet velocity of the fluid for all the heat inputs. But, the heat transfer coefficient remains constant at a particular inlet velocity for different heat inputs (Calmidi and Mahajan (2000)).
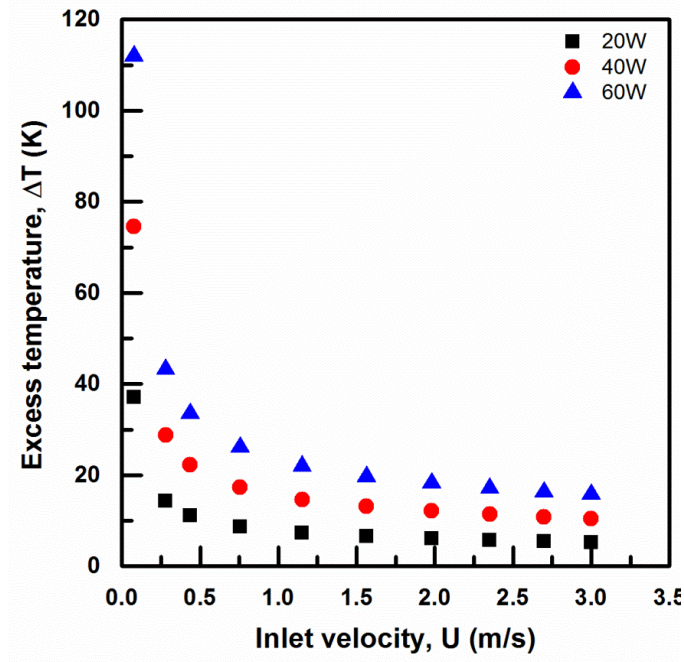
Figure 6.9 Temperature excess variation with fluid inlet velocity for three heat inputs
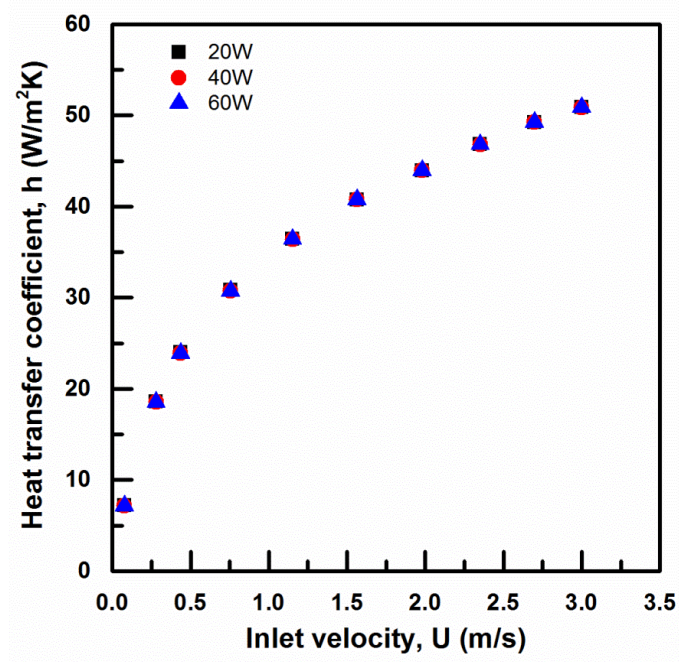
Figure 6.10 Heat transfer coefficient variations for aluminium metal foam of 10 mm thickness

The variation of average Nusselt number for the aluminium and the copper metal foams with respect to the Reynolds number is shown in Figure 6.11 and Figure 6.12. The Nusselt number increases as Reynolds number increases and further, it has been noticed that the presence of metal foams enhances heat transfer compared to the clear channel. The heat transfer rate for copper metal foams is higher compared with aluminium metal foams in the range of Reynolds number studied. Due to the presence of metal foams, the average increase in heat transfer for the aluminium was observed to be 2 times higher than the clear channel and for the copper metal foam it was 2.8 times higher than the clear channel for a thickness of 10 mm. Also, the copper metal foam gives 1.34 times higher heat transfer compared to the aluminium metal foam for the same thickness. As the metal foam thickness increases, the performance of both the metal foams becomes the same.
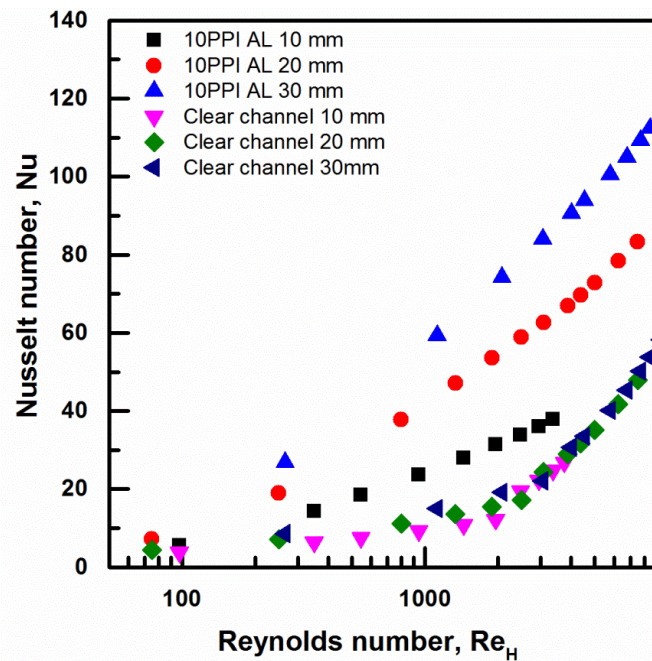
Figure 6.11 Nusselt number variation with Reynolds number for aluminium metal foams
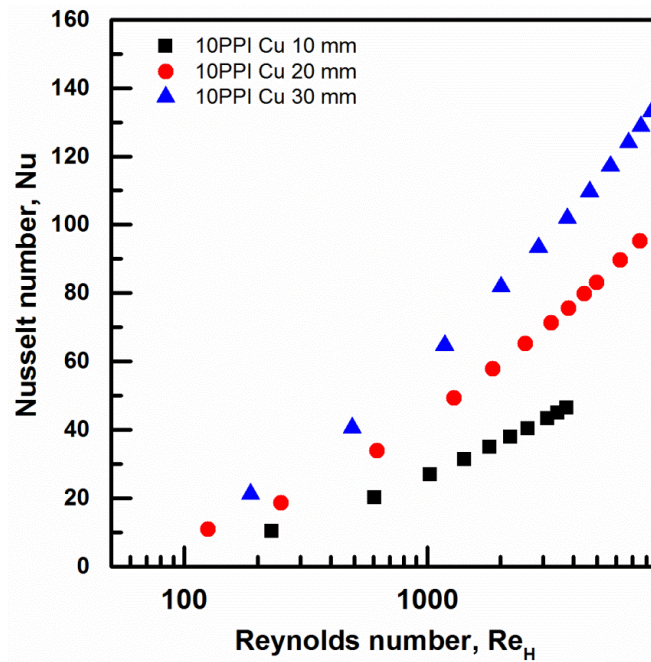
Figure 6.12 Nusselt number variations with Reynolds number for copper metal foams

The thermal performance of a heat exchanging device is presented in terms of Colburn j factor and is given by Eq. (6.5)

$$j = St. Pr^{\frac{2}{3}} \qquad (6.5)$$

The Colburn j factor variations with respect to Reynolds number is shown in Figure 6.13. Colburn j factor decreases with increasing flow rate for all the metal foams considered for the present study. Similar trends are also observed in other porous mediums and foams as reported in literature (Venugopal et al. (2010), Tian et al. (2004), Kim et al. (2004), Boomsma et al. (2003)). All metal foams show higher Colburn j factor when compared to the clear channel in the range of Reynolds number simulated in the present study. Thus, it is seen from the figure that the metals foams give higher heat transfer performance at lower flow rates of the fluid in the Reynolds number range studied. The heat transfer increases with increasing thickness of the metal foams as expected. In order to reaffirm the present case, the Colburn j factor of 10 mm thickness aluminium and copper metal foams is compared with the other porous medium available in literature (refer Table 6.4). It is clear from Figure 6.14

that the results obtained in the present simulations are in agreement with the other porous medium reported in literature.
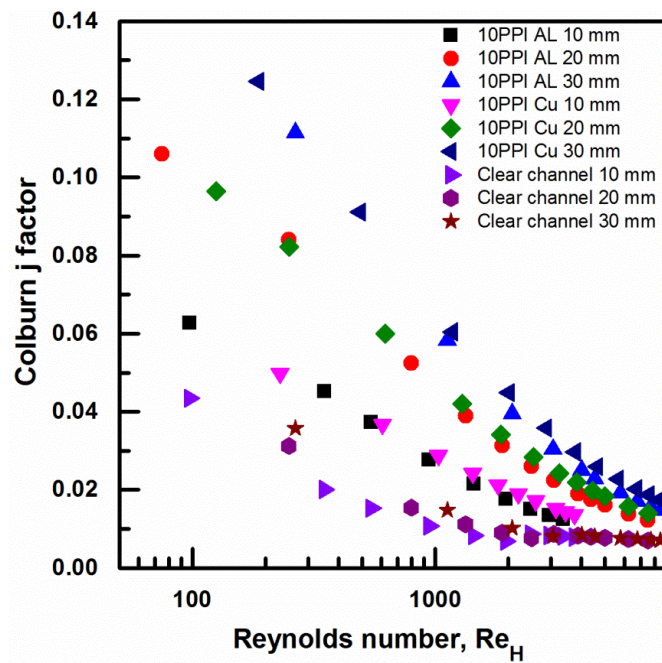
Figure 6.13 Colburn j factor variations with Reynolds number.
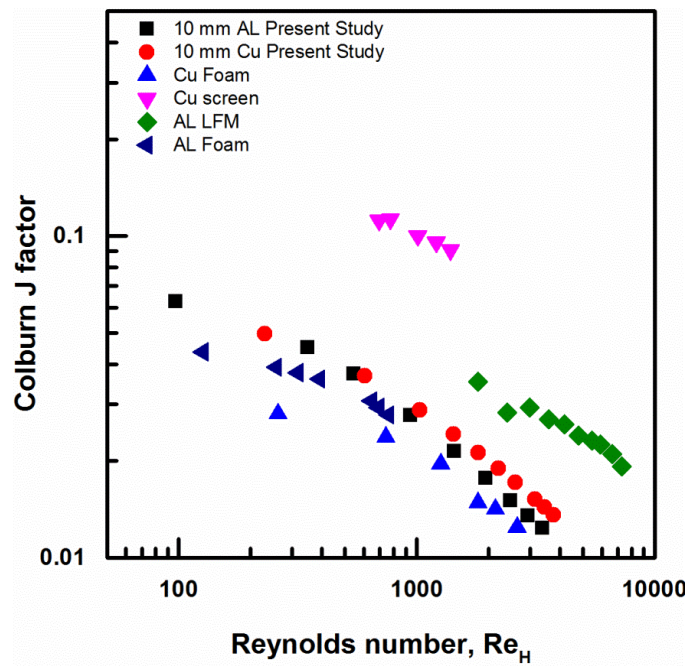
Figure 6.14 Colburn j factor of present study compared with other porous medium.

The overall performance of the metal foams can be analysed by using a performance factor (Manglik (2003), Kurian et al. (2016)) and is given by Eq. (6.6)

$$\lambda_p = \frac{j}{f^{\frac{1}{3}}} \tag{6.6}$$

Figure 6.15 shows variations of performance factor (λ_p) with respect to Reynolds number. The figure shows a decrease in the performance factor with increasing flow rates of the fluid. The metal foams give higher heat transfer performance in the lower flow rates for the range of Reynolds number considered in the present study. As thickness of the metal foams increases the performance factor also increases. It is evident from the plot that the 30 mm thick aluminium and copper metal foams perform almost the same for the range of Reynolds number reported in the present study. It is pertinent to mention here that the effect of thermal conductivity of the metal foam is not significant in the present study.
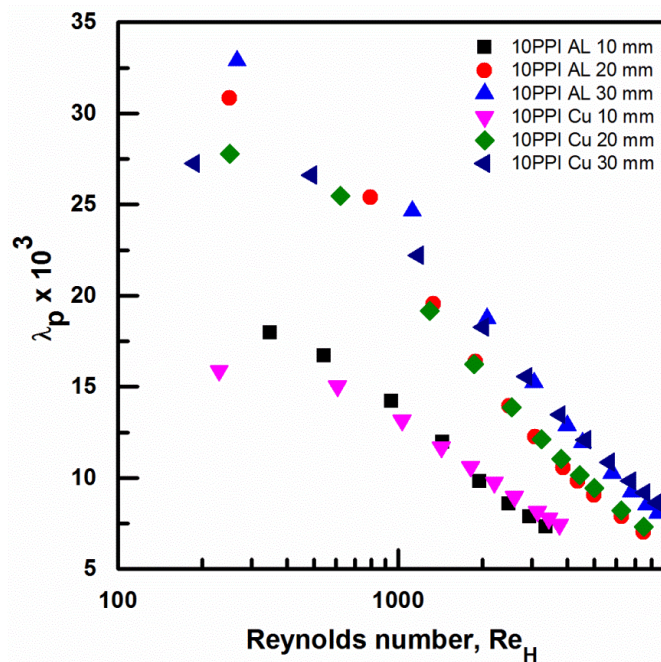
Figure 6.15 Performance factor variations with Reynolds number.

6.6 CONCLUSIONS

Numerical simulations of flow and heat transfer through aluminium and copper metal foams filled in a vertical channel were carried out by using commercially available ANSYS Fluent 15.0 software. In order to enhance heat transfer, high thermal conductivity metal foams were placed on both sides of the aluminium plate and the effect of metal foam thickness was also examined. The proposed parametric study was validated with experimental results available in literature. The following are the concluding remarks observed in the present numerical analysis.

- The pressure drop increases as the inlet velocity of the fluid increases for all the thickness but the variation of pressure drop with respect to the thickness is insignificant for both aluminium and copper metal foams.

- Nusselt number increases with increasing thickness of the metal foams for the range of Reynolds number studied. The effect of change of thermal conductivity of the metal foam does not have significant impact on the heat transfer.

- Based on the comparison of overall performance factor, metal foam thickness of 30 mm gives better thermal performance compared to 10 mm and 20 mm thicknesses.

- The increase in heat transfer due to copper metal foams was observed to be only 1.34 times higher than the aluminium metal foams; therefore, there is little to choose between copper and aluminium metal foams in terms of performance.

6.7 CLOSURE

The numerical study of effect of metal foam thickness as well as thermal conductivity on hydrodynamic and thermal performance is explained in this chapter. The next chapter deals with prediction of heat transfer through discrete heat source system along with metal foams in a vertical channel.

CHAPTER 7

A SYNERGISTIC COMBINATION OF THERMAL MODELS FOR OPTIMAL TEMPERATURE DISTRIBUTION OF DISCRETE SOURCES THROUGH METAL FOAMS

7.1 INTRODUCTION

This chapter explains about the prediction of temperature distribution through the discrete heat source assembly with metal foams filled in a vertical channel. Two different thermal models are considered for the metal foam region to predict the heat transfer. The methodology adopted to achieve isothermal condition on all the heaters is presented and discussed.

7.2 PROBLEM STATEMENT

The physical geometry considered for the present numerical study consists of a vertical channel in which a discrete heat source assembly is placed at the centre of channel and metal foams are placed on both sides of the heat source assembly to enhance heat transfer. The physical domain considered for the analysis is shown in Figure 7.1. The aluminium strip is having the dimensions of 20 x 250 x 3 (all in mm) and the Bakelite strip is having the dimensions of 22.5 x 250 x 7 (all in mm). The size of the metal foam is 150 x 250 x 20 (all in mm). In the discrete heat source assembly, the Bakelite and the aluminium heat source are kept alternatively and heaters are placed in between the aluminium heat sources. Four Bakelite strips are considered in between aluminium heat sources that are placed so as to get a total heat source assembly for a length of 150 mm in the flow direction. The aluminium and copper metal foams of 10 PPI with 20 mm thickness are considered for the present numerical investigation. The properties of the metal foams considered for the present study are listed in Table 7.1. The uncertainties measured in the values of permeability and form drag coefficient are also tabulated in Table 7.1.
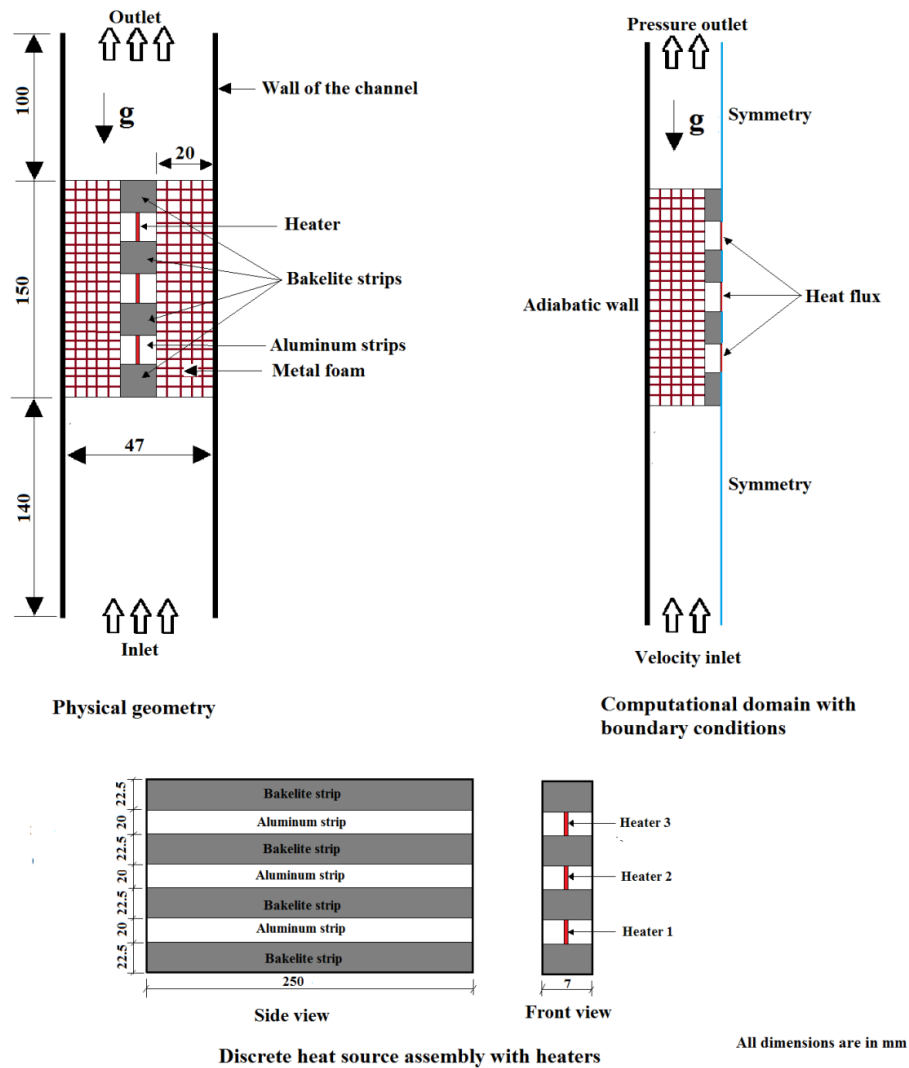
Figure 7.1 Schematic of physical geometry along with computational domain and boundary conditions

Table 7.1 Characteristics of metal foams (Kamath et al. (2013))

Material	PPI	Porosity	Permeability 10^7, m^2	Uncertainty %	Form drag coefficient	Uncertainty %
Aluminium	10	0.9417	6.706	± 29.90	167.56	± 3.34
Copper	10	0.8596	4.779	± 23.24	225.48	± 2.20

7.3 COMPUTATIONAL DOMAIN AND BOUNDARY CONDITIONS

Due to geometrical symmetry about Y axis as seen from Figure 7.1, the two dimensional computational domain considers one half of the vertical channel which consists of heaters, aluminium strips, Bakelite strips, one side metal foam, upstream and downstream of the channel. The computational domain along with the boundary conditions used for the simulation is also shown in Figure 7.1. A uniform velocity at the inlet and zero pressure outlet of the channel are specified as boundary conditions. The side wall of the channel is set to adiabatic condition and the heater placed between the two aluminium heat sources is defined with known heat flux boundary condition. The centreline of the Bakelite strips is assigned with symmetry boundary condition since only half of the geometry is considered for the computations.

7.4 NUMERICAL DETAILS

The commercially available software FLUENT 15.0 (ANSYS (2017)) is used to perform the numerical computations in the present study. Heat conduction in all the solid regions including Bakelite is considered for the analysis; therefore the present analysis becomes a conjugate heat transfer problem. The flow characteristics through the metal foam region are predicted using Darcy Extended Forchheimer model assuming that the metal foam as isotropic homogeneous porous medium. Heat transfer through the metal foam porous medium is predicted using the combination of local thermal equilibrium and local thermal non-equilibrium models as shown in Figure 7.2. The local thermal equilibrium model is used for metal foam regions which are beside the Bakelite strips since these regions are not directly exposed to the temperature gradient. The local thermal non-equilibrium model is used at the metal foam regions which are beside the aluminium strips because the aluminium strips are exposed to the heaters that are defined with heat inputs. The inlet velocity of air is varied between 0.4 and 3.5 m/s and the Reynolds number based on the hydraulic diameter of the channel varies from 2100 to 17000. To capture the turbulent characteristics of the flow, the popular two equation k-ω model is considered in the open region of the channel. Laminar flow is assumed in the porous metal foam region because the Reynolds number based on permeability is less than 150 (Nield and Bejan

(2003)). Air is considered as the working fluid with properties taken at an inlet temperature of 30^0C.
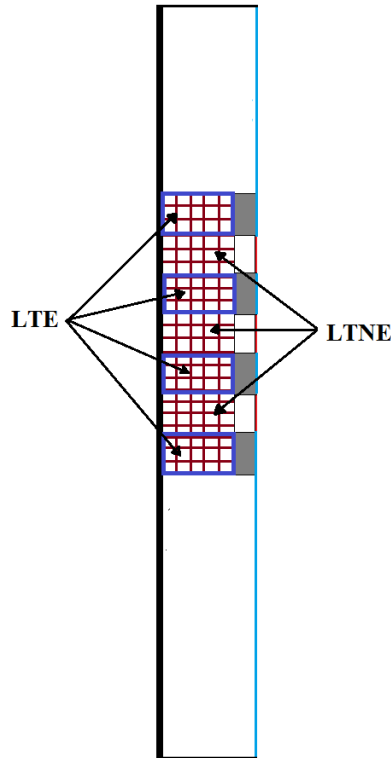
Figure 7.2 Combination of LTE and LTNE thermal model.

The governing equations as well as solver parameter considered for the prediction of flow and heat transfer through the foam free region and foam region in the channel are already mentioned in the section 3.4 of chapter 3.

The surface area density (a_{sf}) and interfacial heat transfer coefficient (h_{sf}) for the metal foams used in the present simulations are calculated based on the correlations proposed by Calmidi and Mahajan (2000) and Zukauskas (1987), respectively. The fiber diameter, pore diameter (Kamath et al. (2013)) and the surface area density calculated for the metal foams used for the simulations are listed in Table 7.2.

Table 7.2 Metal foams surface area density

Material	Pore density (PPI)	Fiber diameter d_f (mm)	Pore diameter d_p (mm)	Porosity ε	Surface area density a_{sf} (m^{-1})
Aluminum	10	0.526	4.982	0.9481	440.25
Copper	10	0.703	4.732	0.8596	824.72

7.5 RESULTS AND DISCUSSION

7.5.1 Grid Independence Study

A detailed grid sensitivity study is carried out for the clear channel to fix the optimal number of grids. Numerical computations are performed for three different grids (49060, 76464 and 102860) to get the optimal size of the mesh. Table 7.3 lists the pressure drop and maximum excess temperature obtained for 3 grids for an inlet velocity of 1.23 m/s and a heat input of 9.2 W for individual heaters. From the grid independency study listed in Table 7.3, the grid size of 76464 is selected for further computations as it shows less deviation in terms of pressure drop and excess temperature.

Table 7.3 Results of the grid independence study

Cells	Pressure Drop (ΔP)	Temperature Difference (ΔT)	Deviation (%) $|\Delta P|$	$|\Delta T|$
49060	7.1060	32.8194	3.21	1.59
76464	6.8307	33.5179	0.78	0.50
102860	6.8847	33.35	Base Line	

7.5.2 Validation of Numerical Results

To validate the numerical methodology adopted, the numerical results of 10PPI metal foam for completely filled channel is compared with experimental results of Kamath et al. (2011). The results of pressure drop and excess temperature showed fairly good agreement with experimental results and are already shown in section 3.6 of chapter 3.

7.5.3 Combination of LTE and LTNE

Heat transfer through the metal foam porous medium is predicted using the combination of LTE and LTNE thermal models as mentioned earlier. The reason to use such a combination is to exploit the concept of two different thermal models in which there exist a temperature gradient between the aluminium heat source and the metal foam wherein LTNE model can be used, on the other hand, there is no temperature gradient between the Bakelite and the metal foam as a result LTE model can be used. Furthermore, the metal foam region besides the Bakelite strips gets heat from the bottom metal foam, since the Bakelite strips are assigned with symmetry condition and are acting as impediment to heat transfer. So, in this region conduction dominates and the air flowing through this metal foam comes in local thermal equilibrium with solid part of the metal foam. Hence, the metal foam regions beside the Bakelite strips are assigned with LTE thermal model. Figure 7.3 shows the temperature distribution contours for the vertical channel predicted using LTNE alone and the combination of LTE and LTNE thermal models for unequal heat inputs. It is clear from the temperature contour that the overall temperature of the vertical channel is higher in LTNE model compared to combined model (LTE and LTNE). The excess temperature obtained by the combined model in the present simulation for the bottom heater (heater 1) is compared with the available experimental results of Kamath et al. (2014) and is shown in Figure 7.4. The average percentage deviation between the numerically predicted excess temperatures and the experimental excess temperatures is found to be 8%. The combined model used in the present study is also compared with the only LTE and only LTNE cases and is shown in Figure 6. It is clear from the plot that the LTE thermal model under predicts and LTNE thermal model over

predicts the excess temperature compared to the experimental results. Hence, the combined LTE and LTNE model used in the present study is best suited for prediction of heat transfer for the present discrete heat source problem.
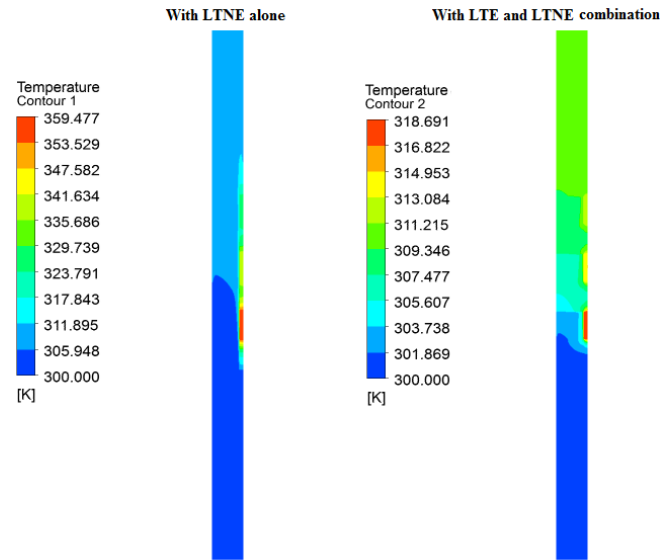
Figure 7.3 Temperature contours for LTNE and combination of LTE –LTNE
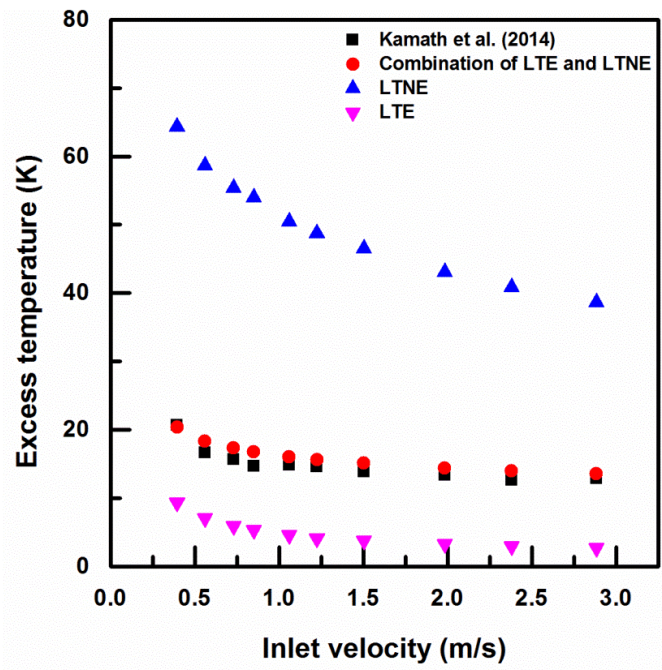
Figure 7.4 Comparison of excess temperature for bottom heater

7.5.4 Temperature Results

In the present study, the aluminium and copper metal foams are considered to enhance the heat transfer in the channel from the discrete heat sources. The values of the thermal conductivity of aluminium and copper metal foams are considered to be 165 and 380 W/mK, respectively. The excess temperature is defined based on the temperature difference between the heater surface and ambient air. The variation of excess temperature with inlet velocity of the fluid for discrete heat sources for an equal heat input of 9.2W is shown in Figure 7.5. The excess temperature decreases with increasing inlet velocity of the fluid for the heater surfaces. It is evident from the plot that the bottom heater takes more heat load compared to other two heaters.
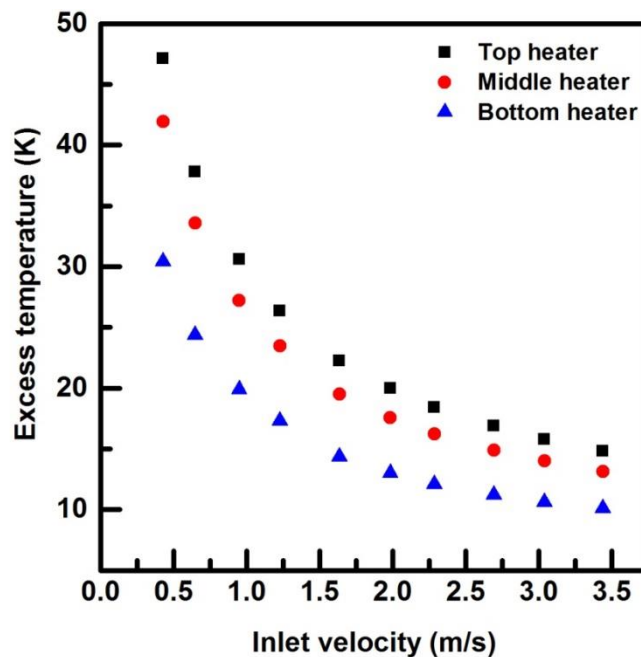
Figure 7.5 Variation of excess temperature on heater surfaces for equal heat input of 9.2 W.

Figure 7.6 shows the excess temperature variation on the heater surfaces for different heat inputs to the heaters for both empty and aluminium metal foam filled channel. The bottom heater is assigned with 40 W, middle heater is assigned with 20 W and the top heater is assigned with 10 W so as to get a total input of 70 W. The heat inputs are divided in such a way that middle heater contains half the heat input of bottom

heater and similarly the top heater contains half the heat input of middle heater. From the figure it is clear that the aluminium metal foam enhances the heat transfer by almost 5 times compared to empty channel case. The excess temperature reduces by 100 ^{0}C due to the use of metal foam compared to clear channel at an inlet velocity of 0.5 m/s, similar result was reported by Kamath et al. (2014) in his experimental study.
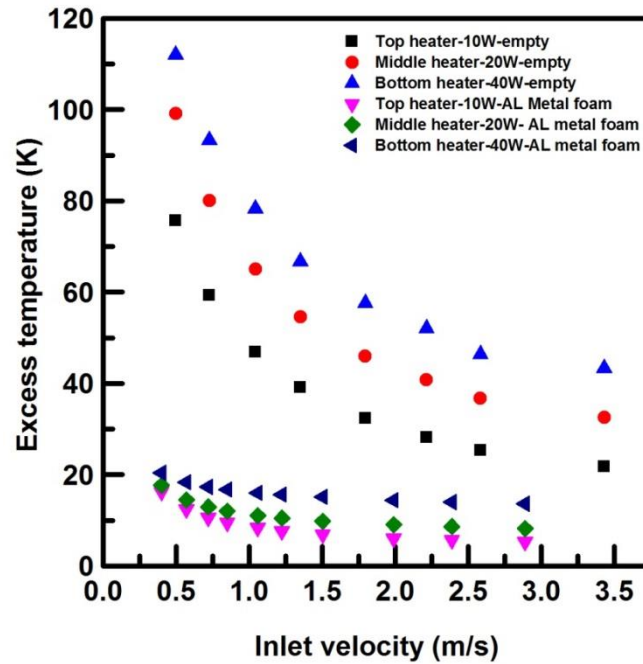
Figure 7.6 Variation of excess temperature on heater surfaces for different heat input.

The variation of excess temperature for both the aluminium and the copper metal foams for unequal heat inputs of 40W, 20W and 10W for the bottom heater, middle heater and top heater, respectively is shown in Figure 7.7. It is clear from the plot that the copper metal foam does not show much significant in the enhancement of heat transfer compared to aluminium metal foam.
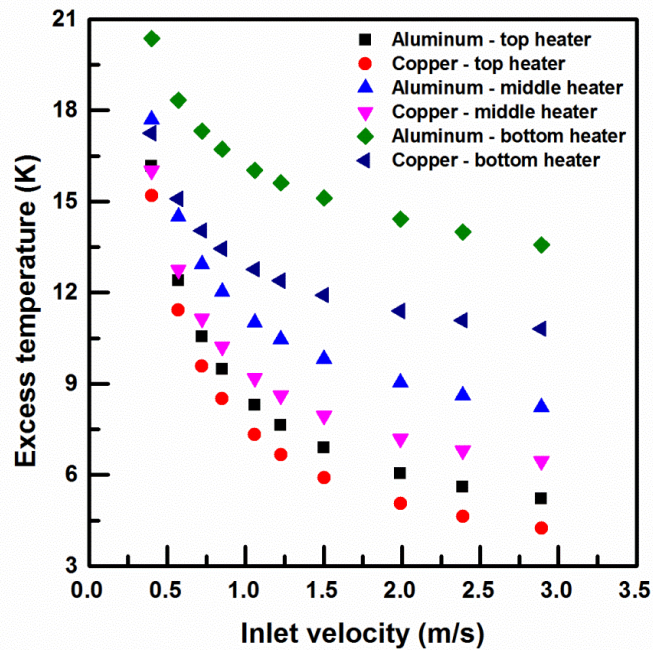
Figure 7.7 Variation of excess temperature on heater surfaces for aluminium and copper metal foams

It is very important to have equal surface temperature on all the heater surfaces to minimize the heat losses. To achieve this, total heat input of 70 W is distributed by trial and error method in such a way that all the heater surfaces show same temperature at a particular inlet velocity. The fluid inlet velocity is taken equal to 0.54 m/s (Kamath et al. (2014)) and varied the heat inputs to the heaters. Figure 7.8 shows the isothermal condition obtained for aluminium metal foam filled vertical channel for unequal heat inputs. The optimal design condition for the aluminium metal foam case is 32W for the bottom heater, 22W for the middle heater and 16W for the top heater and all the heater surfaces are showing an average temperature of 42 ^{0}C. The copper metal foam filled vertical channel shows optimal design condition at a heat input of 34W for bottom heater, 21W for middle heater and 15W for top heater; the heater surfaces shows an average temperature of 40 ^{0}C and the corresponding temperature is shown in Figure 7.9. It is clear from these two plots that the copper metal foam having higher thermal conductivity compared to aluminium metal foam, the excess temperature on all the heat sources reduces only by 2^0 C. The study suggests that the aluminium metal foams can be paramount choice compared to copper metal foam due

to two reasons: (1) there is no significant reduction in the surface temperature due to the use of copper metal foams and (2) copper metal foams are very expensive than the aluminium metal foams.
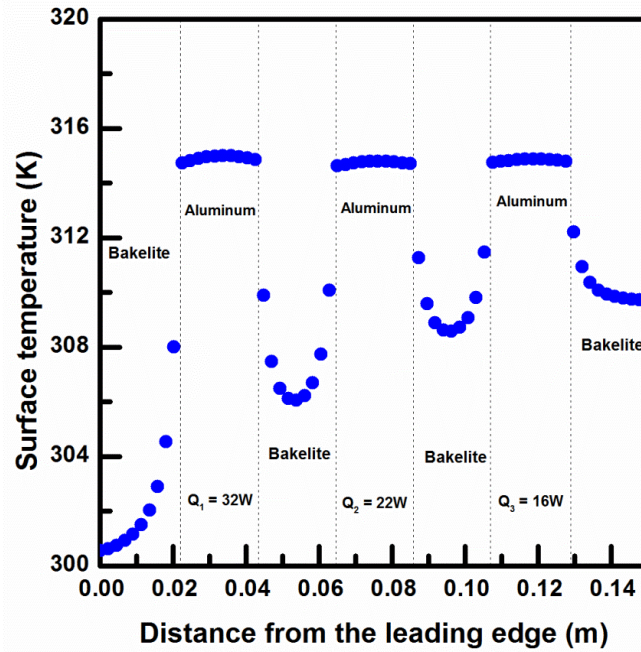
Figure 7.8 Isothermal condition on all heaters for aluminium metal foam
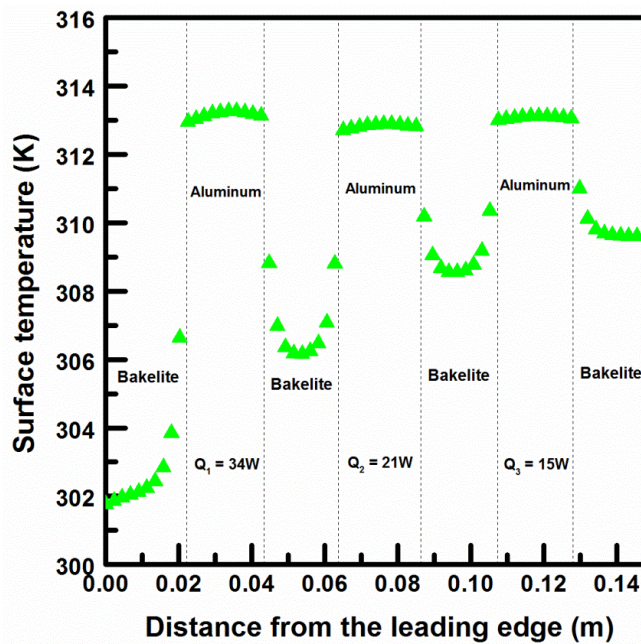
Figure 7.9 Isothermal condition on all heaters for copper metal foam

7.6 CONCLUSIONS

The study of discrete heat sources along with the high thermal conductivity metal foams have been reported in this work. The investigation was carried out in a vertical channel under forced convection heat transfer. The accomplishment of conducive solution to the optimal distribution of temperature has greatly been achieved by employing the synergistic combination of LTE and LTNE models in the vicinity of the discrete sources. Based on the numerical results obtained in this study, some of the concluding remarks are as follows.

- The aluminium metal foams significantly enhance heat transfer compared to the empty channel case. The excess temperature reduces by 100° C at an inlet velocity of 0.54 m/s by the use of aluminium metal foams. It is found that the heat transfer enhancement is higher at lower velocities compared to higher inlet velocities.

- The isothermal condition for the aluminium metal foam was obtained at the optimal heat distribution of 32W for bottom heater, 22W for middle heater and 16W for top heater. Similarly, the copper metal foam gives an optimal heat distribution of 34W for bottom heater, 21W for middle heater and 15W for top heater. The isothermal condition is achieved on all the heaters by varying the heat inputs to the heaters on trial and error basis at a particular inlet velocity of the fluid. Depending upon the temperature requirement on the heater surfaces, the heat input is decreased or increased on a particular heater based on the results of temperature obtained for the previous heat input to the heaters.

- The copper metal foam of 10PPI and $\varepsilon = 0.86$ has not shown significant effect on heat transfer compared to the aluminum metal foam of 10PPI and $\varepsilon = 0.94$ considered in the present study even after having high thermal conductivity that reduces the temperature on all heater surfaces by only 2^0 C. Therefore, the selection of aluminium metal foam becomes indispensable not only to achieve the isothermal condition in electronic cooling but also ensuring easy access and affordable cost.

- The parametric study on heat transfer suggests that the combination of LTE and LTNE thermal models for the proposed study on discrete sources can be used instead of LTNE thermal model alone.

7.7 CLOSURE

In this chapter the heat transfer distribution in metal foams through the discrete heater source system is analysed numerically. The combination of LTE and LTNE thermal model is used in the metal foam region and coined as best suited methodology for the prediction of heat transfer through discrete heat source system. The next chapter explains the study of mixed convection through brass wire mesh porous medium filled a vertical channel.

CHAPTER 8

INTERFACIAL HEAT TRANSFER COEFFICIENT FOR THE FLOW ASSISTED MIXED CONVECTION THROUGH BRASS WIRE MESH

8.1 INTRODUCTION

The wire mesh porous medium received considerable attention by the researchers as it performs almost similar to metal foams in thermal performance. It is very important to calculate the interfacial parameters of the wire mesh to predict flow and heat transfer characteristics numerically. Hence, this chapter elucidates the determination of interfacial heat transfer coefficient for the brass wire mesh porous medium filled in the vertical channel.

8.2 PROBLEM STATEMENT

The physical geometry considered for the numerical study consists of a heater sandwiched between two aluminium plates and placed inside a vertical channel at the centre. The brass wire meshes are placed on both sides of the aluminium plates to enhance heat transfer as shown in Figure 8.1. The dimensions of the aluminium plates are 250 x 150 x 3 (all in mm). The dimensions of the brass wire meshes are 250 x 150 x 10 (all in mm). The dimensions of the channel considered in this study are referred from Kurian et al. (2016) and Kamath et al. (2011).
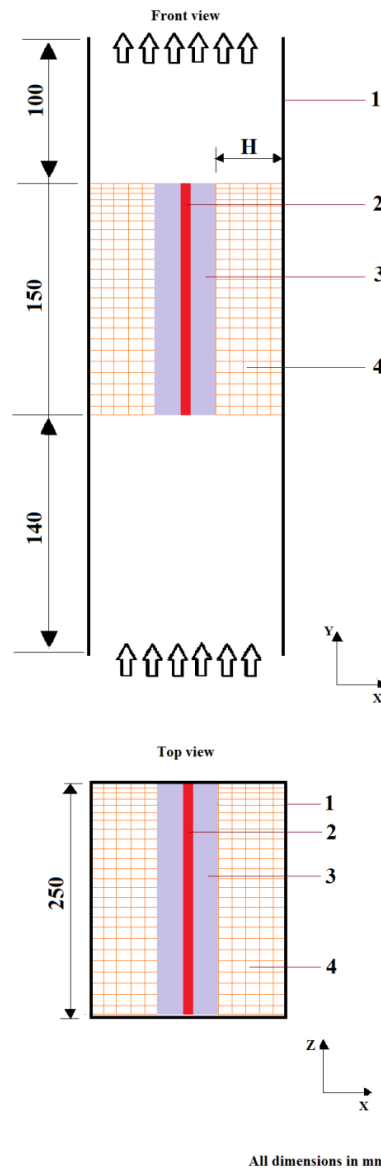
Figure 8.1 Computational domain of the vertical channel (1) side wall of the channel (2) heater (3) aluminium plate (4) brass wire mesh

The properties of the brass wire meshes considered for the present numerical investigation are taken from Kurian et al. (2016) and are shown in Figure 8.2. Three different wire mesh blocks are considered with porosity varying from 0.77 to 0.85. The properties of the brass wire mesh considered for the present study are tabulated in Table 8.1. The inertial and viscous resistance coefficients used in the present simulation are obtained by using form drag coefficient and permeability of the brass wire mesh which is mentioned in Table 8.1. The viscous resistance coefficient is

equal to the reciprocal of permeability of the porous medium and inertial coefficient is nothing but the form drag coefficient of the brass wire mesh porous medium. The values of the viscous resistance coefficients and inertial resistance coefficients used for the present simulations are also tabulated in Table 8.1.

Mesh-1, Porosity = 0.77   Mesh-2, Porosity = 0.81   Mesh-3, Porosity = 0.85
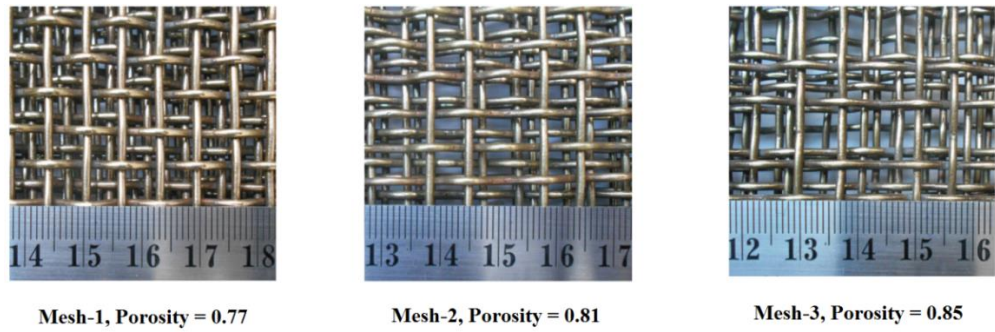
Figure 8.2 Brass wire mesh blocks considered for present numerical study

Table 8.1 Properties of brass wire mesh considered in the present study

Sample	Porosity ε	Permeability 10^7, K, m^2	Form drag coefficient, C, m^{-1}	Viscous resistance coefficient, $1/K$, 10^6, m^{-2}	Inertial resistance coefficient, C, m^{-1}
Mesh - 1	0.77	3.52	66.19	2.84	66.19
Mesh - 2	0.81	4.00	53.87	2.50	53.87
Mesh - 3	0.85	6.54	60.57	1.53	60.57

8.3 BOUNDARY CONDITIONS

In the vertical channel, shown in Figure 8.1, the heater along with the aluminium and the porous medium is symmetrical about the Y-axis, hence only one half of the vertical channel is considered for the numerical computations. The two dimensional computational domain which consists of the heater, the aluminium plate and the brass wire mesh filled on one side of the plate is shown in Figure 8.3. The inlet and outlet of the channel are defined with velocity and pressure, respectively. The heater side of the plate is assigned with known heat flux boundary condition and all side walls of the

channel are set to adiabatic boundary conditions. The channel is symmetric about the vertical axis; therefore, symmetry boundary is assigned to the axis.

$$P = 0, \frac{\partial U}{\partial Y} = 0, \frac{\partial V}{\partial Y} = 0, \text{ T} = \text{T}_\infty$$

Pressure Outlet

Symmetry

$$\frac{\partial T}{\partial X} = 0, \text{ U} = 0, \frac{\partial V}{\partial X} = 0$$

Heat Flux $\frac{Q}{A}$

Adiabatic Wall

$$U = V = 0, \frac{\partial T}{\partial X} = 0$$

Symmetry

$$\frac{\partial T}{\partial X} = 0, \text{ U} = 0, \frac{\partial V}{\partial X} = 0$$

Velocity Inlet

$$U = 0, V = V_\infty, \text{ T} = \text{T}_\infty$$
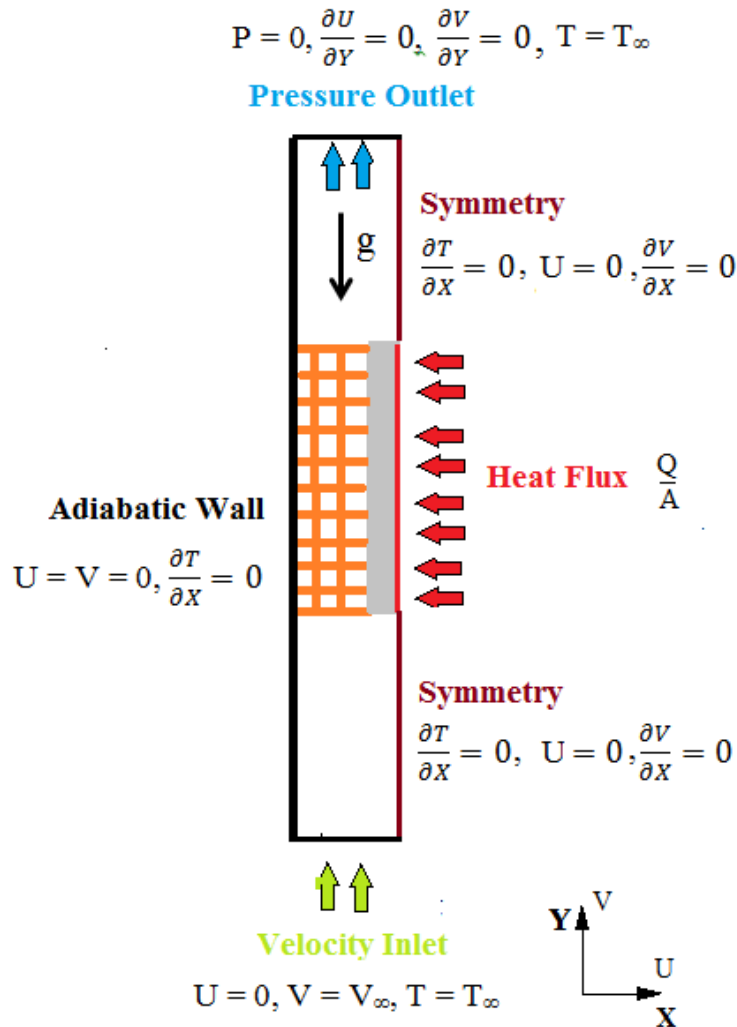
Figure 8.3 Computational domain with boundary conditions

In the present numerical study, the following assumptions are made regarding the fluid and porous medium.

➢ Air is considered as working fluid with constant properties and flows at an inlet temperature of 30° C.

➢ The flow of air in the present study is considered to be steady and incompressible.

➢ The brass wire mesh porous medium is homogeneous and isotropic.

112

- The thermal dispersion through the porous medium is assumed to be negligible and is not considered in the present simulation (Calmidi and Mahajan (2000)).
- The mixing of flow due to the complex structure of the wire mesh is not considered in the present simulations.
- At the interface between the wire mesh porous medium and open channel, the continuity conditions on the velocity, energy and shear stress are applied.

8.4 NUMERICAL SIMULATIONS

Two dimensional computations are performed using the commercially available ANSYS FLUENT 15.0 software (ANSYS (2017)). The velocity of the working fluid is varied between 0.05 and 2.5 m/s; as a result, the Reynolds number based on hydraulic diameter of the channel is varied from 150 to 7800. The transition and turbulent features of the flow in the channel is captured using the k-kl-ω model and the k-ω model is used for the non-porous region. The flow inside the brass wire mesh porous medium is assumed to be laminar since the permeability based Reynolds number is less than 150 (Nield and Bejan (2003)) and turbulence occurs only when it is more than 150.

The governing equations along with numerical details are similar to metal foam filled vertical channel as discussed in section 3.4 of chapter 3. The flow and heat transfer through brass wire mesh porous medium is predicted using Darcy extended Forchheimer flow model and LTNE thermal model.

The surface area density of the wire mesh porous region is calculated based on the expression used by Tian et al. (2004) and is given by

Surface area density:

$$a_{sf} = \frac{\pi}{w + d} \tag{8.1}$$

where 'w' is the width of the cell opening and 'd' is the diameter of the wire mesh. The width of the cell opening and diameter of the brass wire mesh shown in Fig. 8.2 is calculated by using the image analysis software JMicrovision V 1.2.7 (Jmicrovision

(2017)). The brass wire mesh was calibrated using the standard ruler by Kurian et al. (2016). These calibrated images are loaded in the JMicrovision image analysis software and the diameter and width of cell opening of the wire mesh blocks were determined. Figure 8.4 shows the screen shot of JMicrovision software used for the determination of width of the cell and the diameter of the wire of 0.77 porosity brass wire mesh. The surface area calculated for the meshes considered in the present study are tabulated in Table 8.2.
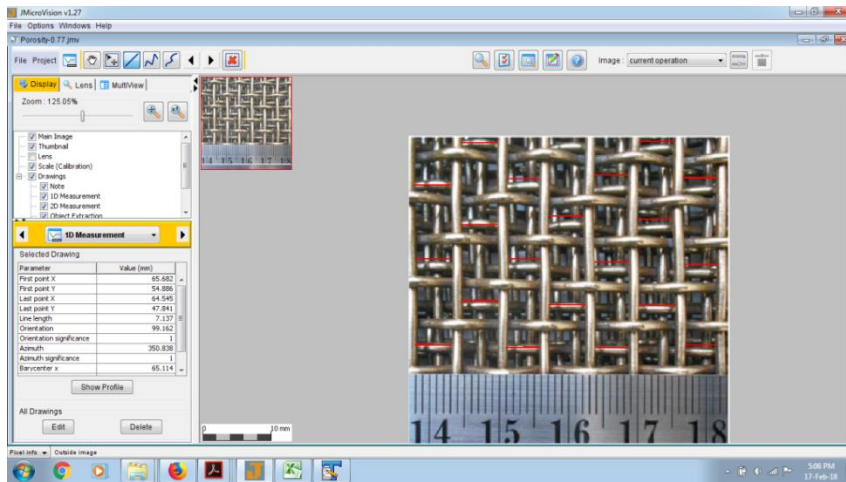
(a)
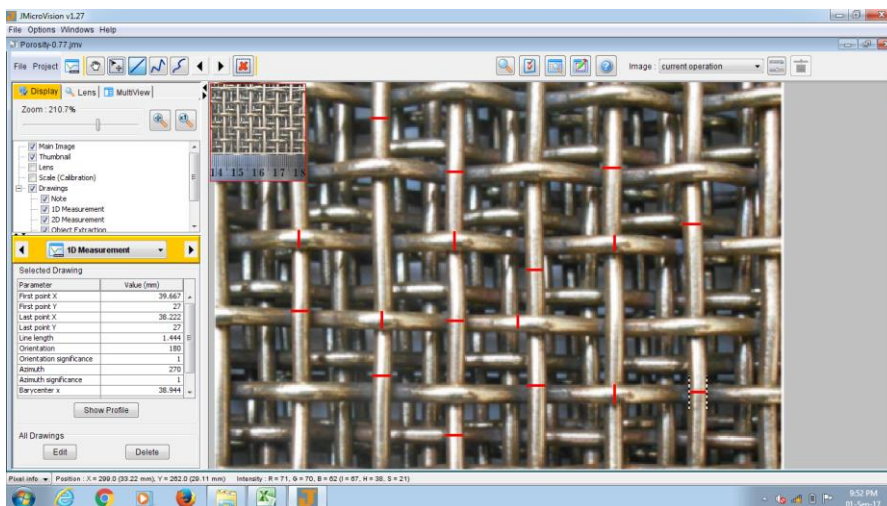
(b)

Figure 8.4 Screen shot of image analysis software (a) Width of the cell opening (b) diameter of the wire

Table 8.2 Surface area density of wire mesh considered in the present study

Sample	Porosity ε	Diameter of the wire d, mm	Width of cell opening w, mm	Surface area density a_{sf}, m^{-1}
Mesh - 1	0.77	1.39	5.15	480.43
Mesh - 2	0.81	1.39	7.57	350.67
Mesh - 3	0.85	1.39	7.80	341.89

It is pertinent to mention here that there is no explicit expression available for calculating the interfacial heat transfer coefficient (h_{sf}) at the solid / fluid interface of the wire mesh porous medium (appearing in Eq. (3.6) and Eq. (3.7)). In view of this, the available interfacial heat transfer coefficient expressions proposed by Wakao et al. (1979), Zukauskas (1987) and Calmidi and Mahajan (2000) in literature are considered and the results from the numerical simulations are then compared with experimental results of Kurian et al. (2016). Finally, a suitable interfacial heat transfer coefficient is selected based on good agreement between simulations and experiments.

Interfacial heat transfer coefficient:

Wakao et al. (1979)

$$Nu_{sf} = 2 + 1.1 \, Re_{d_f}^{\,0.6} Pr^{1/3} \tag{8.2}$$

Zukauskas (1987)

$$Nu_{sf} = \begin{cases} 0.76 \; Re_{d_f}^{\,0.4} Pr^{0.37}, \left(1 \leq Re_{d_f} \leq 40 \right), \\ 0.52 \; Re_{d_f}^{\,0.5} Pr^{0.37}, \left(40 \leq Re_{d_f} \leq 10^3 \right), \\ 0.26 \; Re_{d_f}^{\,0.6} Pr^{0.37}, \left(10^3 \leq Re_{d_f} \leq 2 \times 10^5 \right) \end{cases} \tag{8.3}$$

Calmidi and Mahajan (2000)

$$Nu_{sf} = 0.52 \; Re_{d_f}^{\,0.5} Pr^{0.37} \tag{8.4}$$

8.5 RESULTS AND DISCUSSION

8.5.1 Grid Independence Study

In the present study, a detailed grid independence analysis is carried out in order to fix the optimum size of the mesh. The results of the study are presented in Table 8.3. The

deviation in pressure and temperature is reported for an inlet velocity of 1 m/s and the heat input of 20W. Finally, the grid size of 56700 is considered for the present study since it shows less deviation for both the pressure drop and the excess temperature.

Table 8.3 Results of the grid independence study for 0.77 porosity wire mesh

Cells	Pressure Drop (ΔP)	Temperature Difference (ΔT)	Deviation (%)	
			|ΔP|	|ΔT|
26130	20.00	9.75	2.30	1.10
56700	**19.59**	**9.69**	**0.21**	**0.43**
88400	19.55	9.65	Base Line	

8.5.2 Validation of Numerical Results

8.5.2.1 Pressure drop

Figure 8.5 shows the variation of pressure drop with respect to inlet velocity of the air for the porosity of 0.77. The numerically obtained pressure drop is compared with the experimental results of Kurian et al. (2016). The pressure drop increases with increasing velocity of fluid and the results of numerical simulations match very well with the experimental results at lower velocities whereas at higher velocities numerical results show a deviation of 6% compared to the experimental results.

116
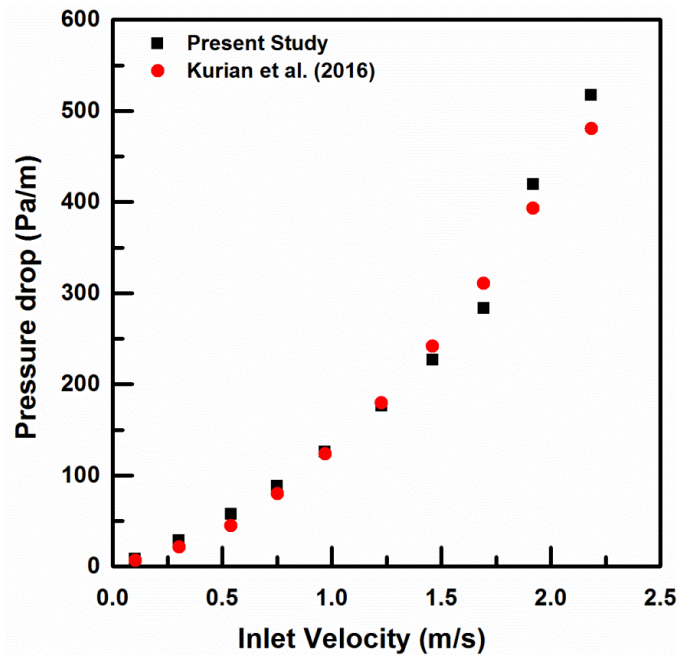
Figure 8.5 Pressure drop comparison with experimental result

8.5.2.2 Identification of Interfacial Heat Transfer Coefficient

As mentioned earlier, there is no distinct expression available for the interfacial heat transfer coefficient for the wire meshes, so the numerical results obtained by considering the available interfacial heat transfer coefficient equations proposed by Wakao et al. (1979), Zukauskas (1987) and Calmidi and Mahajan (2000) for the porous medium are compared with the experimental results. The heat transfer coefficient obtained for the wire mesh with the porosity of 0.77 is compared with the experimental results of Kurian et al. (2016) and is shown in Figure 8.6. From the figure it is clear that the model proposed by Wakao et al. (1979) over predicts and Zukauskas (1987) model under predicts the heat transfer coefficient compared to experimental results. Whereas, the results of the heat transfer coefficient proposed by Calmidi and Mahajan (2000) agrees well with the experimental results up to an inlet velocity of 1.5 m/s with an average deviation of 13% and for velocity greater than 1.5 m/s the deviation is 29% and this may be attributed to the flow transition to turbulence in the porous region of the channel. This deviation can also be due to the approximations made in the present numerical study and probable inaccuracy in the measured experimental data. The experimental uncertainty in heat transfer coefficient

and Nusselt number is reported as ± 2.2% and ± 8.8% respectively by Kurian et al. (2016). The surface area density (a_{sf}) of the wire meshes calculated is based on the two dimensional schematics provided by Kurian et al. (2016) with the use of JMicrovision image analysis software. This introduces some error in accurate prediction of surface area density of the wire meshes considered for the analysis. The surface area density represented in Eq. (3.6) and Eq. (3.7) plays very important role in the solution of energy equation for the wire mesh porous medium. Error can also arise due to the assumption of two dimensional computational domain as opposed to three dimensional experiments. Hence, based on these facts, the interfacial heat transfer coefficient correlation proposed by Calmidi and Mahajan (2000) can be used for the prediction of heat transfer through wire mesh using local thermal non-equilibrium model at lower flow rates.
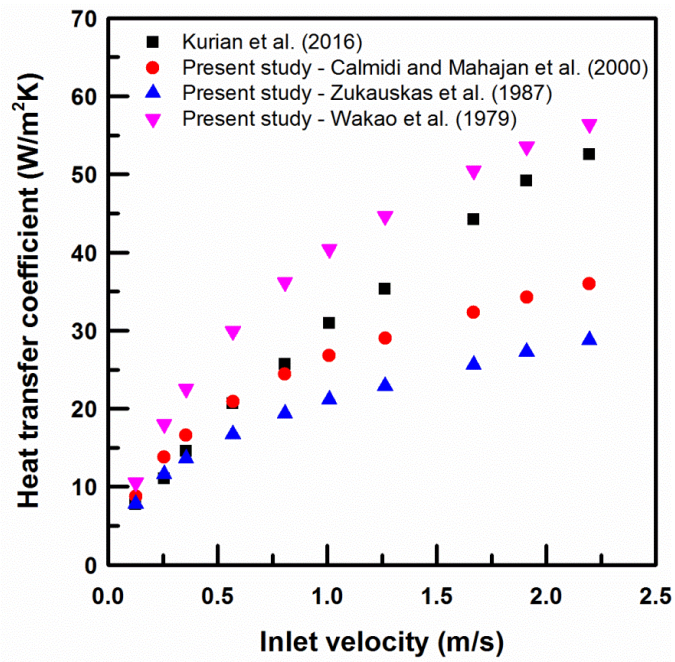
Figure 8.6 Variation of heat transfer coefficient with fluid inlet velocity

The above comparison between the numerical and experimental results serves as the validation of the methodology proposed in this work.

8.5.3 Comparison of LTE and LTNE

The LTE thermal model assumes that the net heat transfer between solid and fluid (pore) at interface of the porous medium is zero because both the solid temperature and the pore fluid temperature remain same. Whereas, the LTNE thermal model considers the existence of temperature gradient at the interface of solid-fluid (pore) of the porous medium, hence the heat transfer takes place from solid to the adjacent fluid flowing through the pores of the porous medium. To further buttress the selection of LTNE thermal model for the wire mesh porous medium, a comparison between LTE and LTNE thermal models is carried out and the variation of heat transfer coefficient with respect to inlet velocity of the fluid is shown in Figure 8.7. From the figure, it is clear that the heat transfer coefficient predicted by LTNE thermal model agrees well with the experimental results of Kurian et al. (2016) whereas the LTE thermal model over predicts the heat transfer coefficient compared to the experimental results. Needless to say that there exists a temperature gradient at the interface of solid-fluid phases of the porous medium. Therefore, it is concluded that the LTNE model is very much suitable for the analysis of heat transfer in the present study.
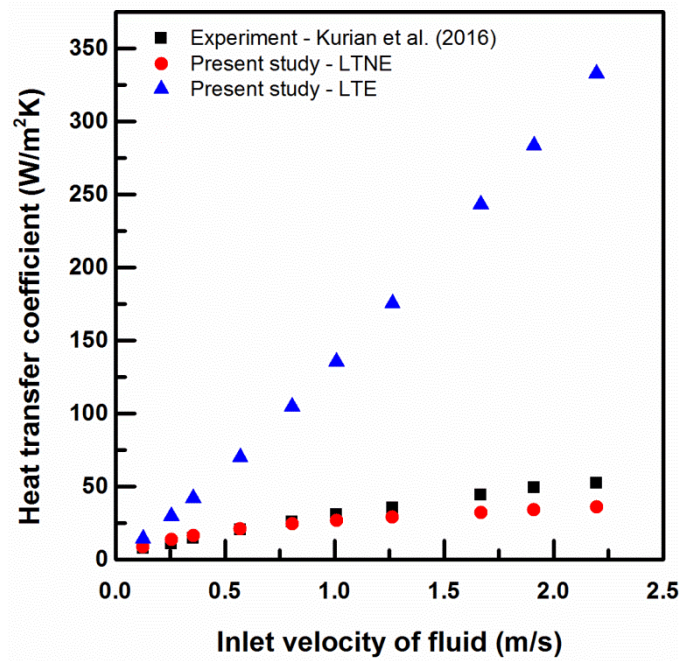
Figure 8.7 Comparison of LTE and LTNE thermal models for wire mesh.

8.5.4 Thermal Dispersion

The thermal dispersion in the present study is assumed to be negligible as mentioned earlier because of high thermal conductivity of metal matrix of the brass wire mesh and low thermal conductivity of the flowing fluid air (Calmidi and Mahajan (2000)). In the present study both the transverse and the longitudinal dispersion is assumed to be negligible. To confirm the assumption made for the longitudinal thermal dispersion, temperature variation in the vertical channel for 0.77 porosity wire mesh for an inlet velocity of 1 m/s is shown in Figure 8.8. From the figure it is clear that the longitudinal temperature difference is smaller than the total temperature difference of the system.
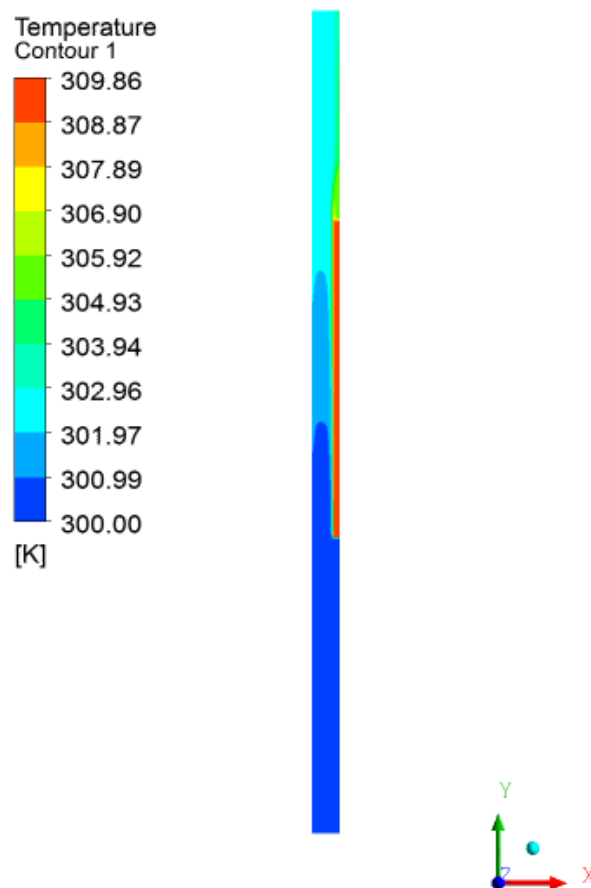
Figure 8.8 Temperature variations in the vertical channel for 0.77 porosity wire mesh.

8.5.5 Hydrodynamic Characteristics

The pressure drop increases as the inlet velocity of fluid increases for all the wire meshes and is shown in Figure 8.9. The pressure drop decreases with increase in the porosity of the wire mesh at a particular inlet velocity. The pressure drop variation at lower velocities is almost linear while at higher velocities the variation is non-linear. The wire mesh of porosity 0.85 shows lesser pressure drop compared to the other two porosities, since the number of wires in the mesh reduces as porosity increases which in turn increases the flow through the wire mesh.
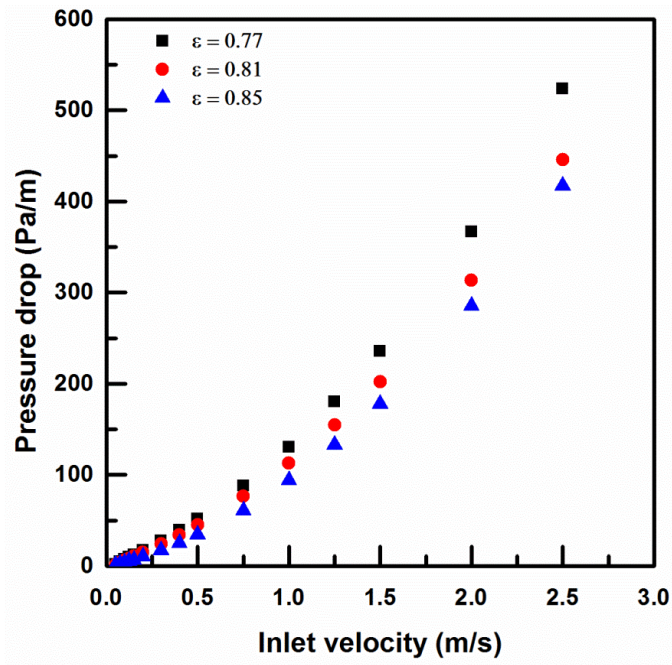
Figure 8.9 Pressure drop variation for wire meshes

The friction factor for the wire meshes is calculated based on the thickness of the mesh and is given in Eq. (8.5)

$$f = \frac{\Delta P}{\left(\frac{L}{H}\right)\left(\frac{\rho V^2}{2}\right)} \tag{8.5}$$

The variation of friction factor obtained for different wire meshes with respect to thickness based Reynolds number is shown in Figure 8.10. Friction factor obtained for 0.85 porosity mesh is lower compared to other two wire mesh porosities since the

pressure drop obtained for 0.85 porosity is less than the other two meshes. As porosity decreases the number of wires in the mesh increases which in turn increases the area of the obstacle for the flow of fluid through the mesh. The friction factor obtained for different wire meshes are compared with the other porous mediums available in the literature for the purpose of verification of the numerical results. The porous mediums used for the comparison are tabulated in Table 8.4. It is clear that the brass wire meshes show lesser friction factor compared to other porous medium for the same porosity.

Table 8.4 Details of porous medium used for comparison

	Type of porous media	Thickness (mm)	Porosity
Tian et al. (2004)	Copper wire screens	10	0.80
Venugopal et al. (2010)	Perforated plates	10	0.85
Kamath et al. (2013)	10 PPI Copper foam	10	0.86
Kim et al. (2004)	Aluminum lattice frame material (LFM)	10	0.94
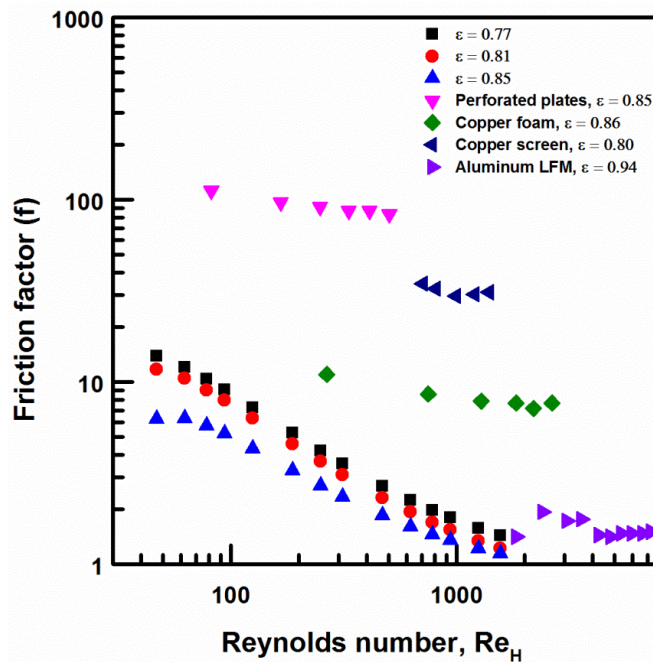
Figure 8.10 Friction factor variation with Reynolds number

8.5.6 Thermal Characteristics

The thermal performance of the brass wire meshes are characterized based on Nusselt number, Colburn j factor and performance factor (λ_p). Since the heater is sandwiched between two aluminium plates the heat input given to the heater is equally divided on both sides of the plates. The thermal conductivity of the brass wire mesh is considered to be 119 W/mK (Kurian et al. (2016)). The heat transfer coefficient and Nusselt number are calculated based on the Eq. (8.6) and (8.7).

Heat transfer coefficient

$$h = \frac{Q}{A\Delta T} \tag{8.6}$$

Nusselt number

$$Nu = \frac{hH}{\lambda_{eff}} \tag{8.7}$$

where ΔT is the temperature difference between average temperatures of the aluminium plate (T_{avg}) and ambient temperature (T_∞) i.e., ($T_{avg} - T_\infty$), λ_{eff} is the effective thermal conductivity of the brass wire mesh high porosity porous medium as mentioned by Nield (1991) and is calculated based on Eq. (8.8) and the working fluid air properties are taken at an inlet temperature of 30°C.

Effective thermal conductivity

$$\lambda_{eff} = \lambda_f{}^\varepsilon . \lambda_s{}^{(1-\varepsilon)} \tag{8.8}$$

The non-dimensional Reynolds number given in Eq. (8.9) is defined based on the thickness of the wire mesh.

Reynolds number

$$Re_H = \frac{VH}{\nu} \tag{8.9}$$

Richardson number

$$Ri_H = \frac{Gr}{Re_H{}^2} \tag{8.10}$$

Where

$$Gr = \frac{g\beta\Delta T H^3}{\nu^2}$$

Figure 8.11 shows the variation of the Nusselt number with Reynolds number for the three wire meshes studied. The Nusselt number increases with increasing flow rate of the fluid for all the porosities considered in the study. At a particular flow rate, the heat transfer rate increases with increase in the porosity of wire mesh for the Reynolds

number range studied. This is because as porosity of the wire mesh increases, more quantity of the fluid flows through the wire mesh porous region which takes more heat from the solid phase of the porous medium and also from the solid aluminium plate. The wire mesh of porosity 0.85 shows higher heat transfer rate compared to other two porosities studied. For the range of Reynolds number considered, it is observed that the wire mesh having porosity of 0.85 gives an average increase of 1.86 and 1.41 times the heat transfer compared to 0.77 porosity and 0.81 porosity wire meshes, respectively. Similarly, wire mesh with the porosity of 0.81 is giving an average increase of 1.32 times the heat transfer rate of 0.77 porosity wire mesh. This confirms that the 0.85 porosity wire mesh gives highest heat transfer performance compared to other two porosity wire meshes.

The flow regimes can be classified based on the slope of the curves as forced convection and mixed convection regimes. The transition of the regimes is observed in the Reynolds number range of $120 < Re_H < 187$. Based on the numerical results, it is clear that at lower flow rates the Nusselt number is weak function of Reynolds number, this regime is identified as mixed convection regime whereas in forced convection regime the Nusselt number is strong function of Reynolds number.
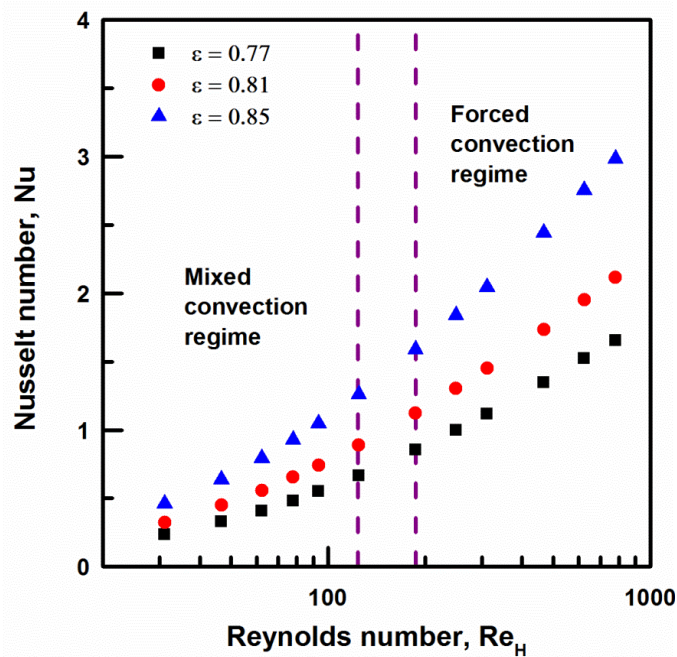
Figure 8.11 Nusselt number variation with Reynolds number

The variation of Nusselt number with respect to Richardson number is shown in Figure 8.12. As Richardson number increases the Nusselt number decreases in the range of Reynolds number studied for the all wire meshes. When Richardson number is less than 0.1 (Ri < 0.1), the Nusselt number is strong function of Richardson number and this regime is identified as forced convection regime. Similarly, when Ri > 0.1, the Nusselt number shows a weak function of Richardson number so this regime is identified as mixed convection regime.
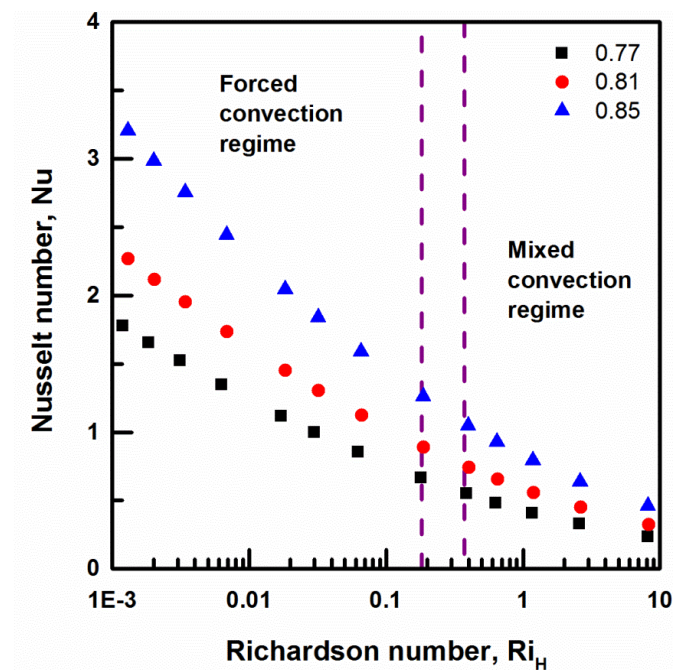
Figure 8.12 Nusselt number variation with Richardson number

The Colburn j factor gives the thermal performance of a heat exchanging device and is represented in Eq. (8.11).

$$j = St. Pr^{\frac{2}{3}} \qquad (8.11)$$

The variation of Colburn j factor with Reynolds number for the wire mesh is shown in Figure 8.13. The Colburn j factor decreases with increasing flow rate of the fluid for all the wire mesh porosities studied. From the plot it is clear that the brass wire mesh shows higher thermal performance compared to the clear channel case, which indicates that the brass wire mesh can also be used for the enhancement of heat transfer. All the porosity wire meshes considered in the present analysis show almost

the same thermal performance. The wire mesh of 0.85 porosity shows slightly higher thermal performance but not that much significant at lower flow rates whereas the lower porosity wire mesh shows a preferable thermal performance at higher flower rates. At lower velocity the quantity of the fluid flowing through the 0.85 porosity wire mesh is higher compared to 0.77 porosity wire mesh, which takes away the heat from the porous structure as well as from the hot aluminium plate. When flow rate increases the fluid flowing through higher porosity wire mesh escapes easily through it and absorbs less heat; on the other hand, the fluid flowing through lower porosity wire mesh takes more heat from the porous structure and also from aluminium plate. As a result, the thermal performance is more or less same irrespective of the porosities considered in the present study. The numerical results of Colburn j factor obtained are compared with other porous mediums tabulated in Table 8.4. From the comparison, it is observed that the numerical results obtained are in good agreement with the values reported in literature.
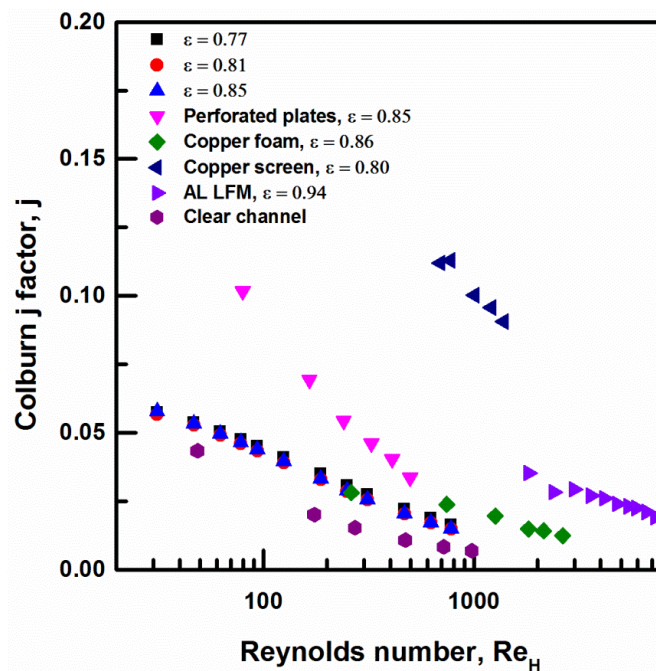
Figure 8.13 Colburn j factor variations with Reynolds number.

The performance factor (λ_p) gives the comparison of heat transfer coefficient to the pumping power of the fluid and it gives the overall performance of the wire meshes defined by Manglik (2003) and is given by Eq. (8.12).

126

$$\lambda_p = \frac{j}{f^{\frac{1}{3}}} \qquad\qquad (8.12)$$

Figure 8.14 shows performance factor (λ_p) variations with Reynolds number. The performance decreases with increasing flow rate of the fluid for all porosity wire meshes considered in the present study. This is due to the fact that as flow rate increases, the pressure drop increases for wire mesh. A similar trend is observed in literature and is shown in the figure for the purpose of comparison. It is also observed that the wire mesh of 0.85 porosity shows higher overall performance compared to the other two wire mesh porosities at lower flow rates. This is due to the fact that at particular flow rate of the fluid, the porosity of 0.85 wire mesh gives higher heat transfer rate with lower pressure drop compared to other two wire meshes studied. For example, at $Re_H = 62$ the wire mesh of 0.85 porosity gives heat transfer rate twice that of the 0.77 porosity wire mesh at approximately 50% reduced pressure drop. The pumping power of the fluid thereby reduces by 50%. This proves that the higher porosity wire meshes can be used for the enhancement of heat transfer in thermal applications where higher heat transfer is achieved with less pumping power of the fluid. When the porosity of the wire mesh or porous medium is lower, the flow rate of the fluid flowing through the porous medium becomes less and thereby increases the pumping power of the fluid in turn increases the operating cost. The brass wire mesh shows higher thermal performance compared to the perforated plates and copper foam for the same porosity range. Based on the comparison results, it is confirmed that the wire meshes can also be used as a better candidate for the enhancement of heat transfer in thermal systems.
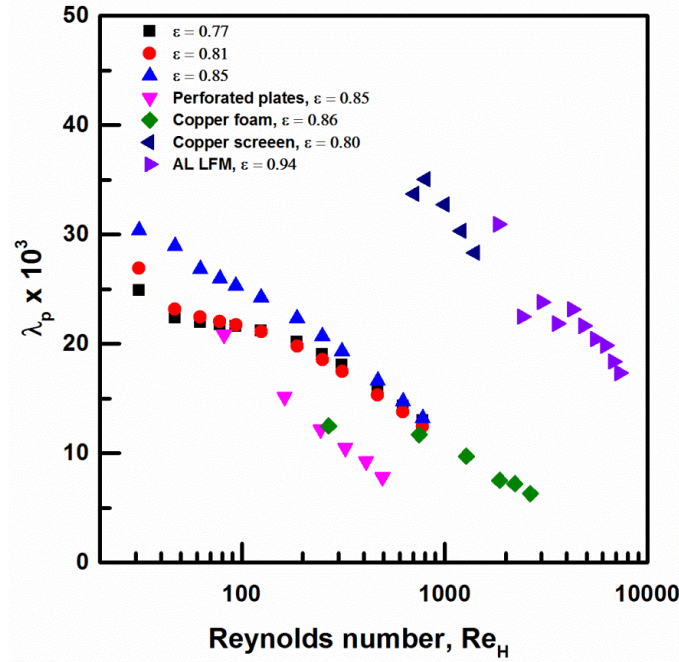
Figure 8.14 Performance factor variations with Reynolds number.

The Nusselt number obtained in the present study is compared with the correlation available in the literature. Kurian et al. (2016) developed a correlation for Nusselt number based on the Reynolds number, Richardson number and porosity of the wire mesh by using the experimental data which is given by Eq. (8.13) and valid for a range of parameters specified in Eq. (8.14). A parity plot, shown in Figure 8.15, between the Nusselt numbers obtained based on correlation proposed in Kurian et al. (2016) and the Nusselt number based on the present simulation, shows good agreement with a deviation of ±20%.

$$Nu_{porous} = 0.124 Re_H{}^{0.707} \varepsilon^{7.57} \left(1 + Ri_H{}^{0.690} Re_H{}^{-0.549}\right) \qquad (8.13)$$

$$
\begin{aligned}
0.001 &\leq Ri_H \leq 11.53 \\
29 &\leq Re_H \leq 1400 \\
0.77 &\leq \varepsilon \leq 0.85
\end{aligned}
\qquad (8.14)
$$
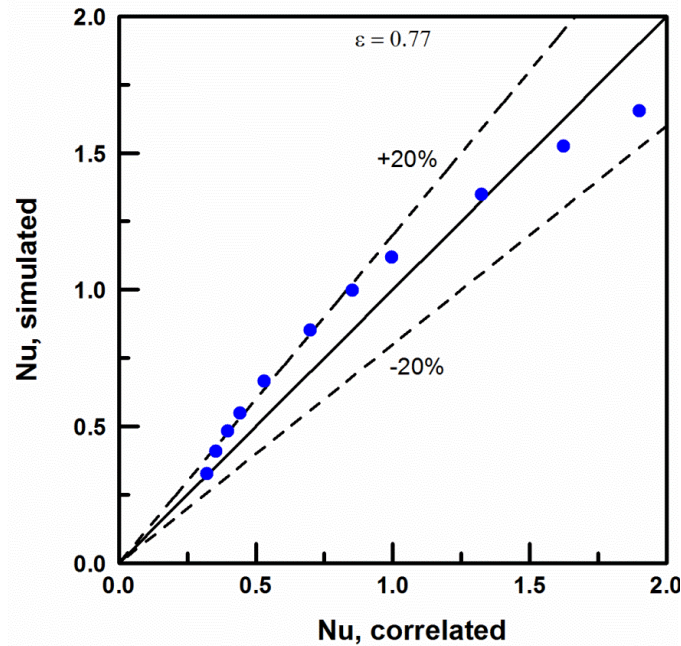
Figure 8.15 Parity plot showing agreement between Nusselt number based on correlation and Nusselt number based on present simulations.

8.5.7 Effect of Partial Filling of Wire Mesh

In the present study two different partial filling of the wire mesh such as 40% and 70% are also considered and compared with completely filled channel to estimate the heat transfer characteristics. Figure 8.16 shows the velocity distribution obtained for the porosity of 0.85 wire mesh partially filled in the vertical channel. The velocity in the open region increases and decreases in the wire mesh region as partial filling rate increases. The results of velocity distribution obtained in the present study agree well with results available in the literature Lu et al. (2016) and Kotresha and Gnanasekaran (2018). For the purpose of comparison, the velocity distribution obtained numerically for 70% filled 10PPI metal foam by Kotresha and Gnanasekaran (2018) is shown in Figure 8.16. The properties of copper metal foam considered for the comparison is given in Table 8.5. The velocity distribution obtained for copper metal foam filled channel is higher in open region and lesser in porous medium compared to brass wire mesh. This is because the permeability of the copper metal foam is less compared to brass wire mesh even after having higher porosity compared to wire mesh.
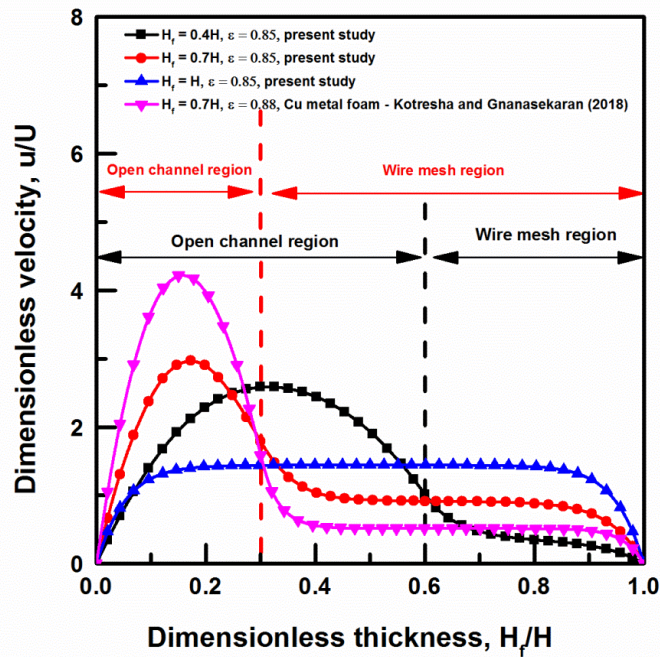
Figure 8.16 Velocity distributions of wire meshes and comparison with metal foams

Table 8.5 Properties of copper metal foam

	Porosity ε	Permeability $K \times 10^7, m^2$	Form drag coefficient C	Surface area density a_{sf}
Copper Metal foam (Kotresha and Gnanasekaran (2018))	0.88	1.742	176.75	822.83

The variation of pressure drop with the inlet velocity of the fluid for partially filled 0.85 porosity wire mesh is shown in Figure 8.17. The pressure drop for partially filled ($H_f = 0.7H$ and $H_f = 0.4H$) channel shows a general increase as similar to completely filled channel ($H_f = H$) with increase in the inlet velocity of the fluid. The pressure drop increases with increase in the partial filling of the wire mesh in the vertical channel, because the volume blockage increases as partial filling increases in the channel which in turn opposes the fluid to flow. For example, at inlet velocity of 1 m/s, the pressure drop obtained in the channel for 40% and 70% filling rate is almost equal to 25% and 59%, respectively, compared to completely filled channel. It is clear

that channel filled with 70% wire mesh gives pressure drop almost half of the completely filled channel.
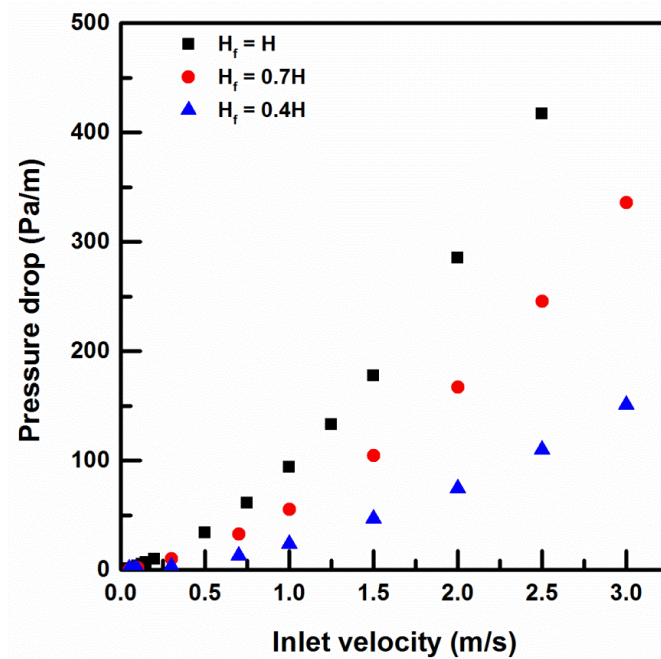
Figure 8.17 Pressure drop variation for partial filled 0.85 porosity wire mesh

The variation of the Nusselt number with the Reynolds number for different filling rate of the 0.85 porosity wire mesh is shown in Figure 8.18. The Nusselt number increases with increasing flow rate of the fluid for all the filling rates considered for the present numerical investigation. Also, it is observed that the Nusselt number increases with increase in wire mesh filling in the vertical channel. At Re = 3100, the channel filled with 40% and 70% filling rate gives an heat transfer rate of 60% and 88%, respectively, of the completely filled channel. The channel filled with 70% filling rate can be considered for the heat transfer enhancement since the pressure drop reduces by almost 50% of the completely filled channel.
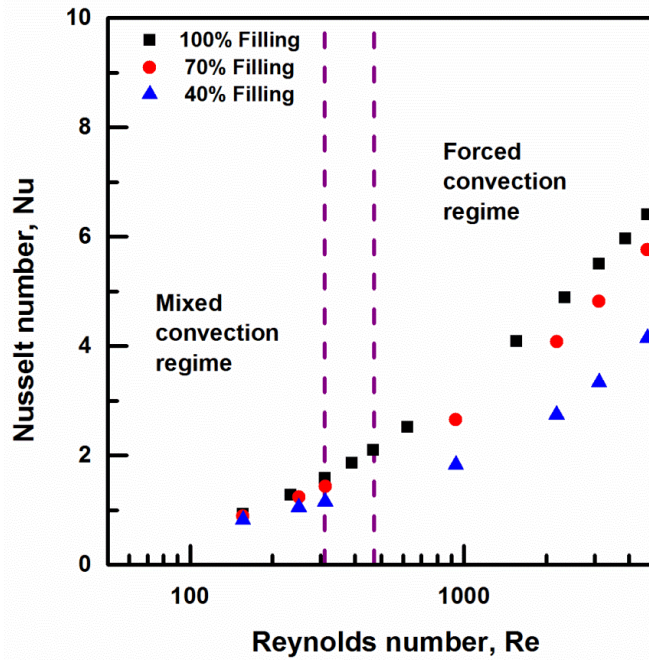
Figure 8.18 Variation of Nusselt number for partial filling of the 0.85 porosity wire mesh

The variation of performance factor with Reynolds number for all filling rate in the vertical channel is shown in Figure 8.19. The performance factor shows a general decrease with increase in the flow rate of fluid for all the filling rates of the wire mesh in the vertical channel studied. At lower flow rates the channel filled with 40% filling rate shows higher thermal performance compared to 70% and 100% filling rates. Whereas at higher flow rates, overall performance of all filling rates of the wire mesh in the channel gives the same performance. For the purpose of comparison and correctness, the numerical result of copper metal foam (Kotresha and Gnanasekaran (2018)) available in the literature is also shown in Figure 8.19. It is clear that the wire mesh gives higher overall performance compared to copper metal foam. Based on the parametric study, it is suggested that the channel filled with 0.85 porosity wire mesh can be used for the enhancement of heat transfer because it gives almost the same overall performance as completely filled case and the pressure drop reduces by almost 50%.
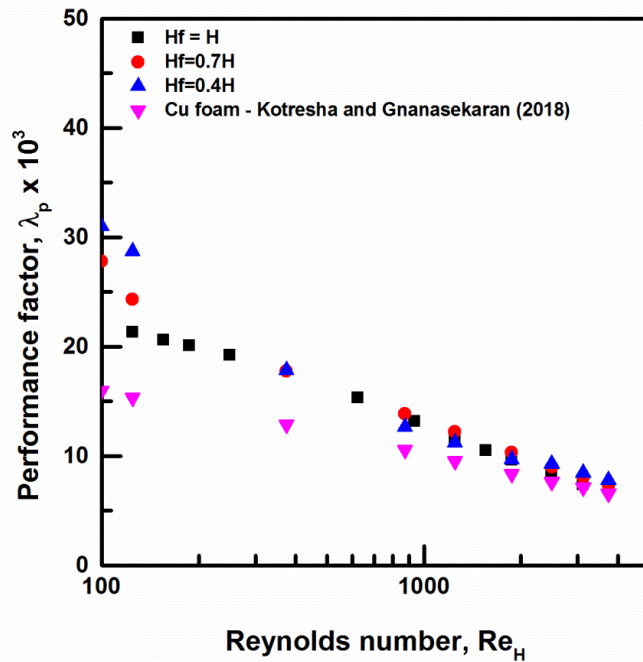
Figure 8.19 Performance factor for partial filled 0.85 porosity wire mesh

8.6 CONCLUSIONS

In the present study, two dimensional numerical simulation of flow assisted mixed convection through brass wire mesh filled in a vertical channel was carried out by using ANSYS FLUENT. The computational domain consists of the heater, the solid aluminium plate and one side brass wire mesh in the vertical channel. The well-established Darcy Extended Forchheimer and LTNE thermal models are synergistically combined to predict the flow and heat transfer through the wire mesh porous medium. The numerical results obtained in the present study are compared with the experimental results available in the literature for the purpose of validation and to check the accuracy of the results. From the study, the concluding remarks are as follows

- The correlation for interfacial heat transfer coefficient expression proposed by Calmidi and Mahajan (2000) was coined as best suited for the case of wire mesh porous medium. At lower flow rates, the numerical results match well with experimental results whereas at higher flow rates the deviation is found to be more between the experimental and the numerical results. This was due to

the turbulence characteristics of the flow especially at higher flow rates and also because of approximations made in the numerical solution.

- The average increase in heat transfer of the brass wire mesh was found to be twice that of the clear channel case. As porosity of the wire mesh increases, the pressure drop and the Nusselt number decreases and increases respectively. The wire mesh of porosity 0.85 gives an average increase of 1.86 and 1.41 times the heat transfer rate compared to 0.77 and 0.81 porosities of the wire mesh.

- Based on the performance factor, the porosity of 0.85 gives highest overall performance compared to 0.77 and 0.81 porosities of the wire mesh.

- The pressure drop increases with respect to increase in the partial filling of the wire mesh in the vertical channel. The pressure drop obtained for 40% and 70% filling rate of the wire mesh is 25% and 59% of the completely filled channel for the same wire mesh porosity. The heat transfer rate increases with increase in the partial filling of the wire mesh in the channel. The partial filling rate of 40% and 70% in the vertical channel gives an average heat transfer rate of 60% and 88% of completely filled channel. It is suggested that 70% filling rate of wire mesh can be used for enhancement of heat transfer with minimum pressure drop.

- As a concluding remark, the commercially available brass wire mesh can be used to enhance heat transfer for effective cooling of electronic equipment since it outperforms compared to the metal foams.

8.7 CLOSURE

This chapter explained the numerical study of mixed convection through brass wire mesh porous medium filled completely/partially in the vertical channel. The detailed description of numerical methodology adopted for the prediction of flow and heat transfer is explained and discussed. Next chapter gives the overall conclusion of the present research work.

CHAPTER 9

CONCLUSIONS AND SCOPE FOR FUTURE WORK

9.1 INTRODUCTION

The present study focused on the numerical prediction of hydrodynamic and thermal characteristics of different metallic porous mediums filled partially or completely in the vertical channel. The metallic porous mediums considered for the analysis are high porosity metal foams (aluminium and copper) and brass wire mesh. The metallic porous structures are placed adjacent to the heater-plate assembly for the enhancement of heat transfer; hence the problem was solved as conjugate heat transfer. The metallic porous mediums are considered as a homogeneous and isotropic in nature. A well-known Darcy Extended Forchheimer flow model is considered for the prediction of flow through the porous medium while the local thermal non-equilibrium model is considered for the prediction of thermal characteristics. Mixed convection is modelled by incorporating Boussinesq buoyancy model in the momentum equations. Two different types of heater plate assemblies are considered for the present numerical investigation.

The thesis started with the introduction which expounds the concepts of porous medium and flow models. It also explains the thermal models available for the prediction of heat transfer through porous medium. The details on metal foam porous medium and their applications along with advantages are highlighted in **Chapter 1**. **Chapter 2** explains the critical review carried out on the literature and conclusions drawn based on the same for carrying out the numerical analysis on the problems identified. The numerical methodology adopted for the solution of fluid flow and heat transfer through the metal foam was detailed in **Chapter 3**. The grid sensitivity analysis along with validation of the methodology was explained in the same chapter. **Chapter 4** presents the results obtained for the mixed convection analysis of high porosity aluminium metal foams having four different pore densities and varying

porosities. The effect of partial filling of the high porosity metal foam in the channel for constant thickness of the channel was detailed in **Chapter 5**. The flow distribution through the porous metal foam was compared with the analytical results for the purpose of correctness. The aftermath of the metal foam thickness and thermal conductivity on thermal performance was presented in **Chapter 6**. Three different thicknesses and two different material of the metal foam are considered for the investigation. An isothermal condition on all the heaters of the discrete heat source assembly with the use of aluminium and copper metal foams was presented and discussed in **Chapter 7**. The **Chapter 8** explains the determination of interfacial heat transfer coefficient for the brass wire mesh porous medium filled in the vertical channel. In the ensuing section, the key conclusions are summarized.

9.2 MAJOR CONCLUSIONS OF THE PRESENT STUDY

- The heat transfer rate increases with increase in pore density of the metal foam at a particular fluid inlet velocity at the expense of friction losses. The metal foam with higher PPI and higher porosity can be considered for the enhancement of heat transfer.

- As partial filling of the metal foam increases in the channel the pressure drop and heat transfer rate increase. The filing rate of 70% with higher PPI metal foam can be preferred for the applications where moderate heat transfer enhancement is required at lower pressure drop. Thereby the pumping power required to pump the fluid reduces almost by 50%.

- The Nusselt number increases with increase in the metal foam thickness for the same PPI metal foam having almost same porosity. The metal foam thermal conductivity does not shown significant effect on the thermal performance. The copper metal foam shown only a 4% increase in heat transfer compared to aluminium metal foam even after having higher thermal conductivity.

- The metal foam heat exchanger showed 5 times increase in heat transfer in discrete heat source system. The isothermal condition on all

the heaters in the discrete heat system was achieved by varying the heat fluxes on all the heaters at a constant velocity.

- The Calmidi and Mahajan (2000) correlation for interfacial heat transfer coefficient matches fairly well with the experimental results for brass wire mesh porous medium. It was found that the brass wire mesh performs almost the same as the metal foams in terms of thermal performance in the range of parameters studied.

9.3 SUGGESTIONS FOR FUTURE WORK

In the present numerical investigation the main aim is to get the flow and heat transfer characteristic through metallic porous mediums without considering the effects of tortuosity and mixing of the fluid flow in the metal foam or wire mesh. The study also neglected the effects of thermal dispersion through both metal foam and wire mesh porous medium. The study can be relaxed by considering the above mentioned aspects into the numerical simulation. The mixed convection study can be extended to graded metal foam filled in the vertical channel since the present study concentrated on uniform filling of the metal foam. The discrete heat source with discrete metal foam study can be carried out in order to find the isothermal condition on heaters in mixed convection regime.

9.4 CLOSURE

The numerical study of hydrodynamic and thermal characteristics through metallic porous mediums is very important to design high performance heat exchangers. This chapter presented the salient conclusions of this study on flow and heat transfer characteristics. Finally, the scope for the future work was also presented.

REFERENCES

Ajmera, S. K., and Mathur, A. N., (2015) "Experimental investigation of mixed convection in multiple ventilated enclosures with discrete heat sources", Experimental Thermal and Fluid Science, 68, pp. 402-411.

Angirasa, D., and Peterson, G. P., (1999) "Forced convection heat transfer augmentation in a channel with a localized heat source using fibrous materials", Journal of Electronic Packaging, 121, pp. 1 – 7.

ANSYS Fluent, (2017); Available from:<http://www.ansys.com/Products/Fluids/ANSYS-Fluent>.

Badruddin, I. A., Zainal, Z. A., Narayana, P. A. A., and Seetharamu, K. N., (2007) "Numerical analysis of convection conduction and radiation using a non-equilibrium model in a square porous cavity", International Journal of Thermal Sciences, Vol. 46, no. 1, pp. 20–29.

Baskaya, S., Erturhan, U., and Sivrioglu, M., (2005) "An experimental study on convection heat transfer from an array of discrete heat sources", International Communications in Heat and Mass Transfer, 32, pp. 248-257.

Bautista, O., and Mendez, F., (2006) "Internal heat generation in a discrete heat source: Conjugate heat transfer analysis", Applied Thermal Engineering, 26, pp. 2201-2208.

Bernardo, B., Ferraro, G., Manca, O., Marinelli, L., and Nardini, S., (2014), "Mixed convection in horizontal channels partially filled with aluminium foam heated from below and with external heat losses on upper plate", Journal of Physics: Conference Series, 501-012005, pp. 1-10.

Bhattacharya, A., Calmidi, V. V. and Mahajan, R. L. (2002), "Thermophysical properties of high porosity metal foams", International Journal of Heat and Mass Transfer, 45, 1017-1031.

Boomsma, K., Poulikakos, D. and Zwick, F. (2003), "Metal foams as compact high performance heat exchangers", Mechanics of Materials, 35, 1161-1176.

Boyd, B. and Hooman, K. (2012). "Air-cooled micro-porous heat exchangers for thermal management of fuel cells", International Communications in Heat and Mass Transfer, 39, 363–367.

Calmidi, V. and Mahajan, R. (2000). "Forced convection in high porosity metal foams", ASME Journal of Heat Transfer, 122, 557–565.

Celik, H., Mobedi, M., Manca, O. and Ozkol, U. (2017), "A pore scale analysis for determination of interfacial convective heat transfer coefficient for thin periodic porous media under mixed convection", International Journal of Numerical Methods for Heat & Fluid Flow, https://doi.org/10.1108/HFF-01-2017-0036

Chen, C. C., Huang, P. C., and Hwang, H. Y., (2013) "Enhanced forced convective cooling of heat sources by metal foam porous layers", International Journal of Heat and Mass Transfer, 58, pp. 356-373.

Cunsolo, S., Baillis, D., Bianco, N., Naso, V. and Oliviero, M. (2016),"Effects of ligaments shape on radiative heat transfer in metal foams", International Journal of Numerical Methods for Heat & Fluid Flow, Vol. 26 (2), 477 – 488.

Da Silva, A. K., Lorente, S., and Bejan, A., (2004) "Optimal distribution of discrete heat sources on a plate with laminar forced convection", International Journal of Heat and Mass Transfer, 47, pp. 2139-2148.

Dogan, A., Sivrioglu, M., and Baskaya, S., (2005) "Experimental investigation of mixed convection heat transfer in a rectangular channel with discrete heat sources at the top and at the bottom", International Communications in Heat and Mass Transfer, 32, pp. 1244-1252.

Dukhan, N., Bağci, Ö. and Özdemir, M. (2014), "Metal foam hydrodynamics: Flow regimes from pre-Darcy to turbulent", International Journal of Heat and Mass Transfer, 77, pp.114-123.

Durgam, S., Venkateshan, S. P., and Sundararajan, T., (2017) "Experimental and numerical investigations on optimal distribution of heat source array under natural and forced convection in a horizontal channel", International Journal of Thermal Sciences, 115, pp. 125-138.

Dyga, R., and Placzek, M, (2010) "Efficiency of heat transfer in heat exchangers with wire mesh packing", International Journal of Heat and Mass Transfer, 53, pp. 5499-5508.

Fu, Y., Wen, J., and Zhang, C., (2017) "An experimental investigation on heat transfer enhancement of sprayed wire-mesh heat exchangers", International Journal of Heat and Mass Transfer, 112, pp. 699-708.

Gan, G., (1998) "A parametric study of Trombe walls for passive cooling of buildings", *Energy and Buildings*, Vol. 27(1), pp.37-43.

Gangapatnam, P., Kurian, R., and Venkateshan, S., P., (2017) "Numerical simulation of heat transfer in metal foams", Heat Mass Transfer, DOI: 10.1007/s00231-017-2149-6.

Ghorab, M. G., (2015) "Forced convection analysis of discrete heated porous convergent channel", Heat Transfer Engineering, 36 (9), pp. 829-846.

Ghosh, I., (2008), "Heat-Transfer Analysis of High Porosity Open-Cell Metal Foam", ASME Journal of Heat Transfer, 130, pp. 034501 (1-6).

Gururaja Rao, C., Balaji, C., and Venkateshan, S. P., (2002) "Effect of surface radiation on conjugate mixed convection in a vertical channel with a discrete heat source in each wall", International Journal of Heat and Mass Transfer, 45, pp. 3331-3347.

Guerroudj, N. and Kahalerras, H. (2012), "Mixed convection in an inclined channel with heated porous blocks", International Journal of Numerical Methods for Heat & Fluid Flow, Vol. 22 (7), 839 – 861.

Hadim, A., and Chen, G., (1994) "Non-Darcy mixed convection in a vertical porous channel with discrete heat sources at the walls", International Communications in Heat and Mass Transfer, 21 (3), pp. 377-387.

Hadim, H. A., and Bethancourt, A., (1995) "Numerical study of forced convection in a partially porous channel with discrete heat sources", Journal of Electronic Packaging, 117, pp. 46 – 51.

Hajipour, M., and Dehkordi, A. M., (2012) "Analysis of nanofluid heat transfer in parallel plate vertical channels partially filled with porous medium", International Journal of Thermal Sciences, 55, pp. 103-113.

Hajipour, M., and Dehkordi, A. M., (2014) "Mixed convection flow of Al2O3-H2O nanofluid in a channel partially filled with porous metal foam: Experimental and numerical study", Experimental Thermal and Fluid Sciences, 53, pp. 49-56.

Hayes, A. M., Khan, J. A., Shaaban, A. H., and Spearing, I. G., (2008) "The thermal modeling of a matrix heat exchanger using a porous medium and the thermal non-equilibrium model", International Journal of Thermal Sciences, Vol. 47 (10), pp. 1306–1315.

Hayes, A. M., (2006) "The Thermal Modeling of a Matrix Heat Exchanger Using Porous Media and the Thermal Non-equilibrium", University of South Carolina.

Hotta, T. K., Muvvala, P., and Venkateshan, S. P., (2013) "Effect of surface radiation heat transfer on the optimal distribution of discrete heat sources under natural convection", Heat and Mass Transfer, 49, pp. 207-217.

Huang, P. C., Yang, C. F., Hwang, J. J., and Chiu, M. T., (2005) "Enhancement of forced convection cooling of multiple heated blocks in a channel using porous covers", International Journal of Heat and Mass Transfer, 48, pp. 647-664.

Huang, P. C., and Chen, C. C., (2012) "Simulation of mixed convection in a vertical channel containing discrete porous-covering heat blocks", International Journal of Heat and Mass Transfer, 55, pp. 3147-3159.

Huang, S., Wan, Z., Wang, Q., Tang, Y., and Yang, X., (2017) "Thermo-hydraulix characteristics of laminar flow in a circular tube with porous metal cylinder inserts", Applied Thermal Engineering, 120, pp. 49-63.

Ismail, S., (2015), "Numerical investigation of heat transfer and fluid flow behaviors of a block type graphite foam heat sink inserted in a rectangular channel", Applied Thermal Engineering, 78, pp. 605-615.

Jeng, T. M., and Tzeng, S. C., (2007) "Forced Convection of Metallic Foam Heat Sink under Laminar Slot Jet Confined by Parallel Wall", Heat Transfer Engineering, Vol. 28 (5), pp. 484-495.

Jiang, P. X., Ren, Z. P., and Wang, B. X., (1999) "Numerical simulation of forced convection heat transfer in porous plate channels using thermal equilibrium and non-thermal equilibrium models", Numerical Heat Transfer (Part A), Vol. 35 (1), pp. 99–113.

Jiang, P. X., and Ren, Z. P., (2001) "Numerical investigation of forced convection heat transfer in porous media using a thermal non-equilibrium model", *International Journal of Heat and Fluid Flow*, Vol. 22 (1), pp. 102–110.

Kamath, P., M., Balaji, C. and Venkateshan, S. P. (2011), "Experimental investigation of flow assisted mixed convection in high porosity foams in vertical channels", International Journal of Heat and Mass Transfer, 54, 5231-5241

Kamat, P. M., Balaji, C. and Venkateshan, S.P. (2013). "Convection heat transfer from aluminium and copper foams in a vertical channel - An experimental study", International Journal of Thermal Sciences, 64, 1-10.

Kamath, P. M., Balaji, C., and Venkateshan, S. P., (2014) "Heat transfer enhancement with discrete sources in a metal foam filled vertical channel", International Communications in Heat and Mass Transfer, 53, pp. 180-184.

Khashan, S. A., and Al-Nimr, M. A., (2005) "Validation of the local thermal equilibrium assumption in forced convection of non-Newtonian fluids through porous channels", Transport in Porous Media, Vol. 61, no. 3, pp. 291–305.

Khashan, S. A., Al-Amiri, A. M., and Pop, I., (2006) "Numerical simulation of natural convectionheat transfer in a porous cavity heated from below using a non-Darcian and thermal non-equilibrium model", International Journal of Heat and Mass Transfer, Vol. 49 (5–6), pp. 1039–1049.

Kim, S. Y., Paek, J. W. and Kang, B. H. (2000), "Flow and Heat Transfer Correlations for Porous Fin in a Plate-Fin Heat Exchanger", ASME Journal of Heat Transfer, Vol.122, 572-578.

Kim, S. Y., Kang, B. H. and Kim, J. H. (2001), "Forced convection from aluminum foam materials in an asymmetrically heated channel", International Journal of Heat and Mass Transfer, 44, 1451-1454.

Kim, T., Zhao, C., Lu, T. and Hodson, H. (2004), "Convective heat dissipation with lattice-frame materials", Mechanics of Material, 36 (8), pp.767–780.

Kopanidis, A., Theodorakakos, A., Gavaises, E. and Bouris, D. (2010), "3D numerical simulation of flow and conjugate heat transfer through pore scale model of high porosity open cell metal foam", International Journal of Heat and Mass Transfer, 53, 2539 - 2550.

Kurian, R., Balaji, C., and Venkateshan, S. P., (2016), "Experimental investigation of convective heat transfer in a vertical channel with brass wire mesh blocks", International Journal of Thermal Sciences, 99, pp. 170-179.

Li, C., and Peterson, G. P., (2006) "The effective thermal conductivity of wire screen", International Journal of Heat and Mass Transfer, 49, pp. 4095-4105.

Lin, W., Xie, G., Yuan, J. and Sundén, B. (2016). "Comparison and Analysis of Heat Transfer in Aluminum Foam Using Local Thermal Equilibrium or Non equilibrium Model", Heat Transfer Engineering, 37:3-4, 314-322.

Linhui, C., Huaizhang, T., Yanzhong, L., and Dongbin, Z., (2006) "Experimental study on natural convective heat transfer from a vertical plate with discrete heat sources mounted on the back", Energy Conversion and Management, 47, pp. 3447-3455.

Liu, H., Yu, Q. N., Qu, Z. G., and Yang, R. Z., (2017) "Simulation and analytical validation of forced convection inside open-cell metal foams", International Journal of Thermal Sciences, Vol. 111, pp. 234-245.

Lu, W., Zhao, C. Y., and Tassou, S. A., (2006) "Thermal analysis on metal-foam filled heat exchangers. Part I: Metal-foam filled pipes", International Journal of Heat and Mass Transfer, Vol. 49(15-16), pp. 2751-2761.

Lu, W., Zhang, T., and Yang, M., (2016), "Analytical solution of forced convection heat transfer in parallel-plate channel partially filled with metallic foams", International Journal of Heat and Mass Transfer, 100, pp. 718-727.

Lu, W., Zhang, T., Yang, M., and Wu, Y., (2017), "Analytical solutions of force convective heat transfer in plate heat exchangers partially filled with metal foams", International Journal of Heat and Mass Transfer, 110, pp. 476-481.

Ly, H., B., Monchiet, V. and Grande, D. (2016), "Computation of permeability with Fast Fourier Transform from 3-D digital images of porous microstructures", International Journal of Numerical Methods for Heat & Fluid Flow, Vol. 26 (5), DOI: http://dx.doi.org/10.1108/HFF-12-2014-0369

Ma, J., Lv, P., Luo, X., Liu, Y., Li, H., and Wen, J., (2016) "Experimental investigation of flow and heat transfer characteristics in double-laminated sintered woven wire mesh", Applied Thermal Engineering, 95, pp. 53-61.

Mancin, S., Zilio, C., Rossetto, L. and Cavallini, A. (2012), "Foam height effects on heat transfer performance of 20 ppi aluminum foams", Applied Thermal Engineering, 49, 55-60.

Mancin, S., Zilio, C., Diani, A. and Rossetto, L. (2012), "Experimental air heat transfer and pressure drop through copper foams", Experimental Thermal and Fluid Science, 36, pp.224-232.

Mancin, S., Zilio, C., Diani, A., and Rossetto, L., (2013) "Air Forced Convection through metal foams: Experimental results and modeling", International Journal of Heat and Mass Transfer, Vol. 62, pp. 112-123.

Manglik, R. M., (2003) "Heat Transfer Enhancement", Heat Transfer Handbook, A. Bejan and A. Kraus, Wiley, Hoboken, New Jersey, United States, pp. 1029-1130.

Muralidhar, K., and Suzuki, K., (2001) "Analysis of flow and heat transfer in a regenerator mesh using a non-Darcy thermally non-equilibrium model", International Journal of Heat and Mass Transfer, 44, pp. 2493-2504.

Nazari, M., Ashouri, M., Kayhani, M., H., and Tamayol, A., (2015), "Experimental study of convective heat transfer of a nanofluid through pipe filled with metal foam", International Journal of Thermal Sciences, 88, pp. 33-39.

Nield, D. A. and Bejan, A. (2005), "Convection in Porous Media", 3rd ed., Springer, Berlin, Germany.

Özdemir, M. and Özgüc, A. F. (1997) "Forced convective heat transfer in porous medium of wire screen meshes", Heat Mass Transfer, 33, pp. 129-136.

Phanikumar, M. S., and Mahajan, R. L., (2002) "Non-Darcy natural convection in high porosity metal foams", International Journal of Heat and Mass Transfer, Vol. 45 (18), pp. 3781-3793.

Radhakrishnan, T. V., Balaji, C., Venkateshan, S. P., (2010) "Optimization of multiple heaters in a vented enclosure – A combined numerical and experimental study", International Journal of Thermal Sciences, 49, pp. 721-732.

Sankar, M., Park, J., Kim, D., and Do, Y., (2013) "Numerical study of natural convection in a vertical porous annulus with an internal heat source: Effect of discrete heating", Numerical Heat Transfer, Part A: Applications, 63 (9), pp. 687-712.

Sener, M., Yataganbaba, A., and Kurtbas, I., (2016), "Forchheimer forced convection in a rectangular channel partially filled with aluminum foam", Experimental Thermal and Fluid Sciences, 75, pp. 162-172.

Sivasankaran, S., Do, Y., and Sankar, M., (2011) "Effect of discrete heating on natural convection in a rectangular porous enclosure", Transport in Porous Medium, 86, pp. 261-281.

Solmus, I., (2015) "Numerical investigation of heat transfer and fluid flow behaviors of a block type graphite foam heat sink inserted in a rectangular channel", Applied Thermal Engineering, 78, pp. 605 - 615.

Sudhakar, T. V. V., Balaji, C., and Venkateshan, S. P., (2009) "Optimal configuration of discrete heat sources in a vertical duct under conjugate mixed convection using artificial neural networks", International Journal of Thermal Sciences, 48, pp. 881-890.

Tamayol, A., and Hooman, K., (2011) "Thermal Assessment of Forced Convection through Metal Foam Heat Exchangers", ASME Journal of Heat Transfer, 133, pp. 11801 (1-7).

Tian, J., Kim, T., Lu, T., Hodson, H., Queheillalt, D., Sypeck, D. and Wadley, H. (2004), "The effects of topology upon fluid flow and heat transfer within cellular copper structures", International Journal of Heat and Mass Transfer 47 (14–16), pp.3171–3186.

Tu, W., Wang, Y., Tang, Y., and Xu, J., (2016) "Heat transfer and pressure drop characteristics in a circular tube with mesh cylinder inserts", International Communications in Heat and Mass Transfer, 75, pp. 130-136.

Venugopal, G., Balaji, C. and Venkateshan, S. P. (2010), "Experimental study of mixed convection heat transfer in a vertical duct filled with metallic porous structures", International Journal of Thermal Sciences, 49, 340-348.

Wang, Y., Wang, J., and Jia, P., (2011) "Performance of Forced Convection Heat Transfer in Porous Media Based on Gibson–Ashby Constitutive Model", Heat Transfer Engineering, Vol. 32 (11-12), pp. 1093-1098.

Wakao, N., Kaguei, S., and Funazkri, T., (1979), "Effect of Fluid Dispersion Coefficients on Particle-to-Fluid Heat transfer coefficients in packed beds", Chemical Engineering Science, 34, pp. 325-336.

Walters, D. K. and Coklja, D. (2008), "A three-equation eddy viscosity model for Reynolds-averaged navier-stokes simulations of transitional flows", Journal of fluids Engineering, 130.

Xu, J., Tian, J., Lu, T. J., and Hodson, H. P., (2007) "On the thermal performance of wire-screen meshes as heat exchanger material", International Journal of Heat and Mass Transfer, 50, pp. 1141-1154.

Xu, H. J., Qu, Z. G., Lu, T. J., He, Y. L., and Tao, W. Q., (2011) "Thermal Modeling of Forced Convection in a Parallel-Plate Channel Partially Filled with Metallic Foams", ASME Journal of Heat Transfer, 133, pp. 1-9.

Yucel, N., and Guven, R. T., (2009) "Numerical study of heat transfer in a rectangular channel with porous covering obstacles", Transport in Porous Medium, 77, pp. 41-58.

Zhao, C.Y., (2012) "Review on thermal transport in high porosity cellular metal foams with open cells", International Journal of Heat and Mass Transfer, Vol. 55 (13-14), pp. 3618–3632.

Zhao, Z., Peles, Y., and Jensen, K., (2013) "Properties of plain weave metallic wire mesh screens", International Journal of Heat and Mass Transfer, 57, pp. 690-697.

Zukauskas, A. A. (1987), "Convective heat transfer in cross-flow", in: S. Kakac, R.K. Shah, W. Aung (Eds.), Handbook of Single-Phase Convective Heat Transfer, Wiley, New York.

LIST OF PUBLICATIONS

INTERNATIONAL JOURNAL

1. **Banjara Kotresha** and N Gnanasekaran (2019). "Effect of thickness and thermal conductivity of metal foams filled in a vertical channel − A numerical study", International Journal of Numerical methods for Heat and Fluid Flow, Vol. 29, Issue 1, pp. 184-203. DOI: 10.1108/HFF-11-2017-0465

2. **Banjara Kotresha** and N Gnanasekaran (2018). "Investigation of Mixed Convection Heat Transfer through Metal Foams Partially Filled in a Vertical Channel by Using Computational Fluid Dynamics", ASME Journal of Heat Transfer, Vol. 140, Issue 11, pp. 112501 (1-11). DOI: 10.1115/1.4040614

3. **Banjara Kotresha**, N Gnanasekaran and C Balaji (2019) "Numerical Simulations of Flow assisted mixed convection in a Vertical Channel Filled with High Porosity Metal Foams", Heat Transfer Engineering, Vol. 41, Issue 8, pp. 112501-11. DOI: 10.1080/01457632.2018.1564208

4. **Banjara Kotresha** and N Gnanasekaran (2019). "A Synergistic Combination of Thermal Models for Optimal Temperature Distribution of Discrete Sources through Metal Foams in a Vertical Channel", ASME Journal of Heat Transfer, Vol. 141, Issue 2, pp. 02200 (1-8). DOI: 10.1115/1.4041955

5. **Banjara Kotresha** and N Gnanasekaran, (2019). "Determination of interfacial heat transfer coefficient for the flow assisted mixed convection through brass wire mesh", International Journal of Thermal Sciences, Vol. 138, pp. 98 − 108. DOI: 10.1016/j.ijthermalsci.2018.12.043

6. **Banjara Kotresha** and N Gnanasekaran (2018) "Numerical Simulations of Fluid Flow and Heat Transfer through Aluminum and Copper Metal Foam Heat Exchanger–A Comparative Study", Heat Transfer Engineering, Vol. 41, Issue 5-6. DOI: 10.1080/01457632.2018.1546969.

7. **Banjara Kotresha** and N Gnanasekaran "Numerical modeling of partially filled wire mesh for the study of mixed convection in a two-sided vertical channel", International Journal of Numerical methods for Heat and Fluid Flow (Under Review)

8. **Banjara Kotresha** and N Gnanasekaran "Comparison of Fluid Flow and Heat Transfer through Metal Foams and Wire Mesh by Using CFD"**,** Recent Patents on Mechanical Engineering. (Accepted for publication)

9. **Banjara Kotresha** and N Gnanasekaran "Nuances of Fluid Flow through a Vertical Channel in the Presence of Metal foam/Solid block – A Hydrodynamic Analysis using CFD"**,** Sadhana (Under Review)

Book Chapter:

1. Banjara Kotresha and N Gnanasekaran, "Analysis of Forced Convection Heat Transfer Through Graded PPI Metal Foams"**,** Numerical Heat Transfer and Fluid Flow**, Lecture Notes in Mechanical Engineering**, pp. 151-158, 2019.

CONFERENCES PROCEEDINGS

1. **Banjara Kotresha** and N Gnanasekaran, "CFD Simulation of Fluid Flow and Heat Transfer Through Aluminium And Copper Metal Foam Heat Exchanger – A Comparative Study", 1st International and 18th ISME Conference on "Mechanical Engineering: Enabling Sustainable Development", (**ISME 18**), National Institute of Technology, Warangal, India, Feb. 23 – 25, 2017.

2. **Banjara Kotresha** and N Gnanasekaran, "Comparison of Fluid Flow and Heat Transfer Through Metal Foams and Wire Mesh by Using CFD", 44th National Conference on Fluid Mechanics and Fluid Power, (**FMFP-2017**), Amrita university, Kollam, India, Dec. 14-16, 2017.

3. **Banjara Kotresha** and N Gnanasekaran, "CFD Simulation of Fluid Flow and Heat Transfer through Aluminum Metal Foam Heat Exchanger", 24th National and 2nd International ISHMT – ASTFE Heat and Mass Transfer Conference (**IHMTC-2017**), BITS Pilani, Hyderabad, India, Dec. 27 – 30, 2017.

4. **Banjara Kotresha** and N Gnanasekaran, "Analysis of Forced Convection Heat Transfer through Graded PPI Metal Foams", International Conference Numerical Heat Transfer and Fluid Flow (**NHTFF-2018**), National Institute of Technology, Warangal, India, Jan. 19 – 21, 2018.

5. **Banjara Kotresha** and N Gnanasekaran, "Prediction of Heat Transfer with Discrete Heat Sources in a Vertical Channel Filled with High Porosity Metal Foam", 5th International Conference on Computational Methods for Thermal Problems (**THERMACOMP2018**), Indian Institute of Science, Bangalore, INDIA, July 9-11, 2018.

6. Prasheel Nakate, **Banjara Kotresha** and N Gnanasekaran, "Asymptotic Approach to obtain Nusselt Number Correlation for Laminar Mixed Convection in a Vertical Channel", 5th International Conference on Computational Methods for Thermal Problems (**THERMACOMP2018**), Indian Institute of Science, Bangalore, INDIA, July 9-11, 2018.

7. **Banjara Kotresha** and N Gnanasekaran, **"Effect of Porosity Grading of the Metal foam in a Mixed Convection Heat Transfer Filled in a Vertical Channel",** 7th International and 45th National Conference on Fluid Mechanics and Fluid Power (FMFP), December 10-12, 2018, IIT Bombay, Mumbai, India.

8. Siva Guru G, **Banjara Kotresha** and N Gnanasekaran, **"**Mixed Convection Heat Transfer through Metal Foams Filled in a Vertical Channel with Thermal Dispersion: A Numerical Study"**,** 7th International and 45th National Conference on Fluid Mechanics and Fluid Power (FMFP), December 10-12, 2018, IIT Bombay, Mumbai, India.

9. **Banjara Kotresha** and N Gnanasekaran, **"Modelling Conjugate Heat Transfer in Conjunction with Highly Conductive Metal Foam in a Vertical Channel",** 11th International Exergy, Energy and Environment Symposium (IEEES-11)), July 14-18, 2019, SRM University, Chennai, India.

Mr. BANJARA KOTRESHA

Mobile: +919945577668

E-mail: bkotresha@gmail.com

Education

Master of Technology from Kuvempu University, Shimoga, Karnataka, India

Sep 2004 - Oct 2006; Mechanical Engineering

Specialization: Thermal Engineering Systems Technology

Bachelor of Engineering from Kuvempu University, Shimoga, Karnataka, India

Sep 1998 – Oct 2002; Mechanical Engineering

Work Experience

Assistant Professor at Government Engineering College, Haveri, Karnataka, India
Mar 2011 – Deputed to pursue Ph.D from 18/07/2016 at NITK
Senior Research Engineer at Fluidyn Softwares & Consultancy Pvt Ltd, Bangalore, India
Nov 2009 – Feb 2011
Research Engineer at Fluidyn Softwares & Consultancy Pvt Ltd, Bangalore, India
Nov 2006 – Oct 2009
Trainee Research Engineer at Fluidyn Softwares & Consultancy Pvt Ltd, Bangalore, India
Aug 2006 – Oct 2006
Work package Engineer at CFD Division, GTRE, Bangalore, India
Jun 2006 – July 2006
Project Trainee at Indian Institute of Science (IISc), Bangalore, India
Aug 2005 - Apr 2006

Achievements

Bagged First Rank to the university in Master of Technology
Bagged 5th Rank to University in Bachelor of Engineering
Gate qualified in the year 2004

Trainings Attended

- Two-week ISTE Workshop on "**Engineering Thermodynamics**" from 11th to 21st December, 2012 Conducted by IIT, Bombay.
- Two-week ISTE Workshop on "**Database Management Systems**" from 21st - 31st May, 2013 Conducted by IIT, Bombay.
- Two-week ISTE Workshop on "**Fluid Mechanics**" from 20th to 30th May 2014 Conducted by IIT, Kharagpur.
- One-week STTP on "**Development of Mechanical Engineering laboratory and Experiments**" from 7th – 11th July, 2014 Conducted by NITTTR, Kolkata.

Computer Skills

      Languages: C, FORTRAN
      Operating Systems: MS Windows, Linux
      CFD Software's: GAMBIT, FLUENT, FLUIDYN-NS, FLUIDYN-MP

Research Interest

Computational Fluid Dynamics, Flow and Heat Transfer Porous Media, Fluid Flow (Incompressible & Compressible flows, Laminar &Turbulent flows), Heat & Mass Transfer Systems, Fluid flow around Bluff-Bodies

Post-Graduation Research Work

      An unsplit relaxation scheme for hyperbolic conservation laws

      Organization: Aerospace Department, Indian Institute of Science (IISc), Bangalore

Personal Details

      Date of birth: 4th April 1981
      Contact Address: Assistant Professor,
                       Department of Mechanical Engineering
                        Government Engineering College
                        Devagiri
                        Haveri – 581110,
                        Karnataka, India
      Marital Status: Married
      Languages Known: Kannada, English and Telugu